A TECHNICAL AND ECONOMIC APPRAISAL FOR OPTIMAL EXPLOITATION OF THE H SUB-INCLINE COMPLEX AT NCHANGA UNDERGROUND MINE

By

ROBERT NYIRENDA

A thesis submitted to the University of Zambia in partial fulfilment of the requirements for the award of Master of Mineral Science (M.Min.Sc) degree in Mining Engineering

UNIVERSITY OF ZAMBIA

LUSAKA

APRIL, 2017

Declaration

I, Robert Nyirenda, hereby declare that this thesis entitled *"A Technical and Economic Appraisal for optimal exploitation of the H Sub-Incline complex at Nchanga Underground Mine"* is my original work. The work contained in this thesis has not been previously published for the award of any other degree or diploma in any university. To the best of my knowledge, where this work comprises of material previously published by any other person, due acknowledgement has been made. I proclaim that the views and opinions expressed in this thesis must only be used for the purpose of reading it. Hence, I declare that this thesis has been carried out and submitted in satisfaction of the nature and standards required for the partial fulfilment of Master of Mineral Sciences degree in Mining Engineering of the University of Zambia.

Author's Signature: .... Date: ....

Certificate of Approval

This is to certify that the thesis, by Robert Nyirenda, is approved as partially fulfilling the requirements for the award of the degree of Master of Mineral Science degree in Mining Engineering of the University of Zambia.

Supervisor

Name: ....

Signature: ....

Date: ....

Internal Examiner

Name: ....

Signature: ....

Date: ....

Internal Examiner

Name: ....

Signature: ....

Date: ....

Internal Examiner

Name: ....

Signature: ....

Date: ....

Dedication

I dedicate this thesis to my mother, Mrs N. L. Nyirenda, my brother, Mr. F. Nyirenda and my late father, Mr F Nyirenda.

Acknowledgements

I am deeply grateful to Dr. Bunda Besa for his guidance, valuable mentorship and selfless efforts to make sure that this research study becomes a success. I also would like to thank Dr. V. Mutambo for his important input in this research study. Special thanks are extended to Mr. Bornwell Hakakwale and Mr. E. Chibomba, my site supervisors, for their contribution which I regard as indispensable for this work to come into fruition.

My most sincere gratitude goes to the University of Zimbabwe for sponsoring my studies at the University of Zambia and Konkola Copper Mines Plc. for allowing me to carry out this research at Nchanga Underground mine, in conjunction with, the School of Mines and Directorate of Research and Graduate Studies of the University of Zambia.

Affectionate compliments are extended to my brother, Francis, and my mother, Mrs Nyirenda, for their support and prayers.

Affable tribute goes to my dear friend, Sherrelyn, for her enduring encouragement and inspiration throughout the course of the research.

Lastly, I wish to thank all individuals who played a role, directly or indirectly, towards contributing to this study.

Abstract

Nchanga Underground mine uses a block caving variant to extract the lower ore body of the Nchanga syncline. The deepest part of the ore body, the H Sub-Incline complex, is thin with 4.39m average thickness, 5.27% weighted average grade of Copper and hosts 1,219,314t in-situ. Operational challenges were being faced including early dilution discharge and premature collapse of secondary developments. In addition, the tramming equipment was failing to meet planned production targets by discrepancies of 35.8% for availability, 25.4% for utilisation and 63.3% for trammed ore. Caved mass evaluations showed that inclined undercutting and a 63.5^{o} angle of draw based on friction angle of the ore zone are suitable for exploiting the complex. Total dilution entry point tonnage of 774,553t was computed for the ore body so as to determine the tonnage which will be drawn before diluted material starts discharging into scraper drifts. Maximum buffer reserve tonnage between development and production was calculated as 192,553t after considering a block recovery factor of 140%, minimum stand-up time for secondary developments (i.e. 0.93years) and annual production rate of 308,500t per year. The calculated buffer reserves will save Konkola Copper Mines $173,231.46 in support costs for developments which are outside the just-in-time range. Additionally, sub systems of dump trucks which had the most impact on loss of machine availability were identified by reliability analysis so as to propose maintenance intervals which coincide with 75% on each reliability curve for the respective trucks. Following this, it was observed that mean time-to-repair of the Sandvik EJC533 truck's transmission was significantly higher at 82.80hrs than that of the other Atlas Copco trucks which averaged at 2.34hrs. It was inferred that this difference was caused by a lack of proficiency to maintain and repair Sandvik EJC533's transmission. Sending artisans to Sandvik for transmission debugging and diagnosis training is expected to reduce repair time and improve reliability. Correspondingly, preliminary investigation showed that Longwall and Cut-and-Fill stoping are the technically superior methods to exploit the complex. Longwall mining was selected as the most appropriate method for extracting future reserves of the complex after a review of documentation on these methods was done using the criteria of operating costs, ore recoveries and productivity per man hour shift. The study established that extracting the complex will increase the life-of-mine by at least 2.42 years, yielding net discounted earnings of $63,006,898.32 excluding interests, taxes and depreciation.

TABLE OF CONTENTS Page

List of Figures

List of Tables

List of Abbreviations and Acronyms

Abbreviation	Description
ADT	Articulated dump truck
AICu	Acid insoluble copper
ARK	Arkose strata
ASCu	Acid soluble copper
BMR	Buffer mineral reserves
Cu	Copper
DCF	Draw control factor
D_e	Equivalent dimension
DEP	Dilution entry point
DORS	Dynamic ore reserves system
EBITDA	Earnings before interests, taxes, depreciation and amortisation
ESR	Excavation-to-support ratio
HIZ	Height of interaction zone
HSI	H Sub-Incline
KCM	Konkola Copper Mines Plc.
LBS	Lower banded shale
MMS	Mining method selection
MRMR	Modified Rock Mass Rating
MTTF	Mean time to failure
MTTR	Mean time to repair
NBG	Nchanga basement granite
NOP	Nchanga Open Pit
NPV	Net present value
NUG	Nchanga Underground Mine
Q	Geomechanics classification
RAM	Reliability, availability and maintainability
RMR	Rock Mass Rating
RQD	Rock Quality Designation
RSR	Rock Structure Rating
RSS	Rock Substance Strength
TBF	Time before failure
TCu	Total of acid soluble and insoluble copper
UBC	University of British Columbia
UCS	Uniaxial Compressive Strength

CHAPTER 1: INTRODUCTION

1.1 Location of Nchanga Mine

Konkola Copper Mines (KCM) is one of Zambia's largest integrated copper producers. Nchanga mine is one of three mines owned by KCM and is located in the municipal town of Chingola, north of the Zambian capital city of Lusaka as shown in Figure 1.1. Nchanga Underground mine (NUG) and Nchanga Open Pit (NOP) are the two main sources of copper and cobalt ore at the mine and they exploit the gently dipping Nchanga syncline ore body.

NUG uses a variant of block caving method to extract the ore body. Presently, the future of NUG production is being focused on extracting the relatively deep, thin yet rich H Sub-Incline (HSI) complex.

Figure 1.1: Location of Nchanga Mine (Source: "Nchanga Open Pit Mines" Google Maps. May 31, 2016)

1.2 Statement of the problem

Exploration has shown that the HSI complex is thin and rich considering a cut-off grade of 1.0% Total Copper (TCu). The in-situ reserve hosts 1,219,314 tonnes of ore with a weighted-average grade by tonnage of 5.27% TCu and an average ore body thickness of 4.39m. Copper ore is mainly hosted in relatively competent Arkose (ARK) strata and also the transitional layer and, to a lesser extent, the Lower Banded Shale (LBS) in blocks east of 2870/3E and 3020/3E levels.

However, operational and economic challenges were being experienced when extracting the HSI complex blocks. Unplanned dilution is undesirably high at 27% such that diluted material is discharging prematurely into scraper drifts mainly due to the following:

- Fines migration, of the relatively less competent hanging wall (LBS) material, through the coarse matrix of fairly competent ore material, during production drawing.
- Reduced gravitational flow zone since there is an unfavourably high phreatic level as shown in Figure A-1 of Appendix A, which is also causing decreases in draw cone radii because of ore and waste caking in the draw zone.
- Short stand-up time of development drives and weak pillar material.

Consequently, costs of operation have increased due to the need to re-mine partially or completely closed development drives as shown in Figures 1.2 and 1.3.

Figure 1.2: Collapsed drift

Figure 1.3: Blocked development drive

Furthermore, the trackless ore conveyance system is failing to meet planned production targets as shown by availability, utilisation and trammed ore percentages in Figure 1.4.

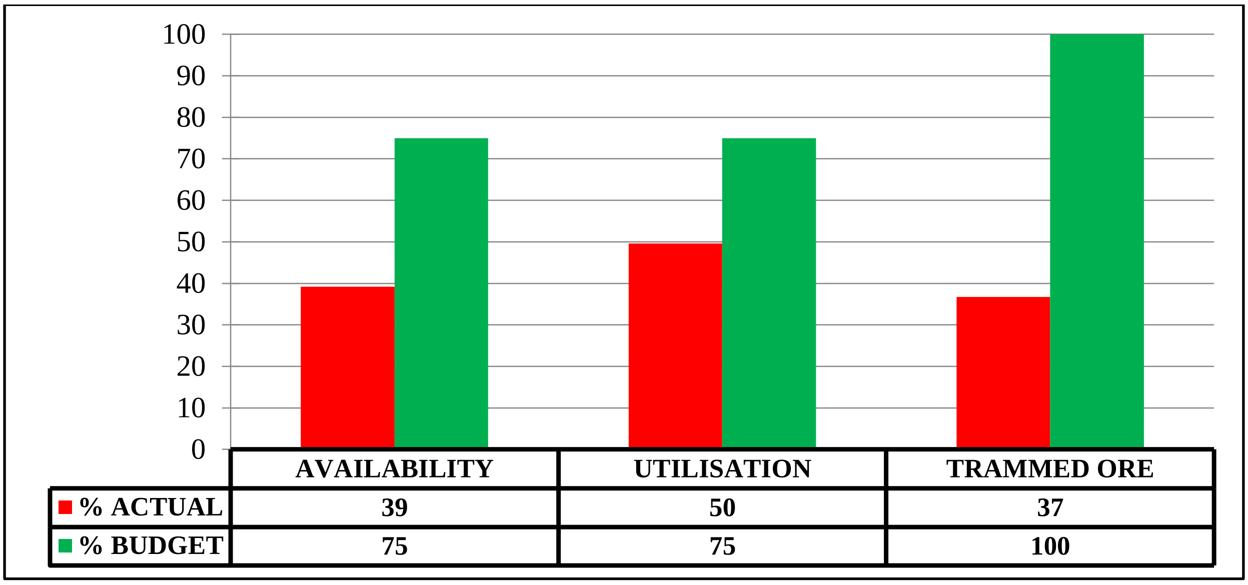

Figure 1.4: Performance indices for dump trucks in the HSI complex

1.3 Study objectives

1.3.1 Main objective

To determine the production potential of the HSI complex and compute the optimal operating strategy which maximises extraction of the complex's blocks east and below 2870/3E and 3020/3E, at KCM's NUG mine.

1.3.2 Sub-objectives

i. Review literature relevant to NUG mining operations using current caving method.
ii. Review of total mineable reserves for the HSI complex blocks east of 2870/3E and 3020/3E.
iii. Compute optimal buffer reserves which can be fully extracted just-in-time before partial or complete closure of development workings.
iv. Analyse the reliability distribution of current trackless equipment such that material conveyance operations are maximised.

1.4 Research questions

- Which Nchanga HSI complex blocks, east and below 2870/3E and 3020/3E, can be efficiently exploited after considering the practicality of mining, economics of extraction and recovery factors?
- How much reserve tonnage can be developed, and provided for production, "just-in time" before the developments reach the end of their stand-up time?
- Are the current hoisting and tramming equipment a viable option for economic extraction of the minable reserves of the complex?
- Is block caving best suited for exploiting future undeveloped reserves of the complex?

1.5 Research methodology

The study spanned over a period of a seven month period from July 2016 to January 2017. Field work included underground site observations, point load testing of irregular rock lumps, collection of discontinuity data, gathering of ore body characteristics and collation of dump truck breakdown data. Secondary data derived from archived geotechnical records were used for rock mass classification purposes because information derived from fieldwork yielded similar results to the secondary data.

A comprehensive description of the research design was presented in Chapter 3. Sections 1.5.1 to 1.5.5 briefly describe activities which were carried out in order to address the different segments of the research problem.

1.5.1 Literature review plan

Current knowledge of the research problem was established by reviewing existing conceptual and data based literature. Information was gathered from KCM and University of Zambia library facilities, and also, the "Google Scholar" service.

1.5.2 Review of HSI complex mineable reserves

Consequently, mineable reserves were reviewed by firstly determining the resource using exploration data from KCM. The cut-off grade was used to remove blocks which are not economical (i.e. 2870/7EC only). Blending options were considered between the 2870/7EC block and the block which contains the highest copper grade of all the blocks (i.e. 3020/7EB). The practicality of mining, dilution and recovery factors was subsequently ascertained by conducting undercut design, calculating the total tonnage which will be drawn before diluted material starts to discharge into scraper drifts and the determination of net discounted earnings before interest, taxes, depreciation and amortisation (EBITDA).

1.5.3 Just-in-time Buffer Mineral Reserves

The maximum reserve tonnage that provides developments just-in-time before their collapse was computed by taking into consideration the excavation stand-up time, annual production rate and mining block recovery factor.

1.5.4 Reliability evaluation of the dump truck fleet

Dump truck failure data was analysed so that components with the most impact on availability were identified. Failure data for these components were subjected to further reliability modelling using the Reliability Analytics Toolkit (Morris, 2010) so as to recommend appropriate maintenance intervals.

1.5.5 Mining method selection

Following a review of mining method selection techniques, a preliminary investigation was done to determine the best method for exploiting future undeveloped reserves using the online UBC mining method selection tool (Edumine, 1999).

1.6 Significance of the study

Successful exploitation of the complex will bring about the following benefits to KCM:

- ✓ Effective extraction of the high grade HSI blocks will help counter copper price fluctuations.
- ✓ The reviewed mineable blocks will increase the life-of-mine (LOM) for KCM.
- ✓ KCM cash in-flows will be significantly improved.
- ✓ Mining the complex will further help KCM gain more geological knowledge of the continuity of mineralisation below and east of 3020FT levels.
- ✓ Production and development excavations for extracting the complex blocks will provide access to sub 3020FT levels for future exploration, developments and production.

1.7 Research scope and limitations

Table 1.1 describes a summary of the study's scope and limitations. Fulfilling the objectives of this study was hindered by constrained study time frame, limited access to fresh diamond drill core samples and unavailable software packages (e.g. Flac 3D, Abaqus 3D, PFC 2D &3D).

Table 1.1: Scope of the study

	Incorporated		Excluded
Calculations	Rock mass classification systems	• Rock mass rating, • Rock quality designation, • Q- Classification, • Lauffer's rock mass classification system. • Laubscher's rock mass classification system	Other rock mass classification methods
	Buffer mineral reserves and development rate	• A technique based on the production rate and excavation stand-up time.	Other methods based on specialised software packages like FLAC 3D
	Review of economic reserves	• Income/loss visibility calculations based on computed dilution entry point at the draw points.	Other calculation techniques suitable for economic review including block modelling.
	Optimisation of materials handling system	• A method based on analysis of reliability, availability and maintainability of the current trackless material conveyance system against planned productive capacity.	Other analysis methods based on specialised software packages like HaulSIM ™.
	Ground support	• Empirical support calculations based on Q- classification.	Numerical modelling
	Caved mass flow analysis	• Methodologies suggested by Heslop & Laubscher (1981), Laubscher (1990), Laubscher (1994), Susaeta (2004) and Munro (2013)	3D particle flow simulations using specialised softwares like PFC 2D or 3D
Modelling	Mining method selection	• University of British Colombia method	Other selection methods like Multiple Criteria Decision Making
	Economic modelling	• Based on review of economic reserves computations • Life-of-mine (LOM), Net present value (NPV) calculations.	Detailed cost overview

Furthermore, the anticipated constraints and inadequacies of the study which were realised during the course of this study were as follows:

- The investigations in this study were only limited to HSI complex blocks east of 2870/3E and 3020/3E.

- Numerical modelling was not done for determining stand-up times, stable stope dimensions and support designs. The reason for not conducting numerical modelling was mainly due to unavailability of appropriate softwares like Fast Lagrangian Analysis of Continua (FLAC) 3D. However, empirical graphs were used as an alternative to provide sufficiently accurate estimates in a timely manner.

- The study did not encompass mineral price forecasting (e.g. time-series analysis, stochastic or dynamic programming) so as to determine the current copper price's position on the global copper price fluctuation cycle at the London Metal Exchange. Knowledge of this position on the cycle will further consolidate this study because it will help to ascertain the optimal commencement time for excavating developments of future HSI complex reserves such that KCM's cash flows are maximised by a minimised payback period.

- The study also did not incorporate cave control evaluations by computer simulations, small scale physical model or full scale mine models. This was due to constraints of unavailability of the computer simulation software packages (e.g. PFC 2D, PFC 3D and ABAQUS 3D) and also the limited time allocated for the study.

Up-to-date cost structure was not used for review of economic reserves due to the KCM's privacy and disclosure policies. However, following frequent consultations with line managers and cost accountants, the estimated values used in the economic evaluation process yielded fairly accurate results.

1.8 Thesis outline

The previously stated objectives and research questions were answered through the following outline of this report:

Chapter 1 introduces the study by describing the background of the problem statement, defining the study's objectives and highlighting the research questions. The objectives were made to be specific, measurable, attainable and realistic such that the research questions are answered adequately.

Chapter 2 provides a review of scholarly knowledge on the different study areas of interest. In addition, it provides general background information of the Nchanga Underground mine including details on the Nchanga syncline geology, current mining method among other things.

Chapter 3 defines the overall strategy which was utilised to achieve the aim of the study. The data sources, study variables, sampling criteria, data collection and analysis techniques were described clearly so as that the different components are integrated in a consistent and logical manner.

Chapter 4 provides an overall description of the processes which were performed in gathering data of the study variables for further processing and analyses. Efforts were made to develop and utilise the appropriate tools in order to avoid gathering superficial, biased or incomplete data.

Chapter 5 presents the meticulous assessment and manipulation of primary and secondary data in order to establish and validate the study's findings.

Chapter 6 describes the deductions made from assessment of the study findings in relation to the objectives defined in Chapter 1. Consequently, conclusions were drawn and recommendations were made based on the inferences established in this study.

CHAPTER 2: BACKGROUND AND LITERATURE REVIEW

2.1 Introduction

The purpose of this Chapter was to elaborate current erudition concerning the variables influencing existing challenges faced in exploiting the HSI complex. Firstly, an assessment of criteria used to design interactive draw zones was done such that the HSI complex blocks can be extracted economically with minimised dilution entry. Secondly, a review of literature regarding just-in-time buffer reserves was undertaken with the aim of obtaining pre-requisite knowledge for computing the maximum allowed reserve development rate which curtails premature collapse of development headings. Thirdly, a discussion was done, regarding reliability analysis of trackless ore haulage systems, so that sufficient information is gained to facilitate an investigation to determine the feasibility of existing NUG trackless fleet to meet production commitments. Lastly, mining method selection techniques were reviewed in a preliminary attempt to aid in the process of selecting the most suitable method for mining future undeveloped reserves of the complex.

2.2 Geological setting of the Lower Ore Body

The Nchanga Syncline is a geological structure which hosts three copper (Cu) ore bodies at NUG mine. The three mineralisations are Upper Ore body (UOB), Intermediate Ore Body and Lower Ore Body (LOB). Figure 2.1 illustrates an idealised section of the Nchanga Syncline highlighting the stratigraphic progression of rock strata at NUG. UOB is about 20m thick and consists of the highly folded Feldspathic Quartzite overlain by Upper Banded Shale. Meanwhile, LOB has a thickness range between 3m to 15m mainly comprising of ARK, transitional layer and LBS.

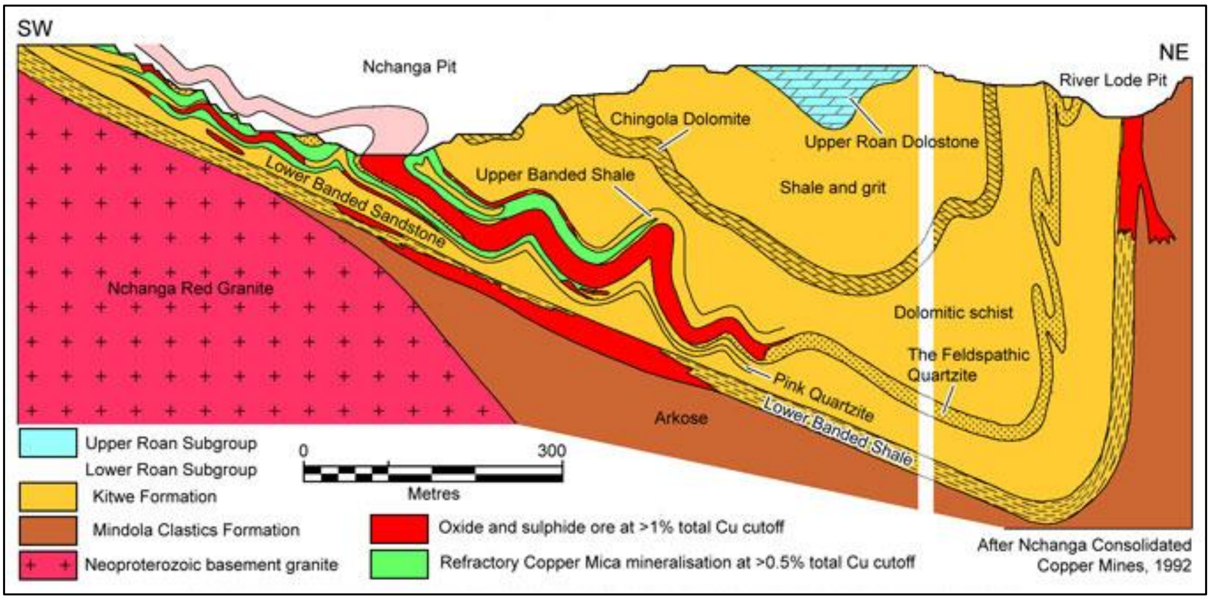

Figure 2.1: Idealised sectional view of Nchanga Syncline (Pearson, 1981)

2.2.1 Stratigraphic assemblage

The basement rock the LOB is the Nchanga Red Granite (NRG) in which the main shafts are sunk. This is overlain by ARK formation in which most of the primary and secondary developments are excavated. Other rock formations in succession are shown in the stratigraphic column in Figure 2.2.

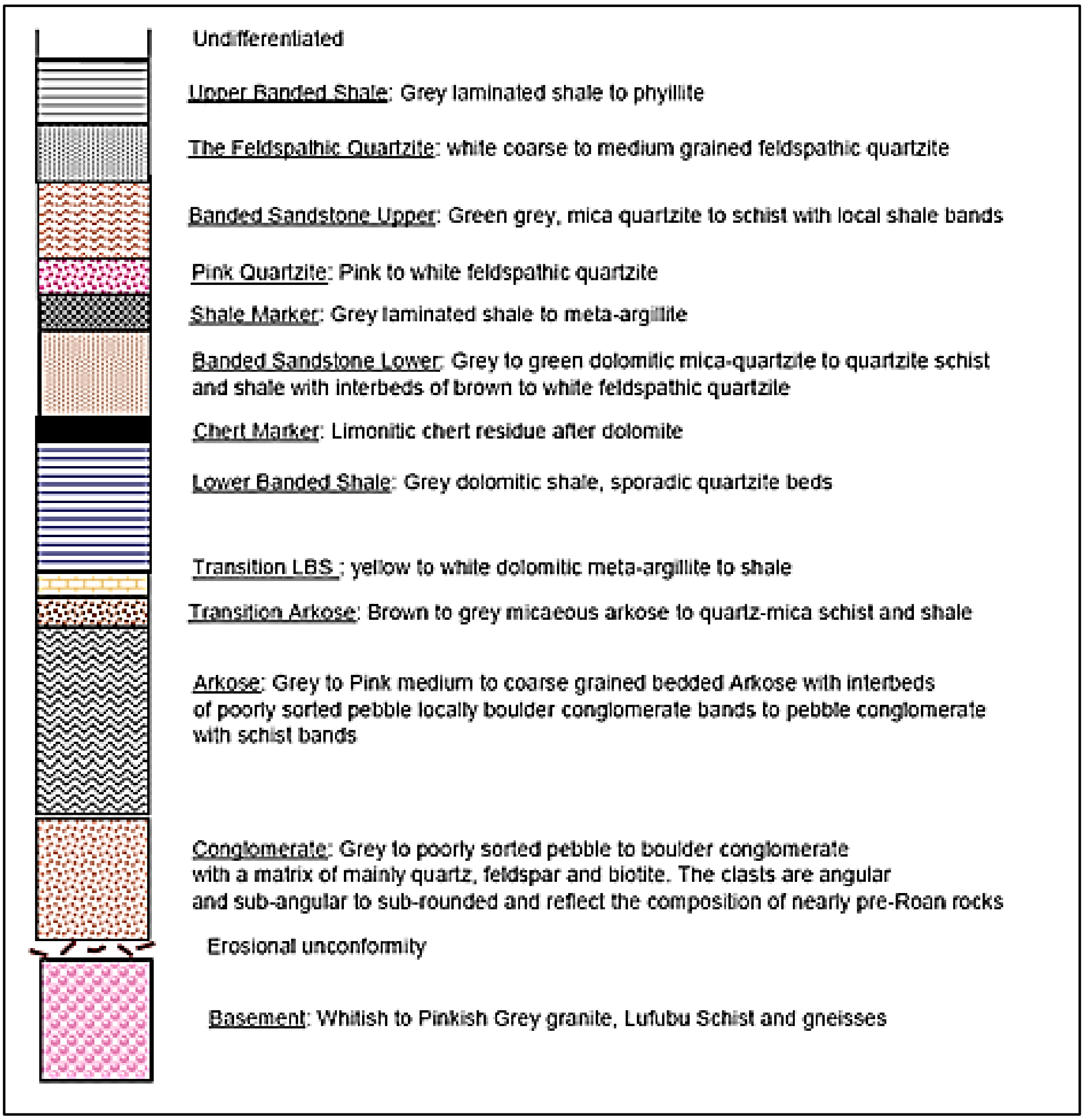

Figure 2.2: Stratigraphic sequence of rock formations in the LOB (Chishimba & Mundike, 2014)

2.2.2 The HSI complex mineralisation

Mineralisation in the HSI complex is essentially an extension of LOB in the deepest part of NUG (i.e. sub 2720FT levels). Exploration has proved that this ore body hosts high grade Cu, however, the thickness is considerably smaller ranging from 0.8m to 9.8m. In addition, the ore zone extends from the top part of ARK into Transition ARK. The total reserve for the complex is 1,219,395t of Cu ore in-situ with a weighted average of 5.27% TCu by tonnage. The HSI complex blocks are illustrated in Figure 2.3.

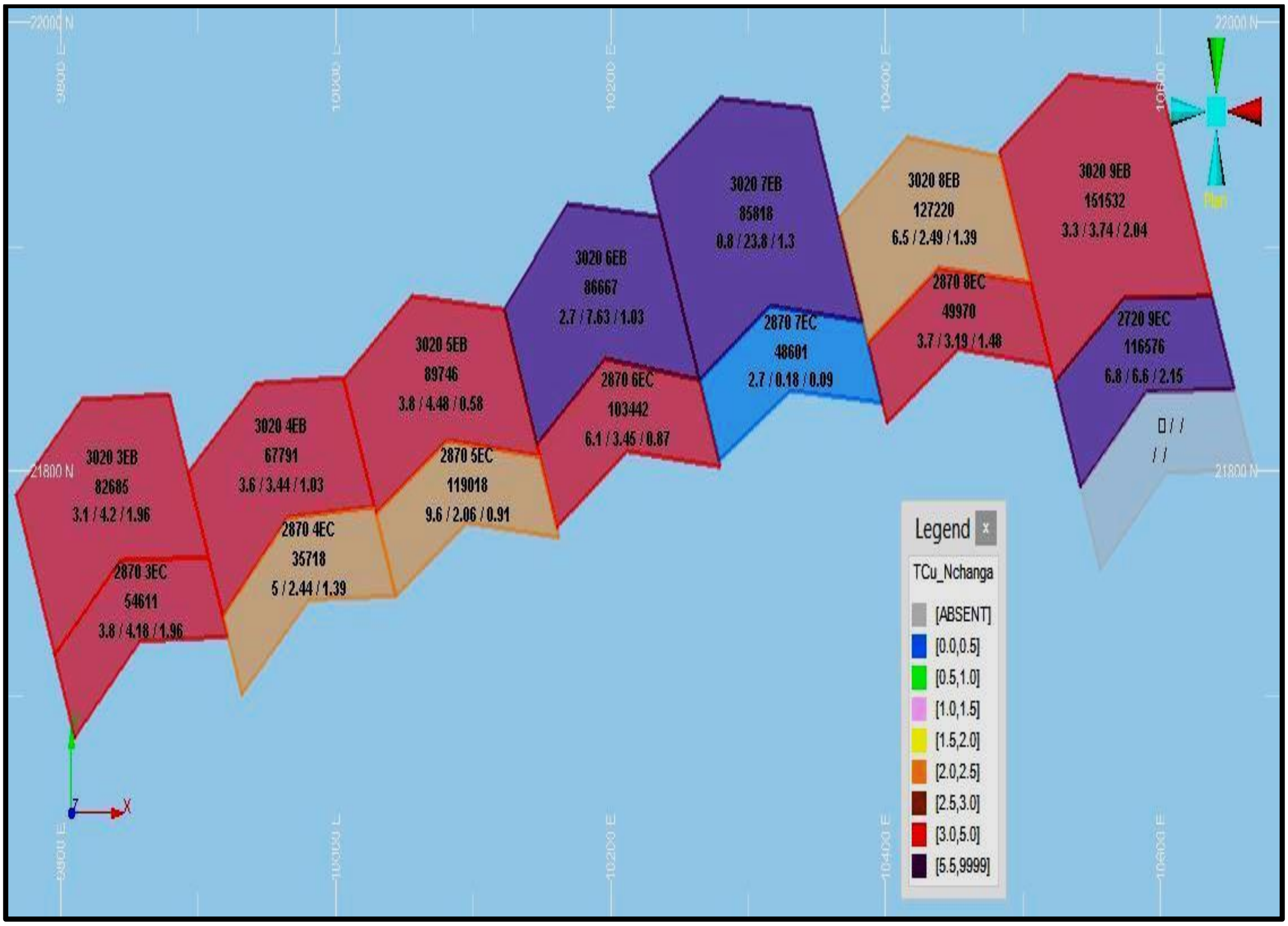

Figure 2.3: HSI complex blocks plan view (KCM, 2016)

In order to interpret Figure 2.3, consider block 3020/3EB. The block tonnage, ore thickness, grade (%TCu) and acid soluble Cu grade (%ASCu) for the block are as follows:

Block Tonnage = 82,685t;

Ore Thickness = 3.1;

Grade (%TCu) = 4.20%; and

Acid-soluble Cu grade = 1.96%.

2.2.3 Structural geology

The results from scan line mapping of geological structures at NUG show dominant discontinuity sets illustrated in Figure 2.4.

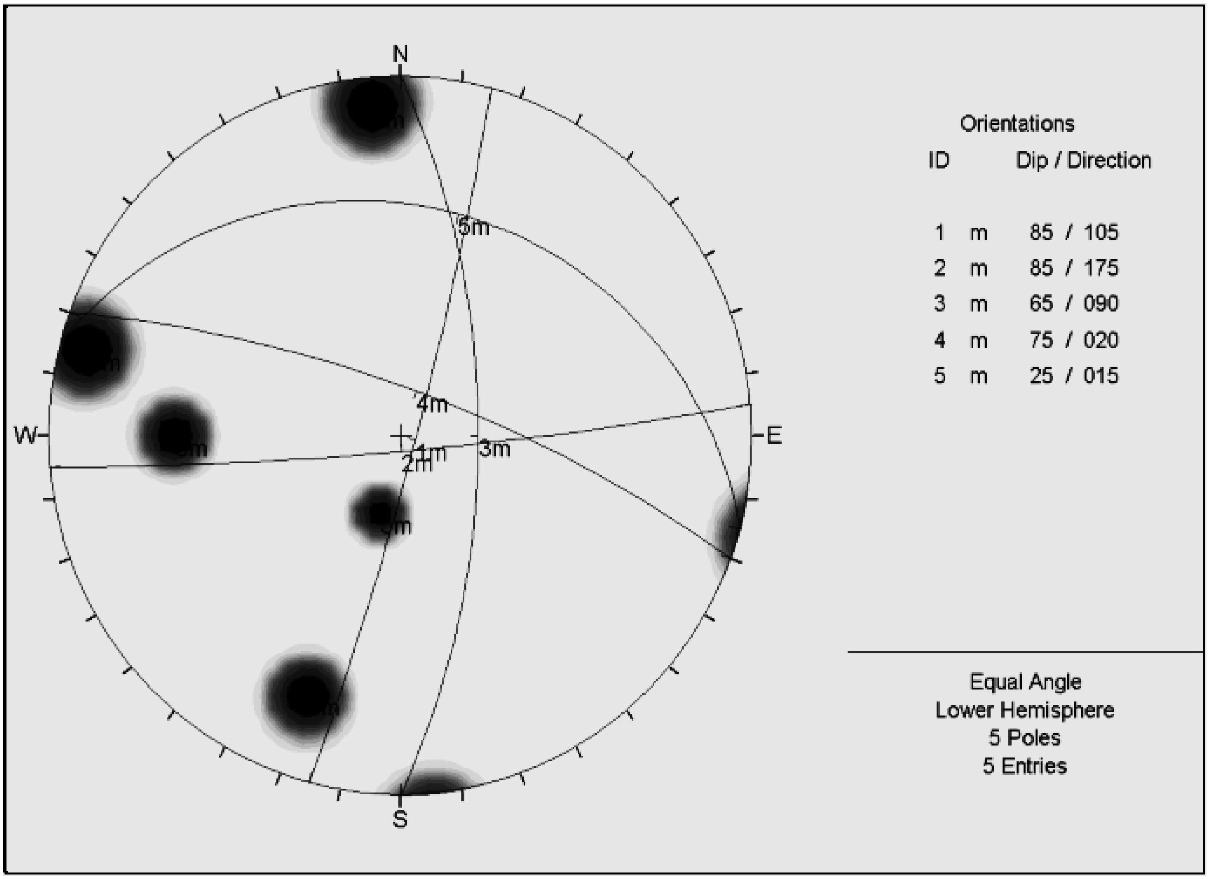

Figure 2.4: Stereographic plot of major discontinuity planes at NUG (Chishimba & Mundike, 2014)

However, no pre-mining stress testing has been done at NUG and KCM geotechnical staff consider overburden load as the major principal stress (Chishimba & Mundike, 2014). Therefore for the purpose of calculating the major principal stress, the traditional empirical relationship shown in Equation 2.1 was used.

$$\delta = \gamma \times z \qquad [2.1]$$

Where: δ = Overburden Stress (Pa);

γ = Unit weight of hanging wall rock (N/m^3); and

z = Depth from surface (m).

2.3 Mining method at Nchanga Underground mine

NUG mine employs a variant of block caving mining method to extract copper ore hosted in the LOB. The governing parameter which was used to select this mining method was geotechnical conditions of the ore zone, hanging and foot wall of LOB. Caveability of the ore body is initiated by low charge fan blasting from undercut excavations (i.e. trough drives) and ore flows by gravity into a system of herring-bone draw points along scraper drifts. Material is then mobilised by firstly scraping from the scraper drifts, subsequently flowing into the transfer drifts and then lastly it reaches the box raises. Figure 2.5 illustrates the NUG design. Further tramming is done by loading locomotives from the box raise chutes and transporting to the shaft hoist. Despite this, ore and waste mobilisation in the HSI complex is done by loading dump trucks from the box raise chutes, tramming the material to the 2600FT tipping points and thereafter locomotives transport the material to the hoist on the 2720FT main tramming level.

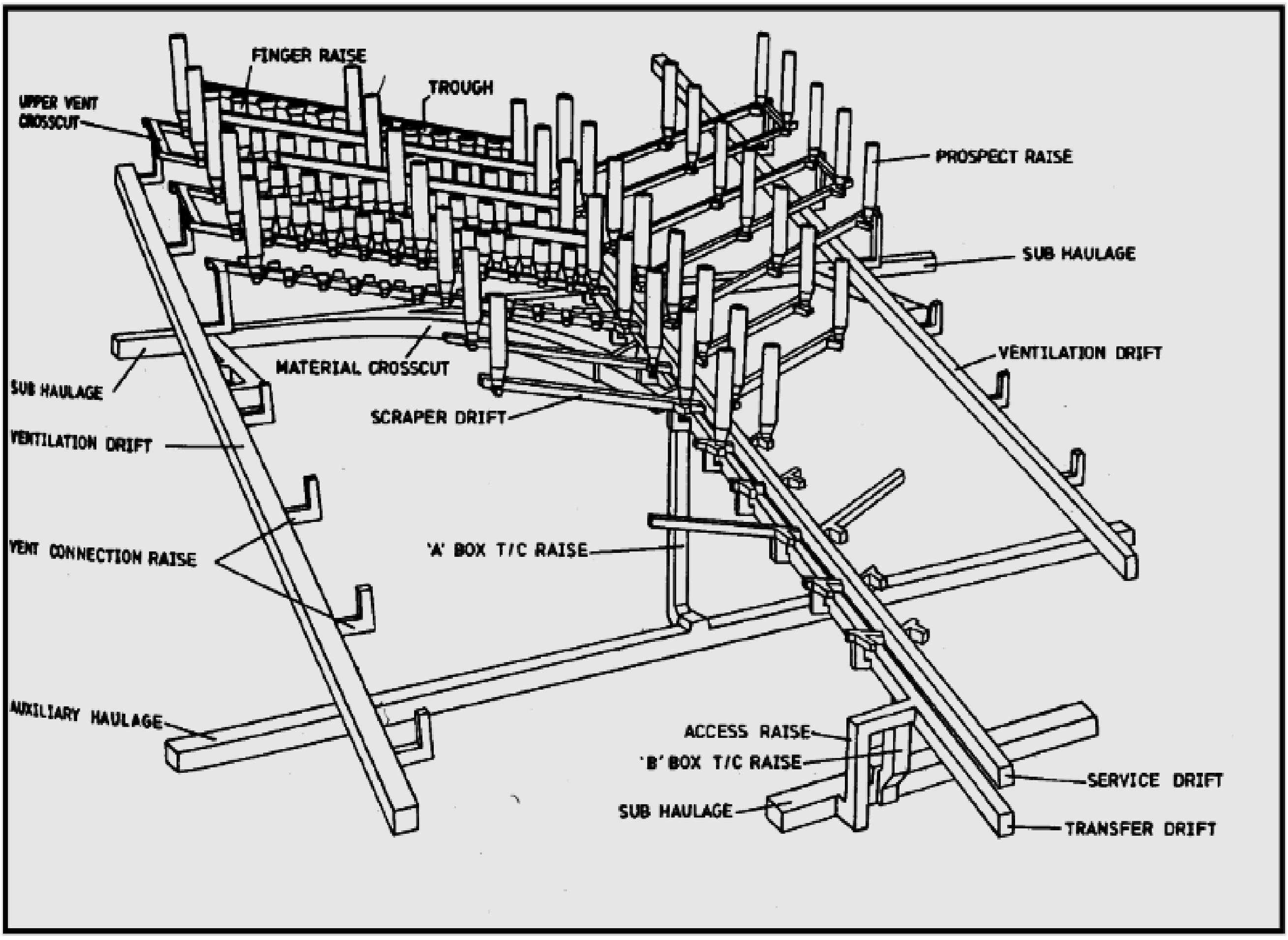

Figure 2.5: NUG mine layout (KCM NUG training manual, 2000)

2.3.1 Draw point geometry

The configuration of draw points at NUG is staggered, as shown in Appendix B-1, with a centre-to-centre spacing of 4.6m for the finger raises. The first and last finger raise crosscuts, on opposite sides of the scraper drift are excavated at 70^{o} from the scraper drift, also shown in Appendix B-1. More dimensions of the draw points are illustrated in Appendix B-2.

2.3.2 NUG cave parameters

A set of factors have been defined by NUG cave control officials for the purpose of minimising premature dilution and maintaining a uniform cave profile. The angle of the cave face must not exceed 60^{o} to the horizontal while the ore/waste interface should be maintained horizontally both in dip and strike. An allowance of ±16^{o} maximum deviation is permitted for horizontal ore-waste interface. Figure 2.6 provides a diagrammatic representation of these cave parameters at NUG.

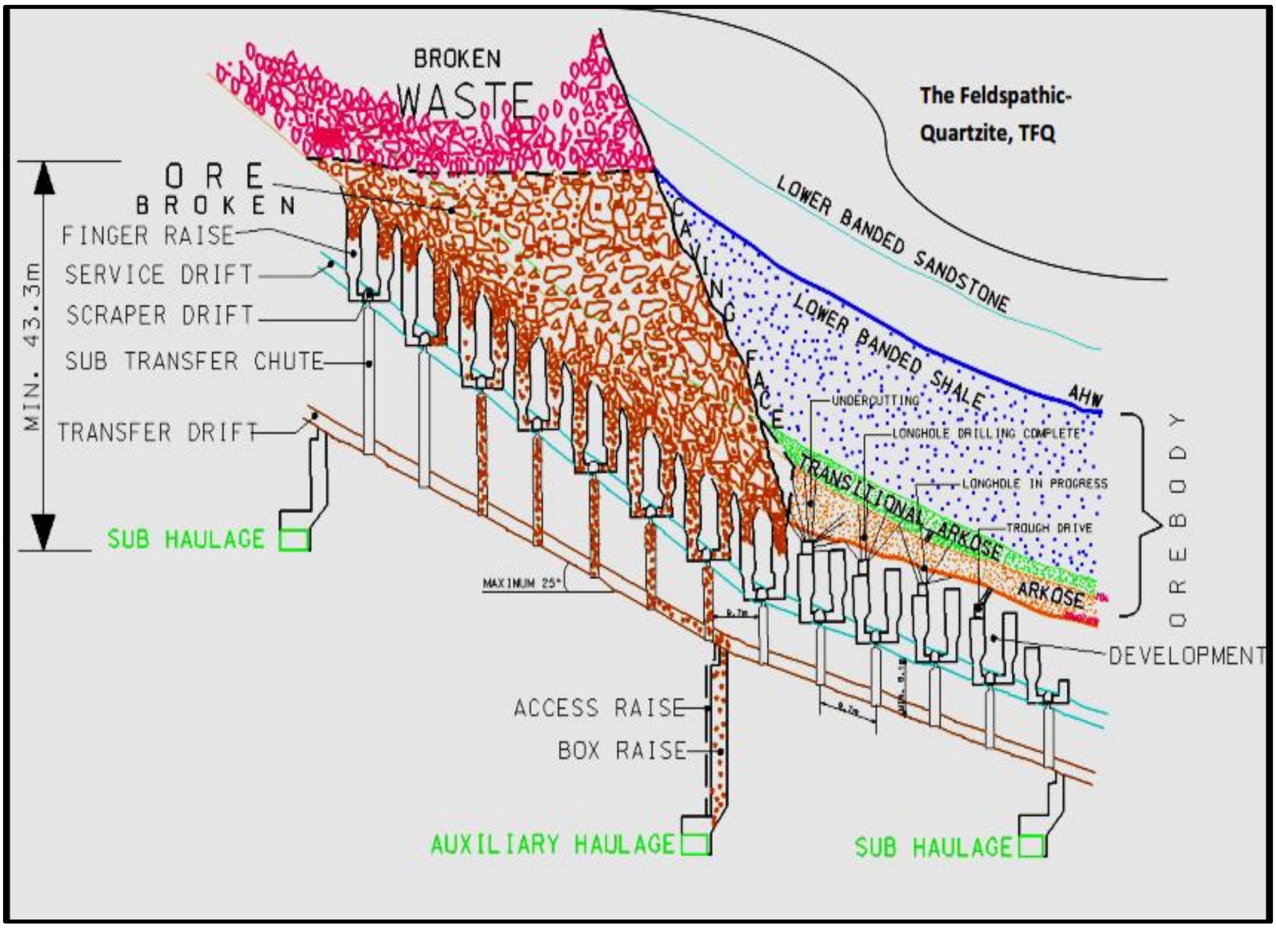

Figure 2.6: NUG cave profile (KCM NUG Training Manual, 2000)

NUG production drawing is constrained by the guidelines highlighted in Table 2.1.

Table 2.1: Technical guidelines for production drawing per drift (KCM Cave Control Manual, 2014)

Exploited % of Ore Reserve	Remark
Less than 15	Extraction is limited to 1000*t* per month
15 to 30	Extraction is limited to 1500*t* per month
30 to 101	Extraction is limited to 2000*t* per month
101 to 125	Extraction is limited to 1000*t* per month
More than 125	Drift is no longer considered in production planning and extraction is limited to 1000*t* per month.

In addition, maximum monthly production is the lower value of one of the following:

- 8% of the ore reserve; or
- 2000*t* per month per drift.

Following the exhausting of drifts and definition of new cave face profile, the Dynamic Ore Reserve System (DORS II) software is then used to extrapolate grades using the Exponential Grade Factor formula (KCM Cave Control Manual, 2014).

2.4 Caved mass flow

2.4.1 Types of flow modes

In block caving, caved material is collected at the draw point. As mucking proceeds, a disturbance zone in the rock mass can be observed above the draw point, traditionally called the ellipsoid of draw (Kvapil, 1998) which is now commonly referred to as an isolated draw zone (Laubscher, 1994), (Halim, 2004), (Munro, 2013). Draw zone diameter is a key parameter of dilution behaviour in block caving (Rubio, 2002). Several authors including Kvapil (1965) and Laubscher (1994) developed empirical charts to compute draw zone diameter mainly based on fragmentation of rock, fragment shape, moisture content and size of opening.

Flow of caved mass is mainly classified as either isolated draw, interactive draw or isolated-interactive draw. Susaeta (2004) used results from a sandbox physical model to distinguish between these three types of draw by comparing the rate of flow through a draw point (Vt_a) to rate of displacement of material overlying the major apex pillar (Vt_i). Figure 2.7 illustrates the diagrammatic relationship between Vt_a and Vt_i, in a draw zone, where the ratio of Vt_a / Vt_i is called the degree of interaction.

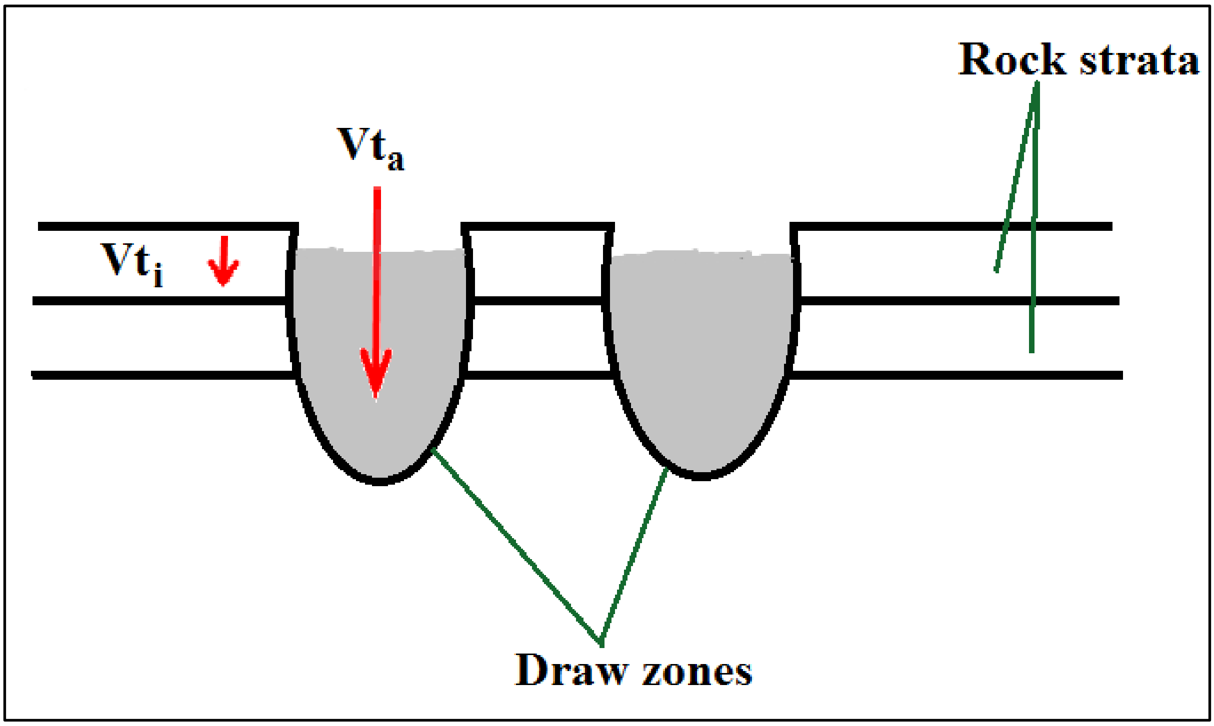

Figure 2.7: The relationship between Vt_a and Vt_i in the draw zone (Susaeta, 2004)

The following deductions were made by Susaeta (2004):

i. $Vt_a > Vt_i$ induces isolated-interactive flow as shown in Figure 2.8 (a),

ii. $Vt_a = Vt_i$ induces interactive flow as presented in Figure 2.8 (b), and

iii. $Vt_a > 0$ and $Vt_i = 0$ induces isolated flow as shown in Figure 2.8 (c).

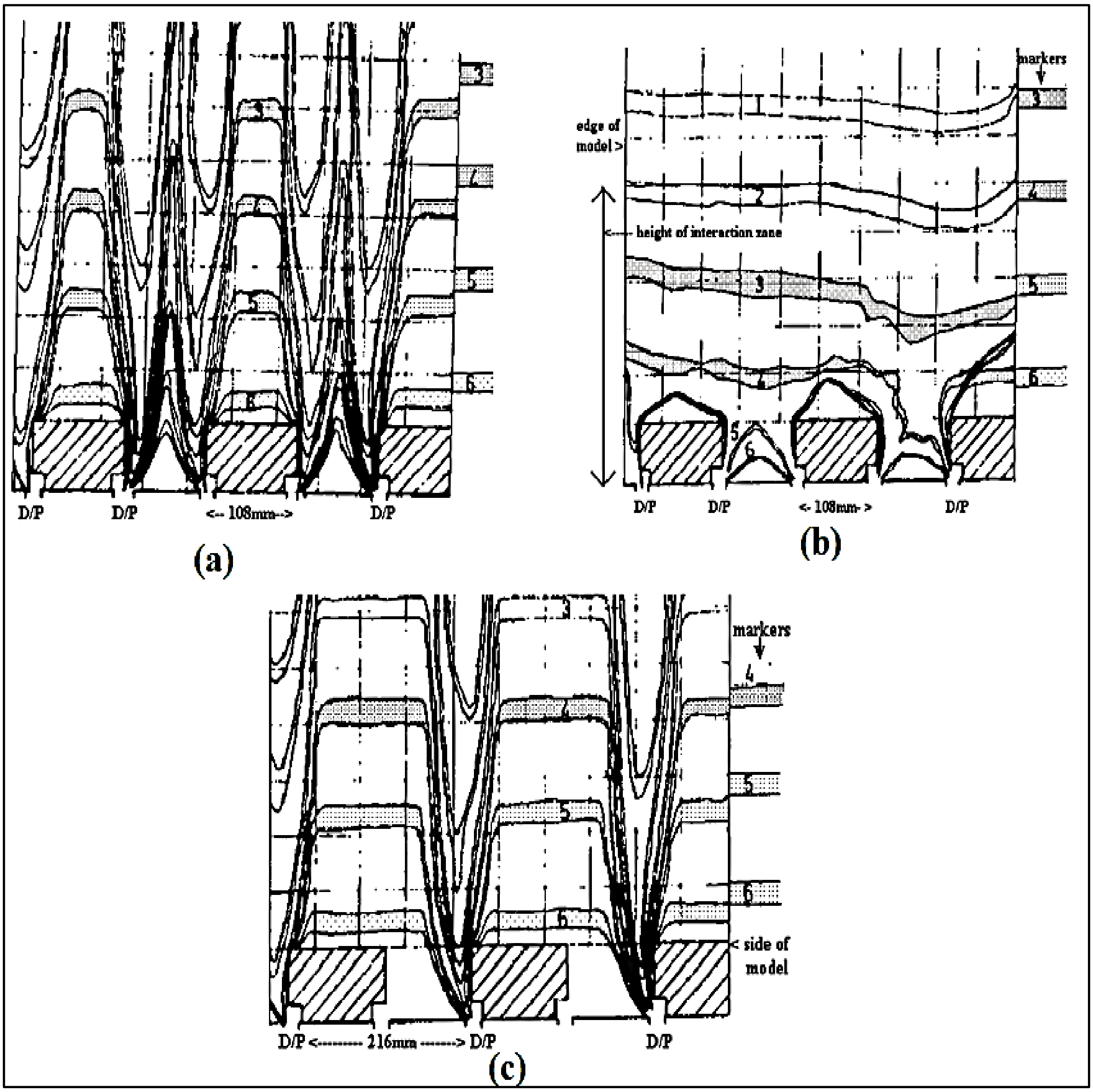

Figure 2.8: Modes of gravity flow (Marano, 1980)

Block caving at NUG favours interactive draw because even horizontal displacement between draw zones is generated so that there are no zones between draw points that may eventually provide a point load on the scraper drifts, damaging them and ultimately resulting in their collapse. In addition, interaction between draw points acts as a barrier to waste material, thus, retarding dilution entry into the draw points.

In order to achieve interactive draw, Kvapil (1965) recommends draw point spacing equivalent to draw zone diameter, while Laubscher (1994) suggests 1.5 times the draw zone diameter. A draw point spacing of 1.6 to 1.7 times the draw zone diameter is recommended for competent rock environments (Susaeta, 2004).

2.4.2 Parameters which influence dilution

Castro and Parades (2014) conducted a review of factors which affect dilution in caving operations. Table 2.2 describes a concise presentation of these parameters.

Table 2.2: Parameters affecting dilution

PARAMETER	EFFECT ON DILUTION	AUTHOR
Uncaved ore/waste interface inclination	To reduce dilution, the interface inclination must be maintained between 45^{o} to 50^{o} by draw control.	Julin (1992)
Ore volume to ore/waste interface surface area	The higher the ratio of ore volume to the ore/waste interface area, the lower the amount of dilution.	Laubscher (2000)
Fragmentation range of ore and waste	Finely fragmented waste and coarse ore translates to pre-mature and extensive dilution, while coarse waste and fine ore means a low overall dilution percentage.	Laubscher (2000)
Height of the interaction zone	Good draw zone interaction and parallel flow will represent the best conditions. Poor draw zone interaction and angled draw zones result in high dilution.	Laubscher (2000)
Variations in waste and ore densities	High density waste and low density ore lead to high dilution. The converse is also true.	Laubscher (2000)
Block or panel caving strategy	A block cave strategy will lead to more horizontal dilution mixing than panel caving	Laubscher (2000)
Uniformity of draw	Low uniformity of tonnages drawn from neighbouring draw points will result in low interaction and early dilution entry.	Julin (1992) and Susaeta (2004)

2.4.3 Dilution characteristics in draw zones

Leonardi et al. (2011) defined only three key mechanisms of dilution in block caving as shown in Figure 2.9:

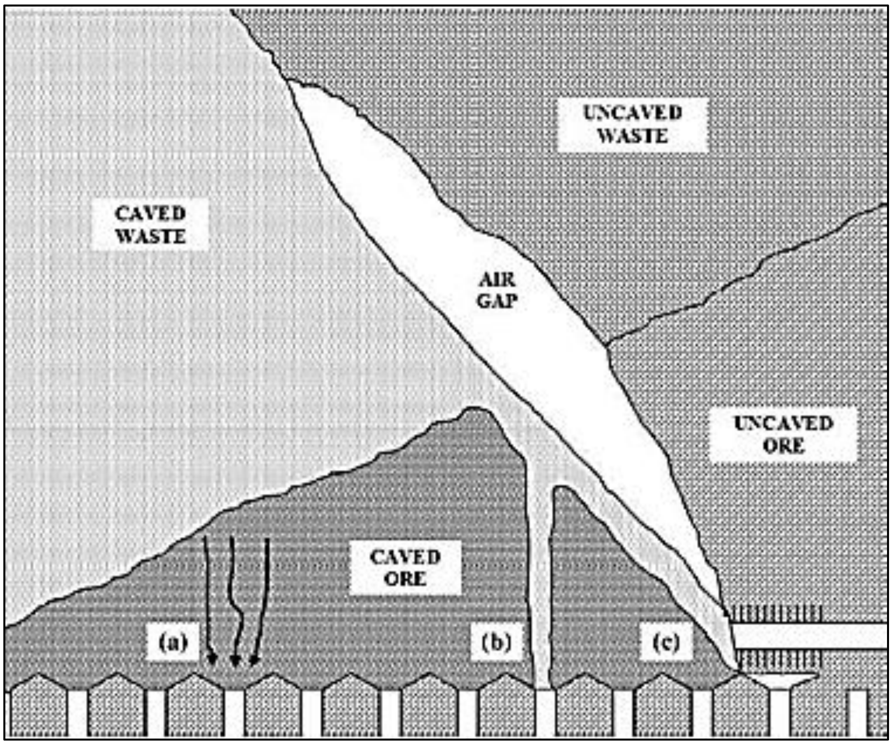

Figure 2.9: The primary mechanisms of dilution (a) fines migration, (b) isolated draw and (c) rilling (Leonardi et al., 2011)

However, Table 2.3 further expounds other essential dilution mechanisms in block caving extraction.

Table 2.3: Dilution mechanisms (Diering, 2007)

MECHANISM	DIRECTION OF INFLUENCE	COMMENT
Vertical Mixing	Vertical	Different velocities for broken material
Horizontal Mixing	Horizontal	Failure of near pillars and draw cones
Toppling	Horizontal	Toppling failure at the cave surface
Rilling	Horizontal	Failure at fragmented/solid rock interface
Regional Lateral Movement	Horizontal	Mostly at distinct interfaces like the sides of kimberlitic pipes
Cone erosion	Vertical	The increase of draw cone radius
Stagnation	Vertical	The decrease of draw cone radius due to ore caking as a result of presence of moisture
Fines migration	Vertical	Rapid downward movement of fine material within a coarser matrix
Piping	Vertical	Small direct path for fines migration
Mud rush	Multi-directional	Fluid flow within a coarse matrix
Open pit failures	Vertical	Abrupt failure of overlying strata
Variable cave back with time	Vertical	Incremental changes to cave back

Figure 2.10 illustrates vertical and horizontal mixing, otherwise known as gravity and lateral dilution respectively.

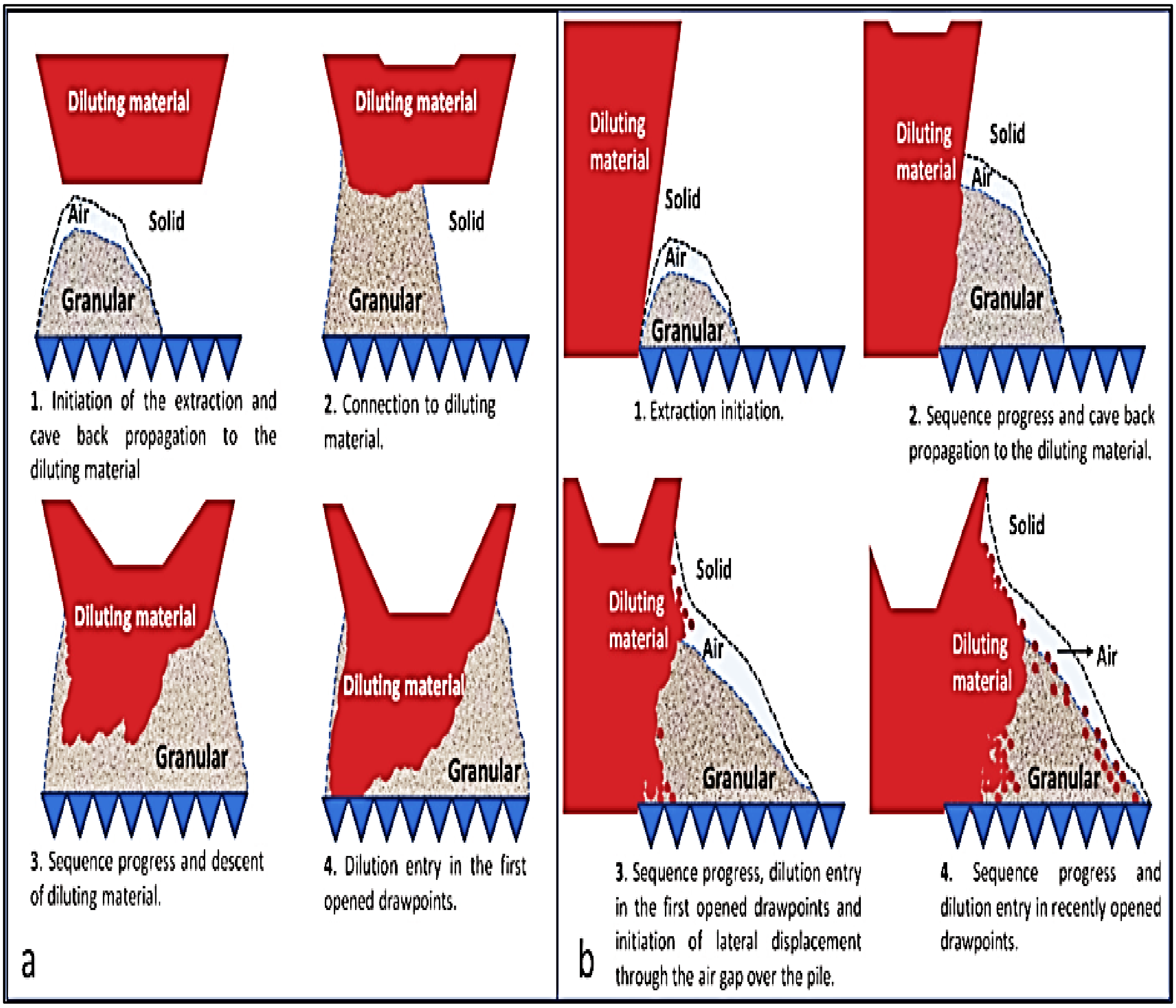

Figure 2.10: Schematic sections of draw points (a) Vertical mixing and (b) Horizontal mixing (Castro and Parades, 2014)

2.4.4 Mixing process within draw zones

Table 2.3 highlighted various modes of dilution within draw zones in block caving mines, however, simulation of mixing processes within the caved area must be performed. This is so because waste material can be transformed to ore if fines ingress high grade ore. The converse is also true because the same ore material can be sterilised if mixed with waste material. Thus, a mixing algorithm is critical when computing economical reserves in block caving mining operations.

Laubscher (1994) proposed a number of guidelines which can be utilised to simulate the mixing process so that better grades can be obtained as the scheduled mining perpetuates. Laubscher inferred that material flows uniformly in the draw zone until it reaches the zone of interaction where the descending flow is characterised as chaotic to the point that material might even discharge in neighbouring draw points. Therefore, height of the interaction zone (HIZ) is the main parameter to simulate mixing process. Equation 2.2 presents the relationship between fragmentation of the rock mass, draw point spacing and draw control practices (i.e. draw control factor).

$$DEP = \frac{[(H_C \times \beta) - HIZ]}{(H_C \times \beta)} \times DCF \times 100\% \qquad [2.2]$$

Where: DEP = Dilution Entry Point is the percentage drawn from the draw zone after which first dilution is observed;

H_C = Height of the draw zone;

β = Swell factor (ratio between in-situ and caved rock densities); and

DCF = Draw control factor which measures how even draw is being done.

Conventionally, the more even draw points are drawn, the higher the DEP. A value close to unity for DCF indicates even draw, while a value significantly different from unity signifies isolated draw (Rubio, 2002). As a result, a DCF value of 1 was used in this study since the objective is to achieve an even and interactive draw which maximises DEP.

The concept of DCF was first proposed by Heslop and Laubscher (1981). Equation 2.3 has been customarily used to calculate DCF.

$$DCF = \frac{\left[\frac{\sum_{k=1}^{K}\left(d_i - d_k{}^i\right)^2}{K}\right]^{0.5}}{\frac{1}{K+1}\sum_{k=1}^{K+1} d_k} \qquad [2.3]$$

Where: d_i is tonnage drawn from draw point *i* in a period of time;

$d_k{}^i$ is tonnage drawn from draw point *k*, a neighbour of draw point *i* in the same period of time;

k is the lower bound for the number of neighbours of draw point *i*;

K is the total number of neighbours of draw point *i*; and

d_k is the tonnage drawn from draw point *k*.

Another formula has been consistently used and, unlike Equation 2.3 which computes DCF on a draw point by draw point basis, it considers the overall performance of the draw points. The formula is presented as Equation 2.4:

$$DCF = \frac{Max\{d_k\}}{Min\{d_k\}} \qquad [2.4]$$

Where: $1 \leq k \leq K + 1$ including the draw point *i*.

2.4.5 Economic boundary of production drawing

Definition of the economically mineable part of an ore body is a critical facet in production planning. This is a complex process in block caving methods because searching for the most suitable combination of production level and height of each draw zone will probably involve millions of permutations (Rubio, 2002). Nevertheless, the process of reviewing economic reserves of the HSI complex was done by using 1.0% (TCu) marginal cut-off grade and current NUG production level-to-level vertical displacement as the height of the draw zone.

DEP also aided in ascertaining the minimum expected tonnage to be drawn before dilution enters the draw zone and starts discharging into the scraper drifts.

Additionally, Rubio (2002) conceded that traditional practice of calculating undiscounted earnings for each draw zone, before dilution enters, encompasses a revenue factor (i.e. metallurgical recovery multiplied by the net smelter returns) and a cost factor which includes expenditures involved in mining and processing. Nonetheless, capital expenditure throughout the ore circuit and associated interests accrued were also incorporated in reviewing the HSI complex reserves.

2.4.6 Sequence of undercutting

The sequence of undercutting characterises where to begin caving on the mine layout and how to continue caving. The dip and geometry of the cave front are essential to defining the sequence, at the same time, commencing caving where the weak rock is located is also recommended (Bartlett, 1992). This allows early capital recoupment because the required hydraulic radius can be reached earlier in the life of mine.

On the other hand, undercutting can start where high grade ore is hosted leading to early payback periods and higher net present values (NPV's). In spite of this, excessive secondary blasting might be needed so as to quickly achieve required hydraulic radius and fragmentation for production. Therefore, the latter approach of extracting higher grades early is the best undercut sequence philosophy because the main goal is to realise a strong economic model.

Standard practice is to maintain a cave face that is always perpendicular to the main geological structures, so that fragmentation is improved and production is maximised. In addition, implementing a concave cave front than a flat one is also recommended because it mitigates uncontrolled caving processes and air blasts since an arched cave back is more stable than a flat one (Rubio, 2002).

2.4.7 Buffer mineral reserves

Musingwini et al. (2003) defined buffer mineral reserves (BMR) as primary/proved reserves which a mine can continue to extract at a specified production rate if all development operations have been stopped. Therefore BMR is a function of the rate of development. This rate defines the minimum number of draw points that have to be developed in order to achieve the required production targets.

Traditional practice in mineral reserves management is to maintain the largest possible BMR so that mining can continue as long as possible if development has been ceased. Despite this, in some cases adopting the “largest buffer reserves” policy is not justified due to high costs of excavating developments. As a result, in most cases the mine’s production capacity limits the development rate. Nonetheless, poor ground conditions at NUG mean that some development ends have to be re-mined because they would have partially or completely collapsed between the time they are excavated and the time when they are utilised. In order to mitigate the collapse of these ends, support density has been increased so as to extend the excavation duty life. Resultantly, support costs have escalated with KCM incurring $173,231.46.

Musingwini et al. (2003) computed the BMR by utilising the economic order quantity of providing development ends when they are needed through correlation and regression analysis of statistics of a database of extracted mineral reserves at Shabanie mine, Zimbabwe, over an 11 year period between 1990 and 2000. Alternatively, BMR can be governed by stand-up time of development headings such that draw points are provided just-in-time for production before their stand-time elapses. Empirical calculation of stand-up time for the developments can be done using a rock mass classification system by Lauffer (1958) which was later adapted by Bieniawski (1989).

Thus, the approach of incorporating stand-up time to compute buffer mineral reserves for the HSI complex was adopted since a sufficient data base of NUG reserve statistics was not available to compare with the method by Musingwini et al. (2003).

2.4.7.1 Derivation of the BMR formula

The block recovery factor has a bearing on the extracted tonnage of BMR as illustrated in Equations 2.5.

$$BMR_e = \gamma \times [B_1 + B_2 + B_3 + \cdots + B_n] \quad [2.5]$$

$$= \gamma \times \sum_{x=1}^{n} B_x$$

Where: BMR_e is the extracted BMR;

γ is the block recovery factor (i.e. ratio of extracted tonnage to in-situ tonnage per given block);

B_x is in-situ tonnage for block "x"; and

n is number of blocks.

However, the summation of B_x yields the in-situ tonnage of BMR. Therefore Equation 2.5 becomes:

$$BMR_e = \gamma \times BMR_I \qquad [2.6]$$

Where: BMR_I is the in-situ tonnage of BMR

If Equation 2.6 is true, then Equation 2.7 is also true.

$$OBMR_e = \gamma \times OBMR_I \qquad [2.7]$$

Where: $OBMR_e$ is the optimal extracted BMR; and

$OBMR_I$ is the optimal in-situ BMR.

Considering the poor ground conditions in the HSI complex, the optimal extracted BMR is a function of the production rate and the excavation stand-up time as shown in Equation 2.8.

$$OBMR_e = P \times T_s \qquad [2.8]$$

Where: P is the production rate (tonnes per year); and

T_s is the excavation stand-up time (years).

Substituting Equation 2.7 into 2.8, therefore the optimal in-situ BMR can be calculated using Equation 2.9.

$$OBMR_I = \frac{P \times T_S}{\gamma} \qquad [2.9]$$

2.4.7.2 Conservative parameters for BMR of the HSI complex

Parameters which yield worst case scenario results for the BMR (i.e. the lowest value of BMR) were used in this study. The parameters are as follows:

1) A block recovery factor of 149% since this is was the highest recovery factor achieved after extracting LOB blocks in the upper levels.
2) The stand-up time of the excavation with the largest roof span was used in calculating the optimal BMR since roof span and stand-up time are inversely proportional.

2.4.7.3 Excavation stand-up time

The first technique which was used to calculate stand-up time for an unsupported roof span was proposed by Lauffer (1958). The stand-up time is the period of time over which a tunnel can stand after excavation. The original method is no longer used since it has been modified by a number of Austrian engineers particularly by Pacher et al. (1974). This technique now forms part of the general system known as New Austrian Tunneling method. The method relates rock mass quality and roof span dimensions as illustrated by Figure 2.11. Although Hoek (2007) conceded that it is prudent not to make the assumption that stability of rock mass surrounding is not time-dependent, it is beneficial to incorporate shortest excavation stand-up time in caving operations to determine the optimal BMR because of the friable nature of the inherent rock mass.

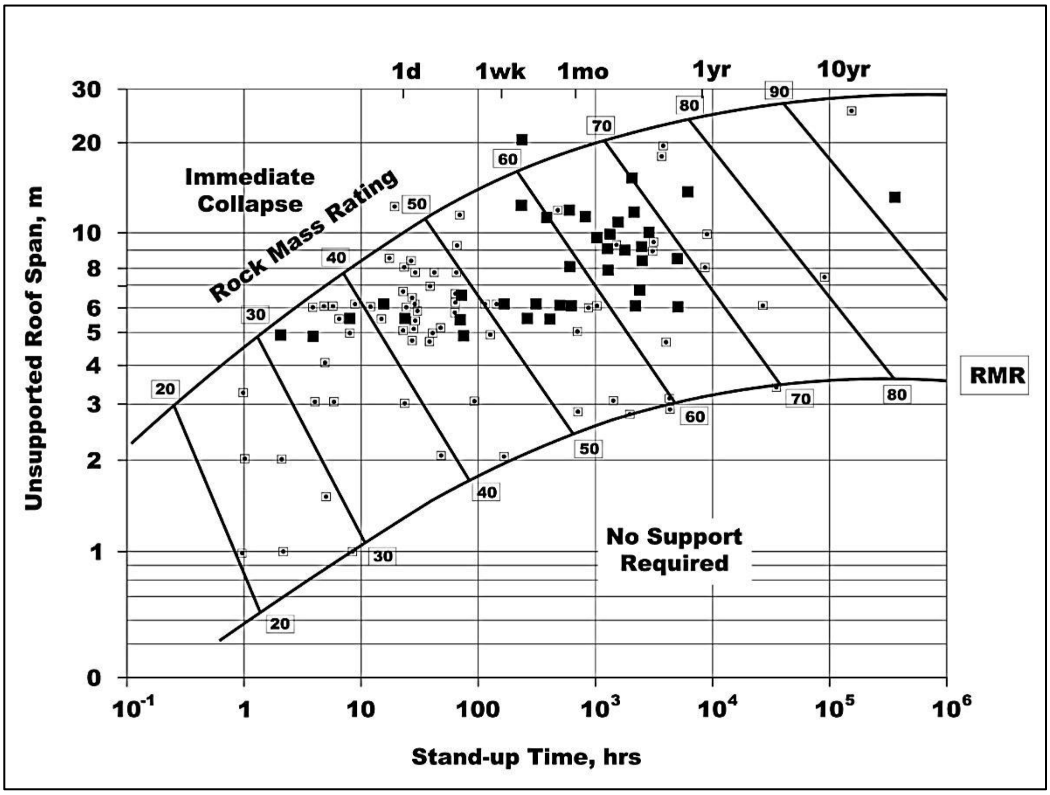

Figure 2.11: Graphical relationship between RMR, roof span and stand-up time after Lauffer (1958), Pacher et al (1974) and Bieniawski (1989)

2.4.8 Drawing rate

The following are the main parameters which define rate of draw:

- ***Equipment.***

  A larger scraper winch bucket allows higher draw rates.

- ***Fragmentation***

  Finer fragment sizes allows for higher draw rates since there is secondary fragmentation required.

- ***Physical properties of the caved rock***

  The presence of water reduces draw rates because draw cone radius is reduced by ore caking. High values of adhesion, angles of internal friction and repose reduce the rate of draw.

- ***Stresses***

  Rocks in high stress environments are likely to burst if exposed to high draw rates. Seismicity significantly affects draw rates by increasing the uncontrolled flow of caved mass.

- ***Mine design***

  The draw cone and discharge drift dimensions have a bearing on the rate of draw. Additionally, the draw height of caved mass has an effect on the draw rate.

Table 2.1 in Section 2.3.2 of this Chapter presents the rate of draw guidelines which are recommended for NUG operations.

2.5 Draw point spacing

Castro et al. (2012) stated that design and operation of most caving operations, including draw point spacing optimisation, is based on the empirical guide by Laubscher (1994 & 2000). 3D simulations can be used to plan the mining scheme of a caving operation with acceptable confidence, even though, the 3D models remain unvalidated due to lack of data to authenticate them (Halim, 2004). However, past research has shown that physical models, with a minimum scale factor of 1:30 to the actual mine parameters, yields findings which can be used reliably for full scale mine modelling. Nevertheless, physical models remain an expensive and time-consuming approach to optimise caving operations, thus, the empirical design criteria was implemented to optimise draw point spacing for NUG.

In literature there have been numerous attempts to establish the optimum draw point spacing for block caving mines. Julin (1992) proposed a guideline based on block caving experiences. He suggested that spacing area must be in the order of $26m^2$ to $236m^2$ as fragmentation increases from fine to coarse. Hustrulid (2000) also used block caving experiences to further aggrandise Julin’s approach by establishing that the radius of the draw zone is 8 to 12 times the mean fragment size. This radius would also translated to draw point spacing using the relationship of 1.7 times the radius of the draw zone. Laubscher (1994) recommended draw point spacing based on RMR of the rock and height of interacting zone as shown by the chart in Figure 2.12. Laubscher (2000) later acknowledged that the following significantly affect draw point spacing decision making:

i) The isolated draw zone diameter;

ii) Fragmentation of the caved material;

iii) The angle of internal friction of the material;

iv) The size of scrapers, and LHD's to be used;

v) The size of draw point loading area;

vi) The number of draw points required for production rate;

vii) The required recovery and dilution;

viii) The possibility of brow wear and failure;

ix) The planned draw strategy; and

x) The possibility of poor draw control.

Another design guide was made for production level layouts based on the rock type, the layout and draw strategy required to minimise dilution (Susaeta et al., 2008). Meanwhile, Kvapil (2004) generated a graphical representation to determine the diameter of isolated draw zones for three types of rock.

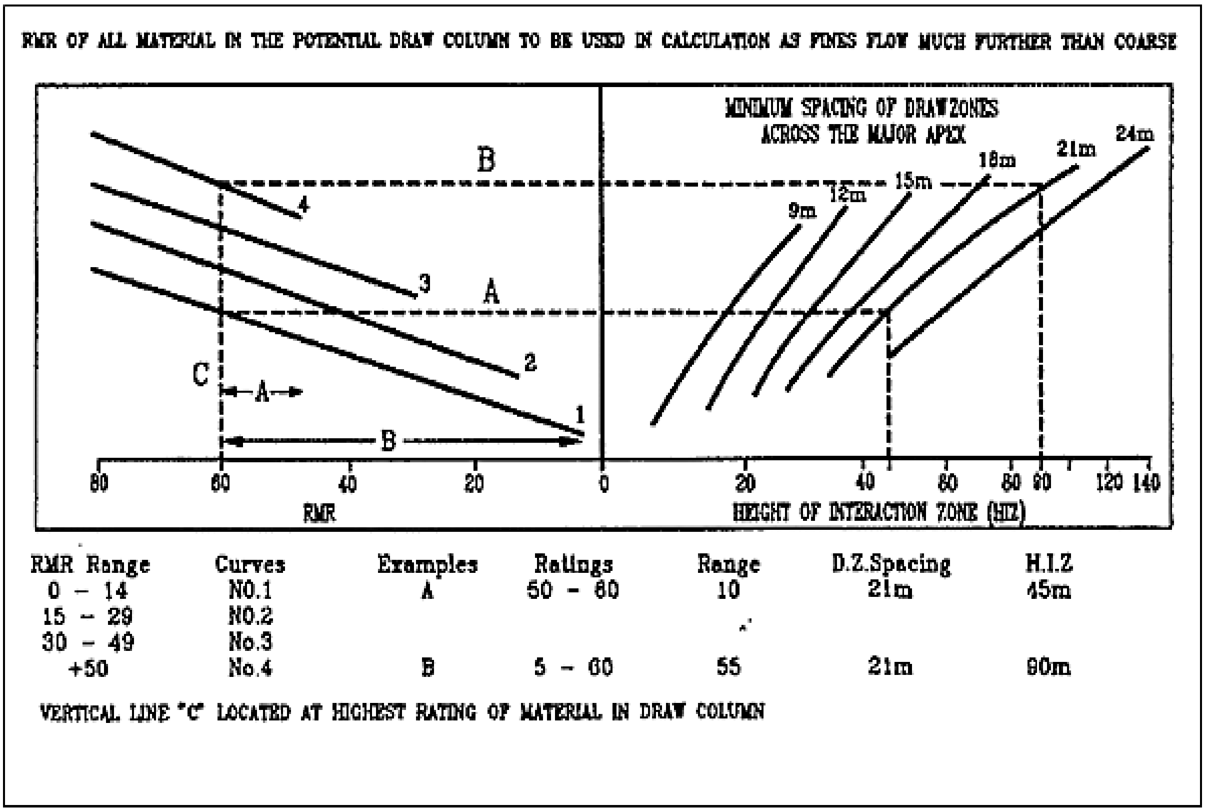

Figure 2.12: Graphical representation of HIZ, RMR and Draw point spacing across major apex (Laubscher, 1994 & 2000)

Castro et al. (2012) established Equations 2.10 and 2.11 which can be used to calculate draw point spacing based on the concept of interaction of adjacent draw zones.

$$HIZ = \left[\frac{d_p - w_p}{2}\right] \tan(\alpha) \qquad [2.10]$$

$$\alpha = \frac{\phi}{2} + 45 \qquad [2.11]$$

Where: d_p is distance between adjacent draw points;

w_p is the face width of the undercut level;

α is the angle of flow of the caved mass; and

ϕ is the angle of internal friction of the caved mass.

2.6 Rock Mass Classification Systems

There are numerous engineering rock mass characterisation systems which are used in the mining industry (Hoek, 2007). Each system puts emphasis on various parameters and it is advised to use at least two techniques at any mine site during its greenfield stages.

2.6.1 Rock Quality Designation Index (RQD)

Quality of the rock mass can be eastimated from drill core logs (Deere et al., 1967). RQD is the percentage of intact core pieces longer than 100*mm* in the total length. The drilled core must be of NW size (i.e. 54.7*mm*). The measuring technique for RQD is shown in Figure 2.13.

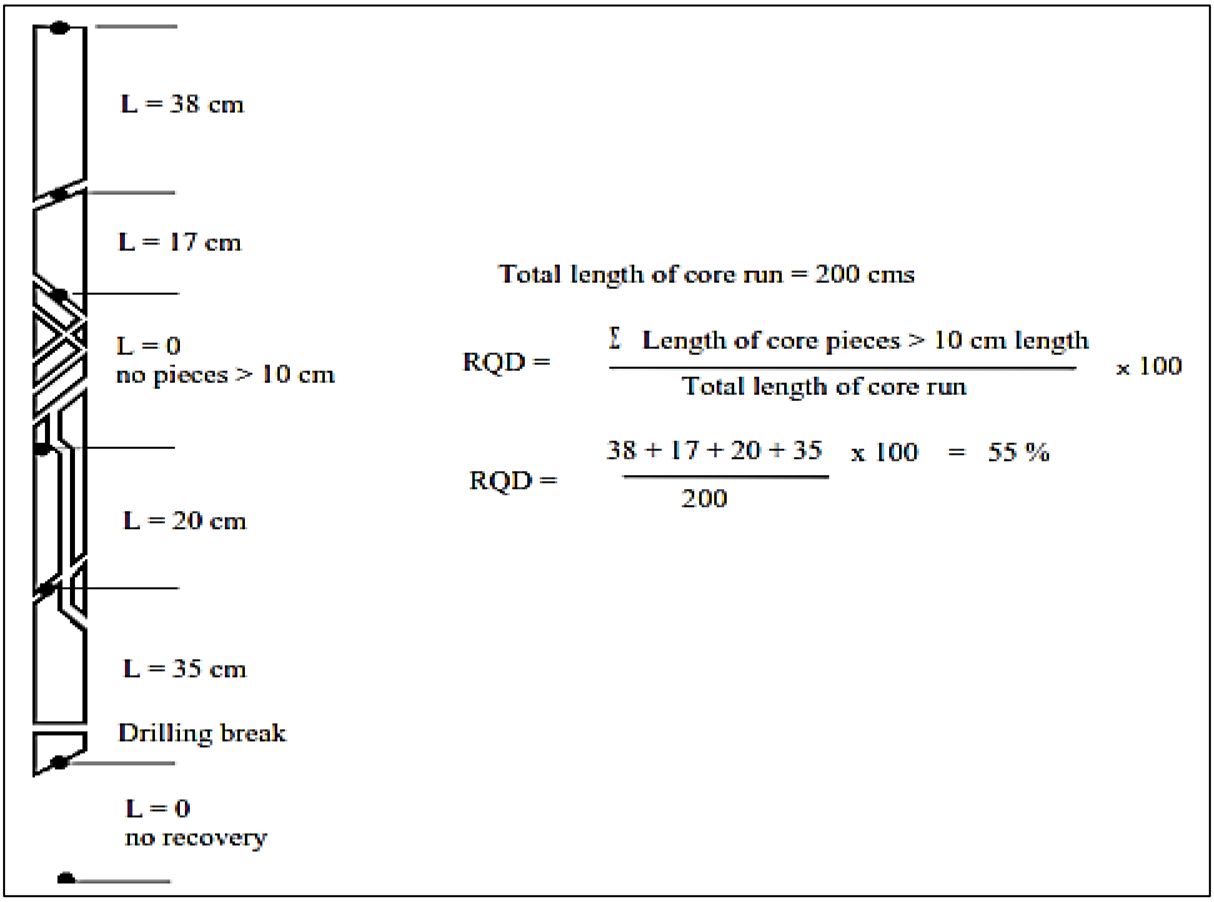

Figure 2.13: Calculation of RQD (Deere, 1989)

RQD can also be estimated for clay free rock from number of discontinuities per unit volume. This empirical relationship shown in Equation 2.12 was proposed by Palmstrom (1982) for use when there are no drill cores available and discontinuities are visible from rock surface exposures in adits or any other excavation.

$$RQD = 115 - 3.3J_V \qquad [2.12]$$

Where: J_V is the sum of number of joints per unit length for all joint sets known.

2.6.2 Rock Structure Rating (RSR)

RSR was introduced by Wickham et al. (1972), as a quantitative method for selecting appropriate support and giving a description of rock mass quality. The biggest limitation of this technique is that most of the case histories reviewed were for relatively small tunnels supported by steel sets. Equation 2.13 presents the formula used to compute RSR.

$$RSR = A + B + C \qquad [2.13]$$

Where:

- Parameter A is general evaluation of geological structure based on geological structures, rock hardness and rock type origin.
- Parameter B is the effect of patterns and orientation of discontinuities with respect to direction of the excavation drive.
- Parameter C is the effect of groundwater inflow and joint conditions.

2.6.3 Geomechanics classification

This system was first introduced by Bieniawski (1976) and it has been refined by numerous authors as more case histories have been reviewed. It is commonly known as the Rock Mass Rating (RMR) system. Based on the 1989 adaptation of the RMR system, the following six parameters are used to classify rock masses (Bieniawski, 1989):

a) RQD;
b) Spacing of joints;
c) Joint conditions;
d) Ground water conditions;
e) Joint orientations; and
f) Uniaxial compressive strength of rock material.

Tables 2.4 to 2.9 present the RMR system showing how to determine ratings for each of the six parameters listed above.

Table 2.4: Classification of RMR parameters and their ratings (Bieniawski, 1989)

<table>
<tr><th colspan="2">PARAMETER</th><th colspan="7">RANGE OF VALUES</th></tr>
<tr><td rowspan="2">STRENGTH OF INTACT ROCK MATERIAL</td><td>POINT-LOAD STRENGTH INDEX (MPa)</td><td>>10</td><td>4-10</td><td>2-4</td><td>1-2</td><td colspan="3">For this low range – UCS test is preferred</td></tr>
<tr><td>UNIAXIAL COMPRESSIVE STRENGTH (MPa)</td><td>>250</td><td>100-250</td><td>50-100</td><td>25-50</td><td>5-25</td><td>1-5</td><td><1</td></tr>
<tr><td colspan="2">RATING</td><td>15</td><td>12</td><td>7</td><td>4</td><td>2</td><td>1</td><td>0</td></tr>
<tr><td colspan="2">DRILL CORE QUALITY RQD (%)</td><td>90-100</td><td>75-90</td><td>50-75</td><td>25-50</td><td colspan="3"><25</td></tr>
<tr><td colspan="2">RATING</td><td>20</td><td>17</td><td>13</td><td>8</td><td colspan="3">3</td></tr>
<tr><td colspan="2">JOINT SPACING (m)</td><td>>2</td><td>0.6-2</td><td>0.2-0.6</td><td>0.06-0.2</td><td colspan="3"><0.06</td></tr>
<tr><td colspan="2">RATING</td><td>20</td><td>15</td><td>10</td><td>8</td><td colspan="3">5</td></tr>
<tr><td colspan="2">JOINT CONDITIONS (See Table 2.8)</td><td>Very rough surfaces, Not continuous, No separation, Unweathered wall rock</td><td>Slightly rough surfaces, Separation <1mm, Slightly weathered walls</td><td>Slightly rough surfaces, Separation <1mm, Highly weathered walls</td><td>Slicken-sided surfaces or Gouge <5mm thick or Separation 1to 5mm Continuous</td><td colspan="3">Soft gouge >5mm thick or Separation > 5mm Continuous</td></tr>
<tr><td colspan="2">RATING</td><td>30</td><td>15</td><td>10</td><td>8</td><td colspan="3">5</td></tr>
<tr><td rowspan="3">GROUND WATER CONDITIONS</td><td>Inflow per 10m tunnel length (l/minute)</td><td>None</td><td><10</td><td>10-25</td><td>25-125</td><td colspan="3">>125</td></tr>
<tr><td>(Joint water pressure)/ (Major Principal Stress)</td><td>0</td><td><0.1</td><td>0.1-0.2</td><td>0.2-0.5</td><td colspan="3">>0.5</td></tr>
<tr><td>General conditions</td><td>Completely dry</td><td>Damp</td><td>Wet</td><td>Dripping</td><td colspan="3">Flowing</td></tr>
<tr><td colspan="2">RATING</td><td>15</td><td>10</td><td>7</td><td>4</td><td colspan="3">0</td></tr>
</table>

Table 2.5: Rating adjustment for discontinuity orientations, with reference to Table 2.9 (Bieniawski, 1989)

<table>
<tr><th colspan="2">STRIKE AND DIP ORIENTATIONS</th><th>Very favourable</th><th>Favourable</th><th>Fair</th><th>Unfavourable</th><th>Very Unfavourable</th></tr>
<tr><td rowspan="3">RATINGS</td><td>Tunnels and mines</td><td>0</td><td>-2</td><td>-5</td><td>-10</td><td>-12</td></tr>
<tr><td>Foundations</td><td>0</td><td>-2</td><td>-7</td><td>-15</td><td>-25</td></tr>
<tr><td>Slopes</td><td>0</td><td>-5</td><td>-25</td><td>-50</td><td></td></tr>
</table>

Table 2.6: Rock mass classes for RMR determined from total ratings (Bieniawski, 1989)

<table>
<tr><th>CLASSIFICATION CRITERIA</th><th colspan="5">CATEGORIES</th></tr>
<tr><td>RATING</td><td>100-81</td><td>80-61</td><td>60-41</td><td>40-21</td><td><21</td></tr>
<tr><td>CLASS NUMBER</td><td>I</td><td>II</td><td>III</td><td>IV</td><td>V</td></tr>
<tr><td>DESCRIPTION</td><td>Very good rock</td><td>Good rock</td><td>Fair rock</td><td>Poor rock</td><td>Very poor rock</td></tr>
</table>

Table 2.7: Meaning of the RMR rock classes (Bieniawski, 1989)

CLASSIFICATION CRITERIA	RANGE OF VALUES				
Class number	I	II	III	IV	V
Average stand-up time	20yrs for 15m span	1 year for 10m span	1 week for 5m span	10hrs for 2.5m span	0.5hrs for 1m span
Cohesion for rock mass (kPa)	>400	300-400	200-300	100-200	<100
Friction angle of rock mass (deg.)	>45	35-45	25-35	15-25	<15

Table 2.8: Guidelines for classification of joint conditions in the RMR system (Bieniawski, 1989)

JOINT FEATURE	RANGE OF VALUES				
Discontinuity length (persistence)	<1m	1-3m	3-10m	10-20m	>20m
RATING	**6**	**4**	**2**	**1**	**0**
Separation (aperture)	None	<0.1mm	0.1-1mm	1-5mm	>5mm
RATING	**6**	**5**	**4**	**1**	**0**
Roughness	Very rough	Rough	Slightly rough	Smooth	Slicken-sided
RATING	**6**	**5**	**3**	**1**	**0**
Infilling (gouge)	None	Hard filling <5mm	Hard filling >5mm	Soft filling <5mm	Soft filling >5mm
RATING	**6**	**4**	**2**	**2**	**0**
Weathering	Unweathered	Slightly weathered	Moderately weathered	Highly weathered	Decomposed
RATING	6	5	3	1	0

Table 2.9: Effects of discontinuity strike and dip orientation in tunnelling for the RMR system (Bieniawski, 1989)

STRIKE PERPENDICULAR TO TUNNEL AXIS		STRIKE PARALLEL TO TUNNEL AXIS	
Drive with dip: Dip 45-90^0	Drive with dip: Dip 20-45^0	Dip 45-90^0	Dip 20-45^0
Very favourable	Favourable	Very unfavourable	Fair
Drive against dip: Dip 45-90^0	Drive against dip: Dip 20-45^0	Dip 0-20^0 Irrespective of strike angle	
Fair	Unfavourable	Fair	

The RMR system has been utilised in this study because of its widespread use in the mining industry and also due to the fact that it has been refined numerous times, thus, making it simpler and effective for rock mass characterisation.

2.6.4 Modified RMR for mining

The original RMR system was established based on case records from civil engineering applications (Bieniawski, 1976). A number of modifications were made, accordingly, to make the system more relevant to the mining industry and it is generally known as Laubscher's MRMR system (Laubscher 1977, 1984), (Laubscher & Taylor, 1976), (Laubscher & Page, 1990). However, the case histories which were used to establish this system were derived from caving operations. Additionally, this system adjusts the RMR to cater for in situ and mining induced stresses, stress variations and the effects of blasting and weathering. For this reason, the MRMR system was used in this study to determine caveability of NUG undercuts in the HSI complex (Diering & Laubscher, 1987). Figure 2.14 highlights the graphical relationship derived by Diering and Laubscher (1987) between MRMR and the shape factor of the stope/tunnel (i.e. hydraulic radius). The hydraulic radius is a ratio of area to perimeter of an excavation's face.

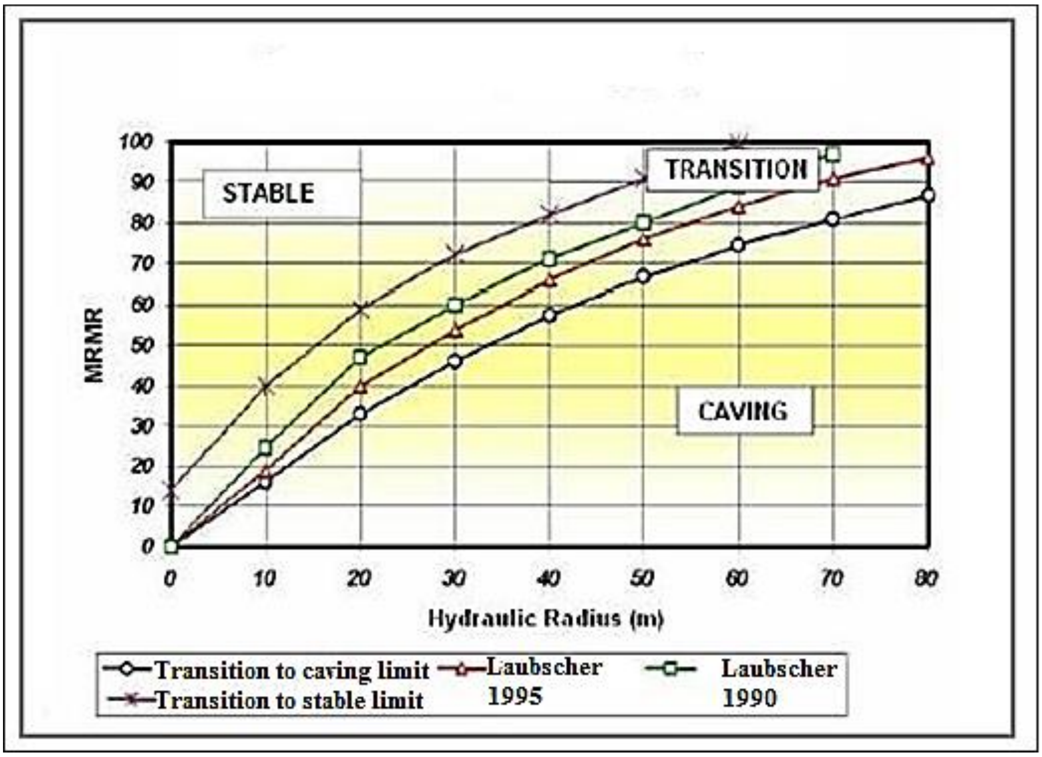

Figure 2.14: Laubscher's Caveability Graph (Laubscher, 2000)

2.6.5 Rock Tunnelling Quality Index "Q"

Barton (1971 & 1974) introduced this rock mass classification system based on a considerably large number of case records of underground excavations. This system is popularly known as the "Q" rating which ranges from 0.001 to 1000 in order of increasing rock competency. The rating is specified by Equation 2.14.

$$Q = \frac{RQD}{J_n} \times \frac{J_r}{J_a} \times \frac{J_w}{SRF} \qquad [2.14]$$

Where: J_n is the joint set number,

J_r is the joint roughness number,

J_a is the joint alteration number,

J_w is the joint water reduction number, and

SRF is the stress reduction factor.

Hoek (2007) stated that this system along with the RMR system are the two most widely applied rock mass classification systems because they both include geological, geometric and engineering paramters to quantify the rock mass quality. Furthermore, the Q rating is widely used in empirical support design, while, the RMR is chiefly implemented for drilling, blastibility designs, etc. Henceforth, the Q rating was used in this study for the purpose of designing the support for secondary developments which are excavated in the fairly competent ARK, as mentioned earlier in Chapter 1.

2.7 Ore and waste mobilisation in the HSI complex

Section 2.3 of this Chapter outlined that the haulage of material from the complex is initially done by low profile articulated dump trucks (ADT's). The ADT's are loaded with material from box raise chutes on the three production levels (i.e. 2720FT, 2870FT and 3020FT). The material is then transported up the H Sub-Incline to tipping points on the 2600FT level. The dumped material will then be loaded from box raise chutes into Gregg and Granby cars on the 2720FT main haulage level. Lastly, the material is transported by locomotives to the hoist. However, Figure 1.4 in Chapter 1 illustrated that the ADT's are not performing to planned capacity. Therefore, this study also encompassed an investigation into the feasibility of achieving the set targets using the current dump truck fleet.

Low profile loaders are also used in the HSI complex for auxiliary operations like haul road cleaning and maintenance, as well as, cleaning refuge cubbies. In some cases, the loaders can be used to boost production by transporting ore from the loading chutes to the tipping points.

2.8 Reliability, Availability and Maintainability (RAM)

2.8.1 Definition of terms

Reliability

Reliability refers to the ability of a machine to perform its specified function under planned operating conditions. It describes the likelihood that a machine will operate appropriately over a specified time. Accordingly, Allahkarami et al. (2016) articulated that reliability is commonly associated with the probability of failure as shown by Equation 2.15.

$$R(t) + F(t) = 1 \quad [2.15]$$

Where: $R(t)$ is the Reliability at time t; and

$F(t)$ is the Cumulative Failure probability function with respect to time.

Therefore, reliability can be specified as the probability that no operational disturbances will happen during a particular time period (Birolini, 2007). Reliability can also be calculated using Equation 2.16 after (Khoshalan et al., 2014):

$$R(t) = 1 - \int_0^t f(t)dt \quad [2.16]$$

Where: $f(t)$ is the failure probability density function.

Availability

Availability is defined as the extent to which equipment is in operable condition such that it can adequately perform an intended function. There are a number of forms of availability depending on applicability and consideration of time (Mohammadi et al., 2015). Two kinds of availability are described below:

A. **Operational Availability**

This form of availability can be computed based on the total calendar period or just on the planned operating time. Equations 2.17 and 2.18 present the two different sub-classes of Operational Availability.

$$A_O = \frac{Total\ calendar\ time - (Planned\ shutdown\ time + Breakdown\ \ time)}{Total\ calendar\ time} \quad [2.17]$$

Where: A_O is the Operational Availability based on calendar time.

$$A'_O = \frac{Planned\ operating\ time - Breakdown\ time}{Planned\ operating\ time} \quad [2.18]$$

Where: A'_O is the Operational Availability based on planned operating time

B. Inherent Availability

This kind of availability is only connected to the intrinsic characteristics of the equipment and its components. Downtimes which are not caused by the equipment design are disregarded in computing this form of availability. Henceforth, it was used in the data analysis process by the researcher because only equipment failure data was made available for the purpose of this study since NUG is presently under care and maintenance. Equation (2.19) is used to compute Inherent Availability.

$$A_i = \frac{MTTF}{MTTF+MTTR} \quad [2.19]$$

Where: *MTTF* is Mean Time To Failure; and
MTTR is Mean Time To Repair.

From Equation 2.19, it can be observed that *MTTF* is a reliability measure while *MTTR* is indicator of ease of repairing or maintaining equipment. Therefore A_i can be expressed as a function of Reliability and Maintainability.

Maintainability

This term refers to how swift equipment can be restored back to operable state. This term is commonly called “Repair time”. Maintainability is also specified as the probability that a machine can be repaired and returned to an operable condition within a stated time interval. The probability of repairing a machine in a specified time is defined by Equation 2.20 below (Birolini, 2007).

$$M(t) = \int_0^t f_r(t)dt \qquad [2.20]$$

Where: $M(t)$ is the Maintainability function at time *t*, and

$f_r(t)$ is the repair time probability density function.

Utilisation

This signifies the productive period of functionality by equipment when it is available for the specified job. It must be known that a machine can be available and still not work; thus, Utilisation can be defined as the availability time lost when the machine was supposed to be working. Equation 2.21 can be used to compute Utilisation.

$$Utilisation = \frac{Available\ hours - (Set\ up\ \&\ Adjustment\ time + Idle\ time)}{Available\ Hours} \qquad [2.21]$$

Bucket-Fill Factor

This parameter defines how much of the available bucket space, on a dump truck or loader, is occupied by the loaded material. Alternatively, this can be specified as the percentage of the bucket capacity that is actually filled with material. The factor is specified by Equation 2.22.

$$Bucket\ fill\ factor = \frac{Volume\ of\ material\ in\ the\ bucket}{Bucket\ capacity} \qquad [2.22]$$

2.8.2 Equipment life failure profile

In the field of reliability analysis of engineering equipment, failure is assumed to be time-dependent and it generally follows the shape of bath tub as shown in Figure 2.15.

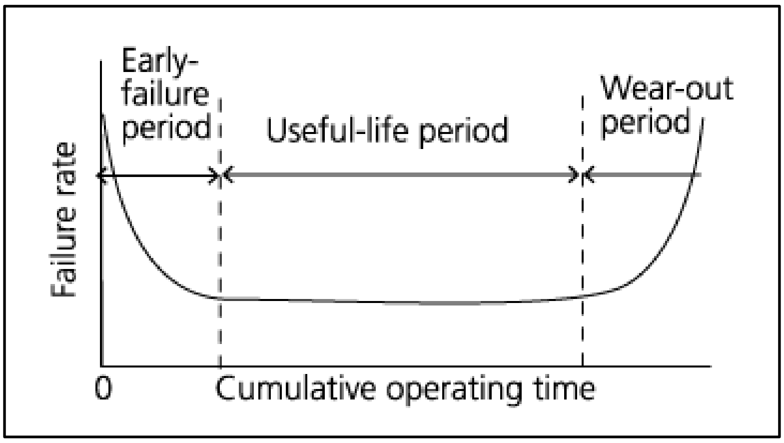

Figure 2.15: The general equipment life failure profile (Allahkarami et al., 2016)

The decreasing failure rate in the early stage of equipment life is mainly caused by debugging of initial set-up and installation errors. The second stage has a constant failure rate because of improved quality control techniques which stabilise early failure rates. Failure rates start to accelerate during the later stage of equipment life due to wear and tear of machine components.

2.8.3 RAM modelling of a dump truck

Numerous authors have performed reliability modelling of a repairable machine in various engineering fields. Samanta et al. (2001a, 2001b & 2004) successfully managed to implement reliability analysis of shovels and dump trucks in the mining industry. Allahkarami et al. (2016) completed a reliability analysis of open pit dump trucks over a 20 month period. Firstly, Allahkarami et al. (2016) divided the dump truck into the following sub systems:

a) Motor,
b) Transmission,
c) Electrical,
d) Hydraulic,
e) Tyre, and
f) Body.

The failure frequency data, over the 20 month period, showed that the motor sub system of the truck was the most significant cause of equipment failure. Subsequently, Allahkarami et al computed a preventative reliability-based maintenance interval of 21hrs for the motor sub system at 90% reliability levels.

Samanta et al. (2004) indicated that the reliability for each individual sub system of a dump truck is calculated by Equation 2.23.

$$R_i(t) = e^{-\lambda_i t} \qquad [2.23]$$

Where: $R_i(t)$ is Reliability of sub system *i* at time *t*; and

λ_i is failure rate of sub system *i*.

Dhillion (2008) highlighted that the reliability for the machine as a whole is achieved by computing the geometric mean of the reliabilities of each sub system as shown by Equation 2.24.

$$R_{ADT}(t) = \prod_{i=1}^{n} R_i\,(t) \qquad [2.24]$$

Similarly, the maintainability for each sub system is found by Equation 2.25:

$$M_i(t) = 1 - e^{-\mu_i t} \qquad [2.25]$$

Where: $M_i(t)$ is Maintainability of sub system *i* at time *t*; and

μ_i is repair rate of sub system *i*.

The maintainability for the dump truck as a whole is determined by Equation 2.26.

$$M_{ADT}(t) = 1 - e^{-\mu_s t} \qquad [2.26]$$

Where: $M_{ADT}(t)$ is the Dump truck maintainability;

μ_s is Machine repair rate$= \frac{1}{MTTR} = \frac{1}{MTTF \times \sum \frac{\lambda_i}{\mu_i}}$; and

$MTTF$ $= \frac{1}{\sum \lambda_i}$.

2.9 Mining method selection techniques

A mining method is basically a description of a combination of variables relating the exploitation process and a deposit's characteristics (Carter, 2011). Parameters that have a bearing on the selection process are (Peskens, 2013):

- Engineering properties of the host rock and the ore body;
- Production rate;
- Characteristic processing behaviour of ore;
- Geotechnical conditions including stress regime and rock mass strength; and
- Economic factors including operating and capital costs combined with mineral price forecast.

Carter (2011) insinuated that the most optimum mining method is the one which maximises economic return. However, Azadeh et al. (2010) proposed that dividing operational and technical factors will result in a technically superior method irrespective of the economic return. Hence, the best approach would be to first select the method based on technical suitability followed by choosing the most appropriate method based on economic return. In this study, a similar approach was adopted, however, economic return for the most feasible methods was not computed. Instead, a review of documented characteristics for the technically suitable methods was done so as to ultimately select the best method.

2.9.1 Mining method selection tools

A number mining method selection tools have been developed over time. All the methods reviewed by the researcher are associated with traditional qualitative or quantitative ranking systems.

2.9.1.1 Boshkov and Wright method

Boshkov and Wright (1973) proposed a qualitative technique which was specifically for underground mines. The factors considered are ore plunge, ore thickness, strength of ore and walls. Table 2.10 illustrates the Boshkov and Wright selection criteria.

Table 2.10: Boshkov and Wright (1973) selection criteria

Type of ore body	Dip	Strength or ore	Strength of walls	Commonly applied mining methods
Thin beds	Flat	Strong	Strong	Open stopes with casual pillars
				Room and pillar
				Longwall
		Weak or strong	Weak	Longwall
Thick beds	Flat	Strong	Strong	Open stopes with casual pillars
				Room and pillar
		Weak or strong	Weak	Top slicing
				Sublevel caving
		Weak or strong	Strong	Underground glory hole
Very narrow veins	Steep	Strong or weak	Strong or weak	Resuing
Narrow veins (widths up to economic length of stull)	Flat	N/A	N/A	Same as for thin beds
	Steep	Strong	Strong	Open stopes
		Weak		Shrinkage stopes
				Cut and fill stopes
			Weak	Cut and fill stopes
				Square set stopes
		Weak	Strong	Open underhand stopes
				Square set stopes
			Weak	Top slicing
				Square set stopes
Wide veins	Flat	N/A	N/A	Same as for Thick beds or Masses
	Steep	Strong	Strong	Open underhand stopes
				Underhand glory hole
				Shrinkage stopes
				Sublevel stoping
				Cut and fill stopes
				Combined methods
			Weak	Cut and fill stopes
				Top slicing
				Sublevel caving
				Square set stopes
				Combined methods
		Weak	Strong	Open underhand stopes
				Top slicing
				Sublevel caving
				Block caving
				Square set stopes
				Combined methods
			Weak	Top slicing
				Sublevel caving
				Square set stopes
				Combined methods
Masses	N/A	Strong	Strong	Underground glory hole
				Shrinkage stopes
				Sublevel stoping
				Cut and fill
				Combined methods
	N/A	Weak	Weak or strong	Top slicing
				Sublevel caving
				Block caving
				Square set stopes
				Combined methods
Very thick beds	N/A	N/A	N/A	Same as for Masses

2.9.1.2 Morrison method

Morrison (1976) divided underground mining methods into three groups as shown in Figure 2.16.

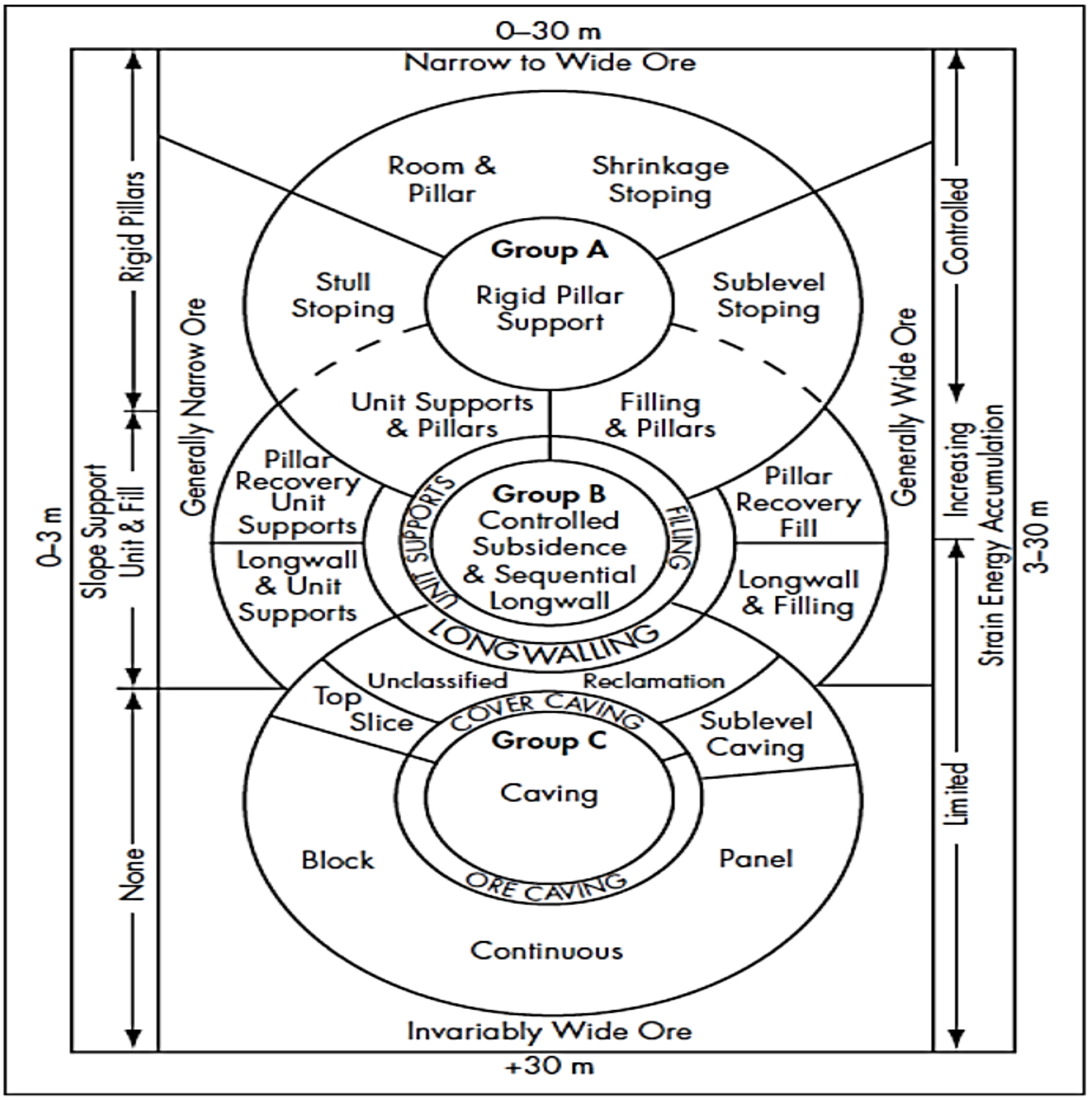

Figure 2.16: Morrison (1976) selection criteria for mining methods

2.9.1.3 Laubscher selection method

Laubscher (1981) established a technique that used RMR of a rock mass. This system was meant for selecting mass mining methods. A later adaptation of this system included hydraulic radius (Laubscher & Page, 1990). This system was the chief actuater of caveability studies for application in caving mining. Figure 2.17 describes the original technique while

Figure 2.14 illustrates the 1990 adaptation which is also a rock mass classification system commonly called “Modified Rock Mass Rating”.

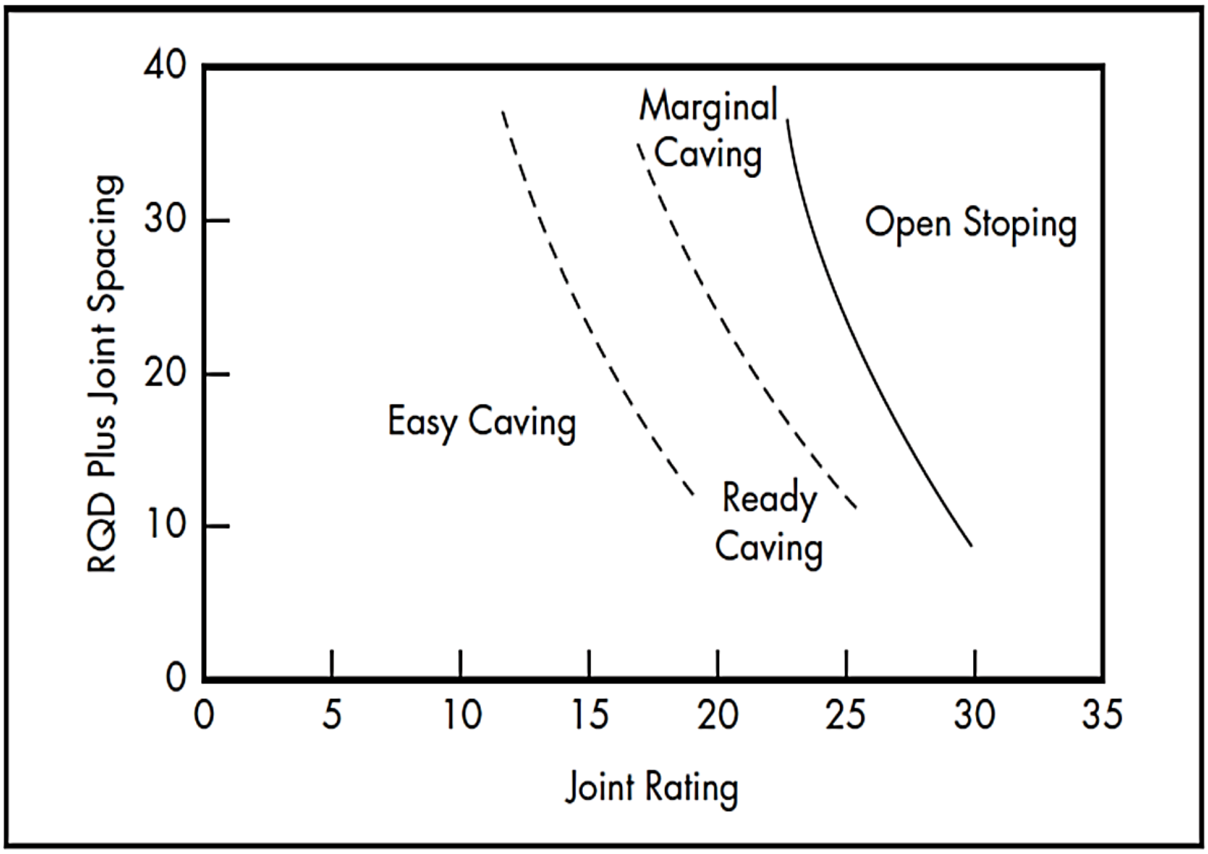

Figure 2.17: Mass mining method selection (Laubscher, 1981)

2.9.1.4 Hartman method

Hartman (1987) generated a flow chart similar to Boshkov and Wright (1973) chart, however, this chart selected specific mining methods for both underground and surface mines. The flow chart is illustrated in Figure 2.18.

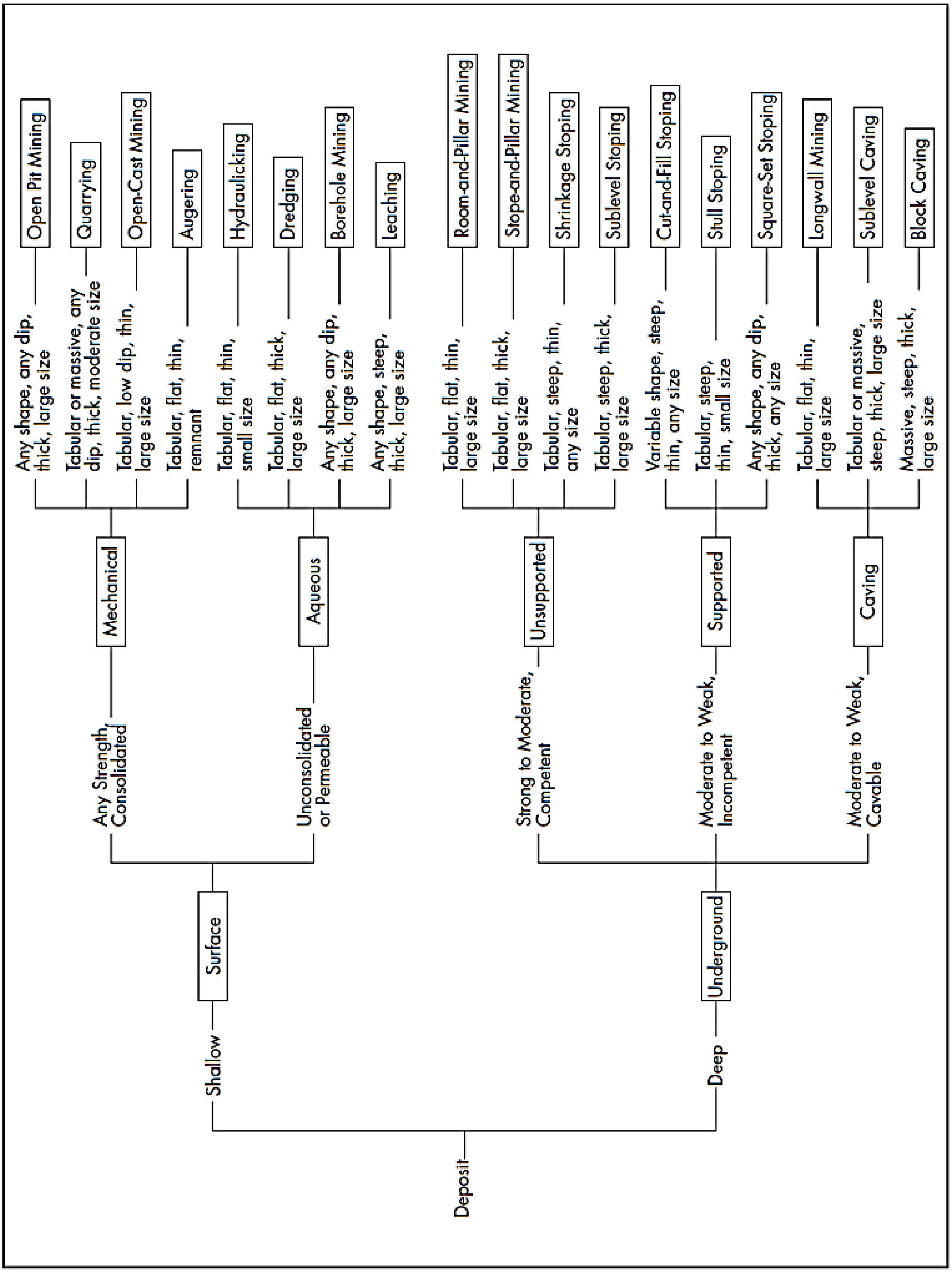

Figure 2.18: Flow chart for mining method selection (Hartman, 1987)

2.9.1.5 Nicholas method

Nicholas (1981) proposed a quantitative method using numerical ranking tables to choose the most suitable method. Table 2.11 indicates that several factors were included in this technique.

Table 2.11: Mining method selection criteria (Nicholas, 1981)

<table>
<tr><th colspan="2">GENERAL SHAPE</th><th colspan="3">ROCK SUBSTANCE STRENGTH (Uniaxial strength/overburden pressure)</th></tr>
<tr><td>Equi-dimensional (E)</td><td>All dimensions are of the same order of magnitude</td><td>Weak (W)</td><td colspan="2"><8</td></tr>
<tr><td>Platy tabular (T/P)</td><td>Two dimensions are many times the thickness which does not exceed 100m</td><td>Moderate (M)</td><td colspan="2">8 to 15</td></tr>
<tr><td>Irregular (I)</td><td>Dimensions vary over short distances</td><td>Strong (S)</td><td colspan="2">>15</td></tr>
<tr><th colspan="2">ORE THICKNESS</th><th>FRACTURE FREQUENCY</th><th>No. of fractures per m</th><th>%RQD</th></tr>
<tr><td>Narrow (N)</td><td><10m</td><td>Very close (VC)</td><td>>16</td><td>0 to 20</td></tr>
<tr><td>Intermediate (I)</td><td>10 to 30m</td><td>Close (C)</td><td>10 to 16</td><td>20 to 40</td></tr>
<tr><td>Thick (T)</td><td>30 to 100m</td><td>Wide (W)</td><td>3 to 10</td><td>40 to 70</td></tr>
<tr><td>Very thick (VT)</td><td>>100m</td><td>Very wide (VW)</td><td><3</td><td>70 to 100</td></tr>
<tr><th colspan="2">PLUNGE</th><th colspan="3">FRACTURE SHEAR STRENGTH</th></tr>
<tr><td>Flat (F)</td><td><20</td><td>Weak (W)</td><td colspan="2">Clean joint with smooth surfaces or fill with material which has strength than the rock substance strength</td></tr>
<tr><td>Intermediate (I)</td><td>20 to 55</td><td>Moderate (M)</td><td colspan="2">Clean joint with rough surface</td></tr>
<tr><td>Steep (S)</td><td>>55</td><td>Strong (S)</td><td colspan="2">Joint filled with material that is equal to or stronger than the rock substance strength</td></tr>
<tr><th>DEPTH BELOW SURFACE</th><td colspan="4">Provide actual depth</td></tr>
<tr><th colspan="5">GRADE DISTRIBUTION</th></tr>
<tr><td>Uniform (U)</td><td colspan="4">Grade at any point in deposit does not vary significantly from mean grade of that deposit</td></tr>
<tr><td>Gradational (G)</td><td colspan="4">Grade values have zonal characteristics and the grades change gradually from one to another</td></tr>
<tr><td>Erratic (E)</td><td colspan="4">Grade values change radically over short distances and do not exhibit any discernible pattern in their change</td></tr>
</table>

Nicholas (1981) assigned ratings to each of ten mining methods per category of the parameters presented in Table 2.11. A description of the assigned ratings for the mining methods is presented in Table 2.12.

Table 2.12: Assigned ratings for each mining method per given parameter (Nicholas, 1981)

MINING METHOD	GENERAL SHAPE			ORE THICKNESS				ORE PLUNGE			GRADE DISTRIBUTION		
	M	T/P	I	N	I	T	VT	F	I	S	U	G	E
Open pit	3	2	3	2	3	4	4	3	3	4	3	3	3
Block caving	4	2	0	-49	0	2	4	3	2	4	4	2	0
Sublevel stoping	2	2	1	1	2	4	3	2	1	4	3	3	1
Sublevel caving	3	4	1	-49	0	4	4	1	1	4	4	2	0
Longwall	-49	4	-49	4	0	-49	-49	4	0	-49	4	2	0
Room and pillar	0	4	2	4	2	-49	-49	4	1	0	3	3	3
Shrinkage stoping	2	2	1	1	2	4	3	2	1	4	3	2	1
Cut and fill	0	4	2	4	4	0	0	0	3	4	3	3	3
Top slicing	3	3	0	-49	0	3	4	4	1	2	4	2	0
Square set	0	2	4	4	4	1	1	2	3	3	3	3	3

MINING METHOD	ROCK SUBSTANCE STRENGTH			FRACTURE SPACING				FRACTURE STRENGTH		
	W	M	S	VC	C	W	VW	W	M	S
ORE ZONE										
Open pit	3	4	4	2	3	4	4	2	3	4
Block caving	4	1	1	4	4	3	0	4	3	0
Sublevel stoping	-49	3	4	0	0	1	4	0	2	4
Sublevel caving	0	3	3	0	2	4	4	0	2	2
Longwall	4	1	0	4	4	0	0	4	3	0
Room and pillar	0	3	4	0	1	2	4	0	2	4
Shrinkage stoping	1	3	4	0	1	3	4	0	2	4
Cut and fill	3	2	2	3	3	2	2	3	3	2
Top slicing	2	3	3	1	1	2	4	1	2	4
Square set	4	1	1	4	4	2	1	4	3	2
HANGING WALL										
Open pit	3	4	4	2	3	4	4	2	3	4
Block caving	4	2	1	3	4	3	0	4	2	0
Sublevel stoping	-49	3	4	-49	0	1	4	0	2	4
Sublevel caving	3	2	1	3	4	3	1	4	2	0
Longwall	4	2	0	4	4	3	0	4	2	0
Room and pillar	0	3	4	0	1	2	4	0	2	4
Shrinkage stoping	4	2	1	4	4	3	0	4	2	0
Cut and fill	3	2	2	3	3	2	2	4	3	2
Top slicing	4	2	1	3	3	3	0	4	2	0
Square set	3	2	2	3	3	2	2	4	3	2
FOOTWALL										
Open pit	3	4	4	2	3	4	4	2	3	4
Block caving	2	3	3	1	3	3	3	1	3	3
Sublevel stoping	0	2	4	0	0	2	4	0	1	4
Sublevel caving	0	2	4	0	1	3	4	0	2	4
Longwall	2	3	3	1	2	4	3	1	3	3
Room and pillar	0	2	4	0	1	3	3	0	3	3
Shrinkage stoping	2	3	3	2	3	3	2	2	2	3
Cut and fill	4	2	2	4	4	2	2	4	4	2
Top slicing	2	3	3	1	3	3	3	1	2	3
Square set	4	2	2	4	4	2	2	4	4	2

2.9.1.6 University of British Columbia (UBC) method

A quantitative mining method selection technique, by Edumine (1999), was formulated based on the Nicholas method but it differs in the sense that this technique considers RMR and not RQD or fracture strength. This method provides a suitability rank for a mining method according to set parameters. The ranking scores range between 1 and 5 with 5 being the most appropriate. If a mining method is completely inappropriate the rank scores in -49. The final score is the sum of suitability ranking scores for each parameter. Table 2.13 describes the selection criteria of the UBC method.

Table 2.13: Mining method selection criteria *(Edumine, 1999)*

General shape	
Equi-dimensional	All dimension are of the same order
Platy-tabular	Two dimensions are larger than the thickness
Irregular	Dimension vary
Orebody thickness	
Narrow	<10 m
Intermediate	10 – 30 m
Thick	30 – 100 m
Very thick	>100 m
Deposit plunge	
Flat	<20°
Intermediate	20° – 55°
Steep	> 55°
Grade distribution	
Uniform	Grade is equal to the mean grade throughout the orebody
Gradational	Grade has a zonal characteristic which gradually changes from zone to zone
Erratic	Grade can change quickly over distance without any pattern
Deposit depth	
Shallow	<100 m
Intermediate	100 – 600 m
Deep	>600 m
RMR	
Very weak	0 – 20
Weak	20 – 40
Medium	40 – 60
Strong	60 – 80
Very strong	80 – 100
RSS	
Very weak	<5
Weak	5 – 10
Medium	10 – 15
Strong	>15

This method was selected by the researcher for mining method selection because it is the most recent of all traditional selection tools. Data specific for the HSI complex was collected and input into the online UBC mining method selection tool by Edumine (1999).

2.10 Summary

Documented records at NUG were reviewed with the intention of gaining adequate knowledge of the different study variables. Academic research work was also evaluated so as to consolidate the pre-requisite knowledge base such that the most appropriate research design which adequately answered the research questions was formulated. Finally evaluation tools and techniques were chosen for implementation in data analysis stage.

CHAPTER 3: RESEARCH DESIGN AND METHODOLOGY

3.1 Introduction

This Chapter gives a comprehensive narrative of the conceptual framework and research approach which was adopted in line with achieving the main objective of the study by fulfilling each and every sub-objective as previously stated in Chapter 1. Firstly, the framework is presented in the form of a process flow chart linking study areas of interest. Subsequently, a description of the study variables, selected sampling criteria, data collection and analysis procedures was presented for each area of interest to the study. Lastly, a discussion was done covering study limitations and ethical considerations.

3.2 Research approach

A quantitative experimental research approach was adopted to establish a solution to the research problem. This research method was chosen because it is applicable where sufficient knowledge of causes for the problem have been established, as presented in Section 1.2 of Chapter 1. Thus, necessitating the need to conduct further investigations to develop and evaluate intervention(s) meant to limit or solve the problem.

3.3 Research design

A conceptual framework was synthesised in order to present the research approach which was used to achieve the study's main objective. Figure 3.1 illustrates the integration of variables for all the study's areas of interest in a logical and consistent manner.

Data which was utilised to complete the review of economic reserves is highlighted in Section A of Table 3.1. Meanwhile, Section B of Table 3.1 presents information which was applied in the process computing BMR. In addition, Equation 2.9, derived in Section 2.4.7.1 of Chapter 2, was used to calculate optimal BMR. Data highlighted in Section C of Table 3.1 was used for the design of interactive drawing. Meanwhile, Section D presents information which was employed in analysis of reliability, availability and maintainability (RAM) for the existing NUG materials ore conveyance system. Lastly, the data for mining method selection process is shown in Section E of Table 3.1.

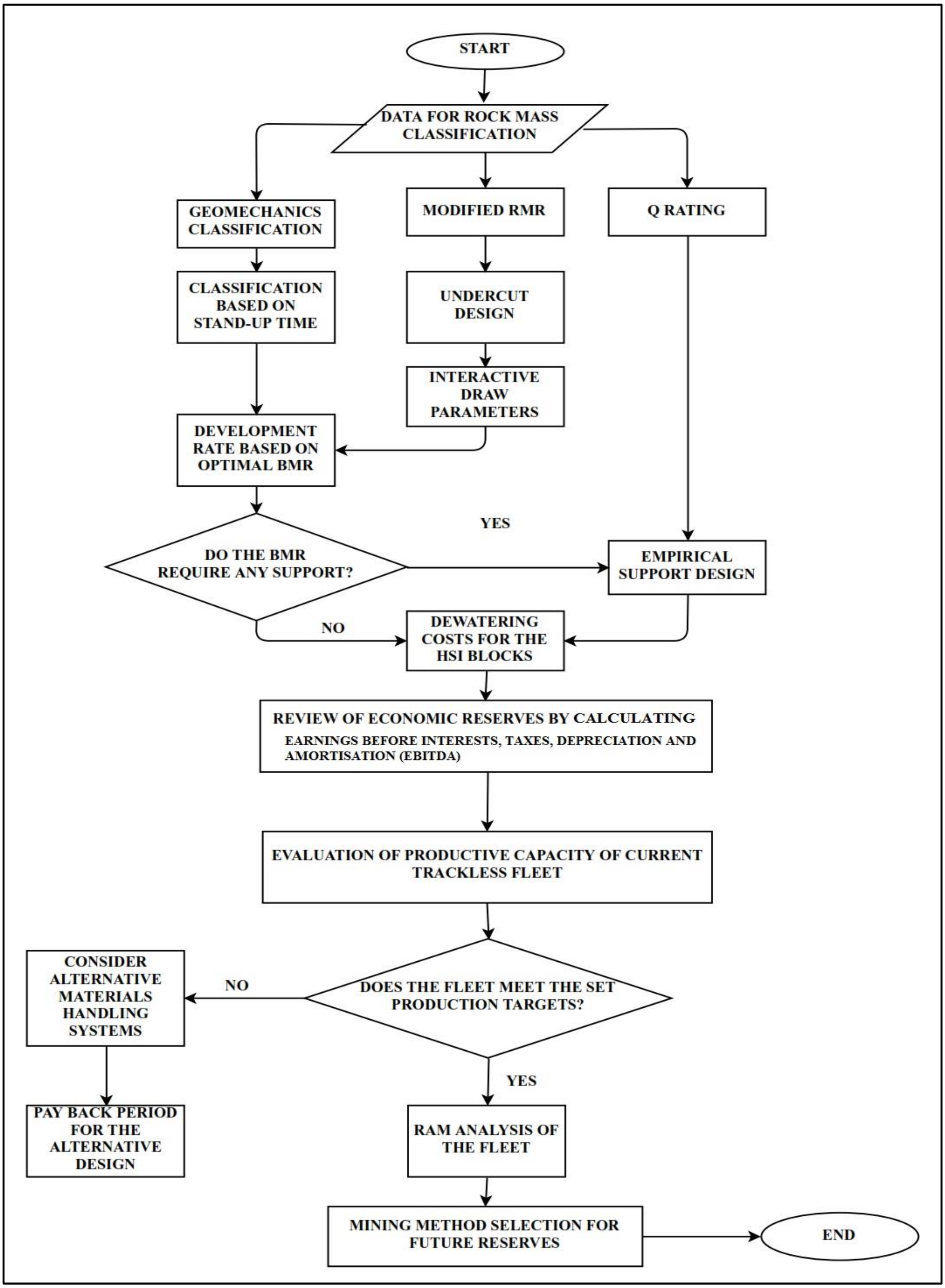

Figure 3.1: Conceptual framework of the study

3.4 Sources of data

Two classes of data, primary and secondary, were used with the intention of accomplishing the aim of the study. It is acknowledged that the primary data utilised in the study possesses a high degree of accuracy, because it was collected directly from the data sources (i.e. sample population), it however, consumed a significant amount of time and effort. Contrariwise, the secondary data which was used is of a lower degree of accuracy than primary data due to the fact that information loses accuracy from its source until it reaches the recipient. Despite this, the secondary data has the benefit of consuming lesser time during the data gathering process than the time taken to collect primary data. For these reasons, the researcher decided to use utilise both primary and secondary data so that highly accurate results were achieved in the limited time frame set for the research.

Primary data used in the research constituted of point load tests on rock samples, discontinuity window mapping, groundwater inflow sampling and focus group discussions with KCM officials. The data gathered on rock mass characteristics was comparable to archived records at NUG. As a result, NUG geotechnical records were adopted in this study. In addition, published information on a variety of subject areas of the study was used as secondary data. This information was gathered from library facilities at the University of Zambia, published journals and research articles accessed from the “Google Scholar” platform, mining standards of best practice obtained from mining practice handbooks and, lastly, documented records at KCM’s Nchanga mine.

3.5 Study variables

The study variables which were incorporated in this research study are highlighted in Table 3.1. A detailed description of different sampling methods and sample size calculations followed this section.

Table 3.1: Data which constituted the study variables of the research

SECTION A: REVIEW OF ECONOMIC RESERVES
In-situ tonnages and grades distribution for HSI complex Blocks (i.e. Exploration data)
Cut-off grade (%TCu)
Net Smelter Return of Cu in concentrates
Net Return of Primary Cu from Leaching plant
Mining costs
Concentrating costs
SECTION B: OPTIMAL BUFFER MINERAL RESERVES
Mining Block Recovery factor γ = 140%
Actual Production Rate
Stand-up time of development headings: (Rock Quality Designation, Joint Spacing, Groundwater conditions, Discontinuity conditions, Joint orientation, Uniaxial Compressive strength)
SECTION C: INTERACTIVE DRAW DESIGN
Trough drift spacing
Draw point spacing
MRMR of footwall
Minimum caving hydraulic radius of trough drives
Caving angle
SECTION D: ANALYSIS OF MATERIALS CONVEYANCE SYSTEM
Remaining useful life of loaders and dump trucks
Availability and utilisation of loaders and trucks
Required spares for equipment and associated costs of procurement
Fleet size and productive capacities
Production tramming target

Index properties of rock (maximum lump size, angle of repose, moisture conditions)
Failure data for the low profile articulated dump trucks
SECTION E: MINING METHOD SELECTION
General ore body shape
Ore body thickness
Deposit plunge
Grade distribution
Depth of ore body from the surface
RMR
Rock substance strength (Ratio of Uniaxial Compressive Strength to Major Principal Stress)

3.6 Sampling criteria

Sampling is the process of selecting a number of units (a sample), from a collection of units (population), and this is used to determine a particular characteristic(s) of the sample which can be generalised for the whole population. A stratified sampling was implemented in this study because it provides the best representation of the study's population for rock mass classification tests (i.e. point load laboratory tests, discontinuity window mapping and groundwater inflow sampling) since the HSI complex is already divided into three levels (i.e. 2720FT, 2870FT and 3020).

3.6.1 Sample sizes

Normally, the larger the sample size, the more likely a study can make accurate inferences of the study population. This is because a large sample size is closer to including every study element in the population, thus, it is more likely to be a better representative of the population.

The issue of inaccurate study findings due to a sample's poor representativeness of the population describes what is commonly called "Error in research". As expected, a large sample results in a lower magnitude of this error. Probabilistic sampling also has a lower error since each study unit has an equal chance of being selected, therefore, a researcher has a better chance of selecting a sample that represents the population.

The size of a sample required for a research basically depends on whether the study is intended to find out the proportion of a particular characteristic or it is meant to find the study mean. The level of accuracy of the answers derived by the research also affects the sample size required. Equations 3.1 is used to determine the sample size required for the purpose of investigating the proportion of a certain quantity, correspondingly, Equation 3.2 is for establishing the sample size for a research aimed at calculating the study mean (Silverman, 1986). It must also be noted that the error in research generally goes up to 4%.

$$E = z\sqrt{\frac{\hat{p}(1-\hat{p})}{n}} \qquad [3.1]$$

$$E = \frac{t \times s}{\sqrt{n}} \qquad [3.2]$$

Where: E = Desired error of research;

z = The score on the z-distribution for a selected confidence interval;

$\hat{p}$ = The prior judgement of the correct value of p[1];

n = The sample size;

t = The score on the t-distribution for a selected confidence interval;

s = Standard deviation[2]

Equation 3.2 was used to determine the sample sizes required for point-load testing considering a 4% error margin and 95% confidence interval.

---

[1] If the initial estimate of $\hat{p}$ is not known, the convention is to assume $\hat{p}$ = 05.

[2] s is typically a guess, rough estimate or based on past experience.

3.7 Data collection techniques

The researcher utilised four data collection techniques in this study as highlighted below:

1) Review of mine records;
2) Focus group discussions;
3) Point load laboratory tests; and
4) Underground site observations (i.e. groundwater inflow sampling and discontinuity window mapping).

3.7.1 Data collection instruments

Table 3.2 highlights the instruments which were used to gather primary data on rock mass properties. Due to unavailability of fresh core samples, secondary tri-axial test results from KCM's Ground Control Manual were collected, specifically friction angle and cohesion data for the HSI complex strata.

Table 3.2: Data collection instruments and related study variables

STUDY VARIABLE	INSTRUMENTS WHICH WERE USED
Compressive strength	Point load testing machine, 1kg club hammer and mason's bolster chisel
Groundwater Inflow	Tape measure, stopwatch and volume measuring containers
Discontinuity window mapping	Tape measure and Clar geological compass

3.7.2 Review of mine records

This data collection method was implemented by use of a checklist and data compilation sheets illustrated in Tables C-1 to C-5 of Appendix C. The author chose this tool because it provides a cheap yet effective technique of gathering secondary data.

3.7.3 Focus group discussions

Discussions with KCM Nchanga mine officials, notably with Mr. Chibomba and Mr. Hakakwale, using checklists and data compilation sheets. This data collection procedure was done so as to clarify and gain more secondary data required in this study.

3.7.4 Point load laboratory tests

Experiments were conducted on fragmented rock samples to determine uniaxial compressive strength, using a point load testing machine, at the rock mechanics laboratory of KCM's Nchanga mine. Section 3.6 of Chapter 3 described the different types of sampling criteria and an explanation was given on why stratified sampling was employed in this data collection method. Figure 3.2 provides a description of suggested specimen size limits for the irregular lump point load test. Rock specimens which did not satisfy the recommended dimensions were prepared by using a mason's bolster chisel and 1kg club hammer.

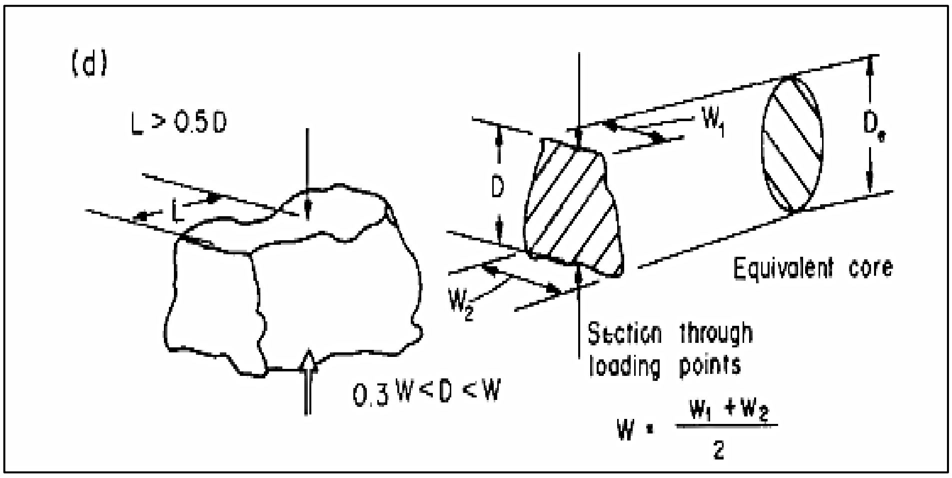

Figure 3.2: Suggested rock specimen size limits for irregular lump point load test

Figure 3.3 shows the point load testing process being done for this study. It must be noted that the two highest and lowest values were excluded in data analysis so as to avoid using extreme values.

Figure 3.3: Point load laboratory testing being done for this study

Following the testing process the slope of a log-log graph, plotting failure load versus the square of specimen equivalent diameter, was implemented as the point load strength index (I_s). Equation 3.3 was used to determine the equivalent diameter (D_e) of the cross-sectional area.

$$D_e = \frac{4 \times WD}{\pi} \qquad [3.3]$$

Where: W = Mean cross-sectional width;

D = Loading platen to platen separation.

Equation 3.4 was utilised to calculate the corrected point load strength index ($I_{s(50)}$)

$$I_{s(50)} = I_s \times \left(\frac{D_e}{50}\right)^{0.45} \qquad [3.4]$$

Equation 3.5 was used to compute uniaxial compressive strength (C_o).

$$C_o = 24 \times I_{s(50)} \qquad [3.5]$$

3.7.5 Groundwater inflow sampling

Groundwater inflow observations were done by placing measuring containers along selected sub haulages and measuring volume of water collected in the container after a 5 minute time lapse. Figure 3.4 illustrates the systematic configuration which was used in the observations.

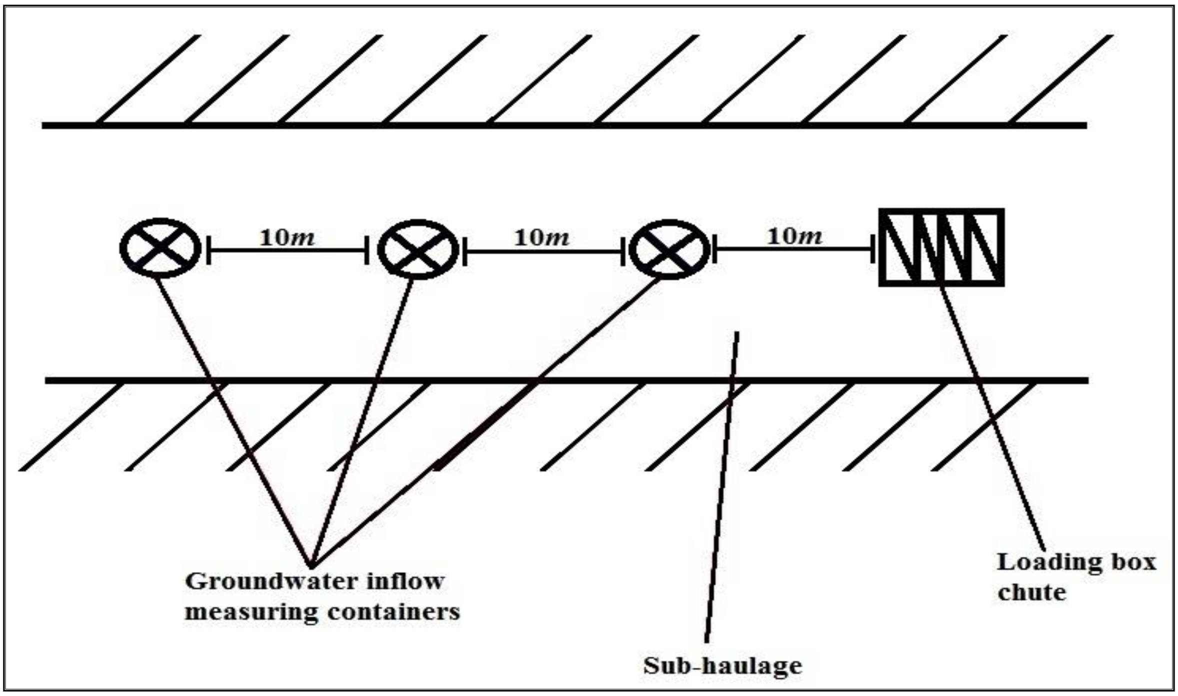

Figure 3.4: Systematic layout for groundwater inflow observations

Stratified sampling was employed by performing the observations separately in sub-haulages on the 2720FT, 2870FT and 3020FT levels. Chutes which were randomly selected for inflow inspections are highlighted in Table 3.3.

Table 3.3: Chutes which were selected for groundwater inflow observations

LEVEL	RANDOMLY CHOSEN CHUTES		
2720FT	9EC	5EB	7EC
2870FT	2EC	6EB	3EB
3020FT	3EB	4EC	8EB

3.7.6 Discontinuity window mapping

The same sub haulages and chutes chosen for inflow inspections were also subjected to discontinuity window mapping of dimensions 2.5m × 2.5m using the Clar geological compass illustrated in Figure 3.5. This data collection process was carried out to determine discontinuity type, orientation, spacing, persistence, roughness, aperture, groundwater seepage, number of joint sets, infill type and width. Stereographic analysis was subsequently done using discontinuity orientations to identify the major and minor joint sets. It must be noted that the discontinuity data gathered in this study was compared with NUG geotechnical records and it was found that the results are equivalent.

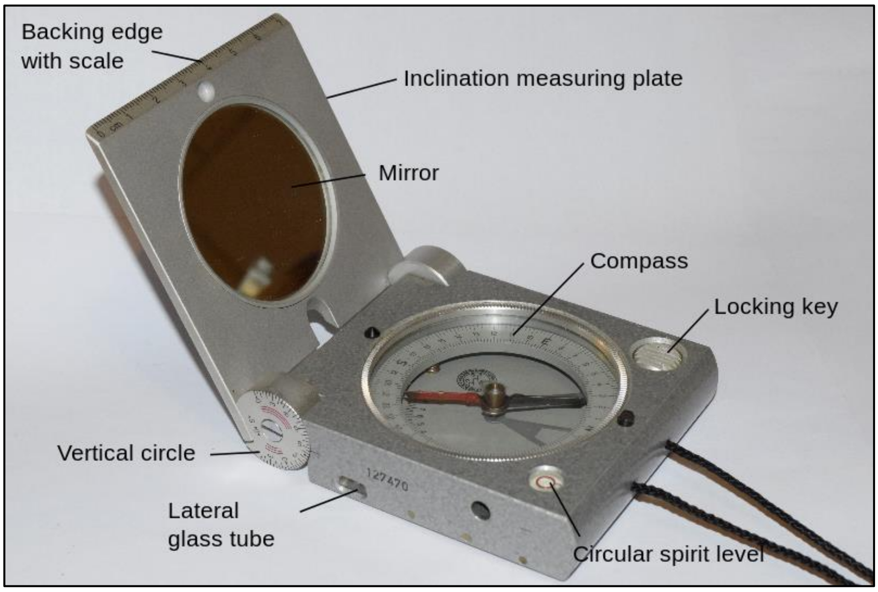

Figure 3.5: Clar geological compass used for discontinuity window mapping

3.8 Data processing and analyses

Data which was gathered was initially organised in a standardised manner by sorting the data into groups respective to the instrument used to collect it. Pre-tests were conducted during the progression of data gathering so that gaps and overlaps (e.g. systematic and random errors) in the collection process were rectified. Following the completion of data collection, the researcher used the tools listed below to process and analyse the data.

a. Empirical graphs by Lauffer (1958); Laubscher (1977) and Barton (1974);
b. UBC mining method selection tool (Edumine, 1999);

c. Reliability Analytics Toolkit (Morris, 2010); and
d. Microsoft Excel software;

3.8.1 Empirical graphs

Ensuing collection of data highlighted in Section B and C of Table 3.1, data processing of geotechnical rock properties was done through application of the empirical graphs stated in the previous section. The data processing mainly involved interpolation of values of Q-rating, Equivalent Dimension, RMR and MRMR such that the following were established:

i. Permanent and Temporary Support estimates;
ii. Stand-up time of the development workings;
iii. Minimum caving hydraulic radius of trough drives; and

3.8.2 Productive capacity evaluation of ore haulage system

Equation 3.6 was used to calculate the design productive capacity (P_C) for the NUG dump trucks. The computed value was then compared with planned annual production rate such that a decision could be made to either recommend an alternative system or perform RAM analysis of current system so that fleet performance can be maximised. It must be noted that maximum dump truck cycle time was determined by consulting with NUG mine captains and reviewing daily fleet production records because operations were suspended during the period of the study.

$$P_C = \frac{\beta \times \rho \times A \times B \times C \times D \times E}{\omega} \qquad [3.6]$$

Where: β is the dump box fill factor = 0.8,

ω is the maximum truck cycle time = 0.5hrs,

ρ is the density of ore = 2.5t/m^3,

A Dump box heaped capacity = 13.0m^3,

B is the planned production duration per shift = 6hrs,

C is the number of shifts per day = 3,

D is the planned production days per year = 300 for 2015/16 financial year, and

E is the fleet size = 4 trucks.

3.8.3 RAM analysis

RAM analysis was done by firstly collecting NUG fleet failure data for the duration between April to August 2016. The data was sorted according to the truck sub systems mentioned in Section 2.8.3 of Chapter 2. Following this, the sorted failure data was imported into the Reliability Analytics Toolkit (Morris, 2010) such that a Reliability decay curve was generated. The computed maintenance interval from the curve was then recommended for each chosen truck sub system in order to improve overall fleet availability.

3.8.4 Mining method selection using the UBC mining method selection tool

The mining method selection (MMS) criteria data, highlighted in Section E of Table 3.1, was gathered and input into the online UBC mining method selection tool.

3.8.5 Application of Microsoft Excel Software

Microsoft Excel was used to produce charts for processed data of the study population, together with, generation of economic evaluation calculations.

3.9 Ethical considerations

Due to the nature of the study, this report did not require any significant ethical considerations. Nonetheless, all materials used in the study were respectfully acknowledged.

3.10 Summary

This chapter explained the entire research design that was implemented in this study. The conceptual framework presented links between areas of interest in the study and further highlighted the logical manner implemented to engage the research problem. A description of the study population was provided. Sampling criteria, data collection and analyses procedures were also discussed with the aim to further emphasise the research approach which was adopted in this study. In conclusion, the study’s constraints, inadequacies and ethical deliberations were conferred.

CHAPTER 4: DATA COLLECTION

4.1 Introduction

This Chapter presents the data set which was collected for further processing and subsequent generation of recommendations. The various data sources used for this study are specified in Section 3.4 and 3.7 of Chapter 3. The data was sorted and pre-tests were done to ensure that all the required information has been gathered.

4.2 Grade-tonnage distribution of the HSI complex

Cut-off grade alone is not a sufficient metric to make a decision on whether to continue or cease production drawing. A parameter called cut-off point was used to determine the theoretical ore tonnage which has to be mucked before production drawing ceases (Cokayne, 1998). Equation 4.1 describes the relationship which was used to calculate the expected ore tonnage to be drawn for a given block after taking into consideration a cut-off grade of 1.0%TCu.

$$Expected\ Ore\ Tonnage = \left[1 - \frac{Cut\ off\ Grade}{In\ situ\ Block\ Grade}\right] \times In\ situ\ Block\ Tonnage \qquad [4.1]$$

Where: $\frac{Cut\ off\ Grade}{In\ situ\ Block\ Grade}$ is the waste-to-ore grade ratio in the caved mass.

However, the researcher concedes that, in practice, the drawn tonnage can be more or even less than the computed values due to unforeseen geological uncertainties, draw control practices, the extent of interaction between draw zones and ore losses as the caved mass flows to the discharge point. Hence the need to conduct continuous sampling and assaying such that grades are monitored throughout the draw life of a block. The Table in Appendix D describes the Cu grade distribution and expected ore tonnages to be drawn for all the blocks.

It is important to realise that the block 2870/7EC has a grade of 0.18% which is well below the cut-off grade (i.e. 1.0%TCu). However, this provides a blending opportunity between 2820/7EC and other blocks. The following computations were done to determine whether blending the blocks with 2870/7EC is beneficial over treating 2870/7EC as waste and mining the remaining blocks as ore.

The weighted average grades for blending 3020/7EB and 2870/7EC blocks are:

$$Average\ grade\ by\ tonnage\ (\%TCu) = \frac{(23.8\% \times 85\,818) + (0.18\% \times 48\,601)}{85\,818 + 48\,601} = 15.26\%$$

$$Average\ grade\ by\ thickness\ (\%TCu) = \frac{(23.8\% \times 0.8) + (0.18\% \times 2.7)}{2.7 + 0.8} = 5.58\%$$

The weighted average grade of the two blocks, by their thickness, provides credible results since production drawing significantly depends on block thickness. Hence, Figure 4.1 was generated to show a comparison between contained Cu tonnage after blending the two blocks and contained Cu tonnage without blending the blocks (i.e. by mining the 3020/7EB and leaving 2870/7EC as waste) after considering weighted average grade by thickness.

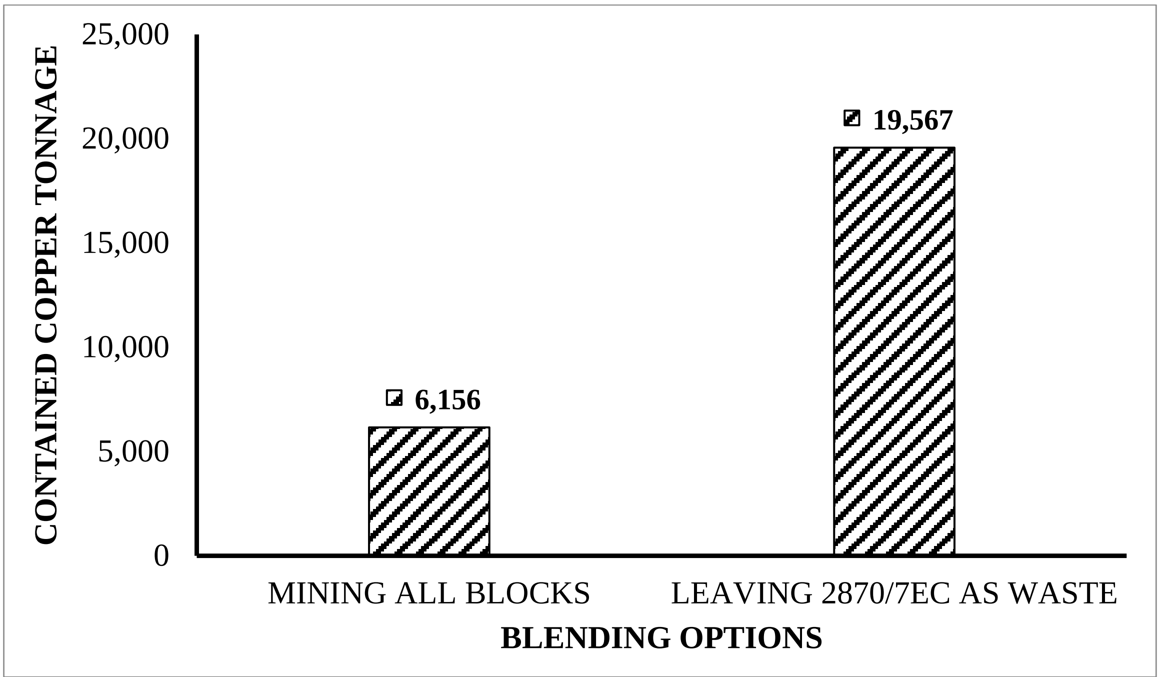

Figure 4.1: Contained Cu tonnages for blending 3020/7EB with 2870/7EC versus leaving 2870/7EC as waste

Figure 4.1 shows that blending 2870/7EC with 3020/7EB yields a lower total tonnage of 6,156t for contained Cu than the alternative of treating the 2870/7EC block as waste while mining 3020/7EC and the other blocks as ore. Figure 4.1 above evidently illustrates that blending with the block 3020/7EB, which has the highest grade of all HSI complex blocks, will fail to yield higher contained Cu tonnages. Therefore the decision to treat 2870/7EC as waste was selected.

4.3 Rock mass classification

Q rating, RMR and modified RMR are the classification systems which were used to determine the rock mass quality. Data was gathered by performing the following activities;

a. A series of point load experiments on rock samples from the hanging wall, foot wall, and ore zone;
b. Underground site observations; and
c. Extensive review of KCM’s Nchanga underground geotechnical records.

4.3.1 Uniaxial compressive strength results

Equation 3.2 was used to calculate the sample size for the purpose of determining uniaxial compressive strength (UCS) of the ore zone, hanging and foot wall rocks. The rock matrix of interest consists of Nchanga basement granite (NBG), ARK and LBS (KCM, 2000). An assumption of 4% error margin of the anticipated UCS values was used, as well as, standard deviations to calculate the sample size as shown in Table 4.1.

Table 4.1: Calculated sample sizes for point load tests

Rock type	Expected UCS range (MPa)	Standard deviation (MPa)	Error margin (MPa)	*t*-Distribution (for 29 degrees of freedom)	Sample size
NBG	>120	10	4.8	2.045	19
ARK	80-150	7	3.20	2.045	21
LBS	25-55	5	2.2	2.045	22

The sample sizes computed in Table 4.1 were used to collect rock samples (i.e. arkose, granite and lower banded shale samples) by employing chosen stratified sampling technique. The samples were separately gathered from eastern sections of 3020FT, 2870FT and 2720FT levels because the western sections have been exhausted. Uniaxial compressive strength of the samples was determined by following the procedure outline in Section 3.7.4 of Chapter 3.

Results of the point load tests are illustrated in Appendix E. Figure 4.2 presents the calculated values of uniaxial compressive strengths for ARK, NBG and LBS.

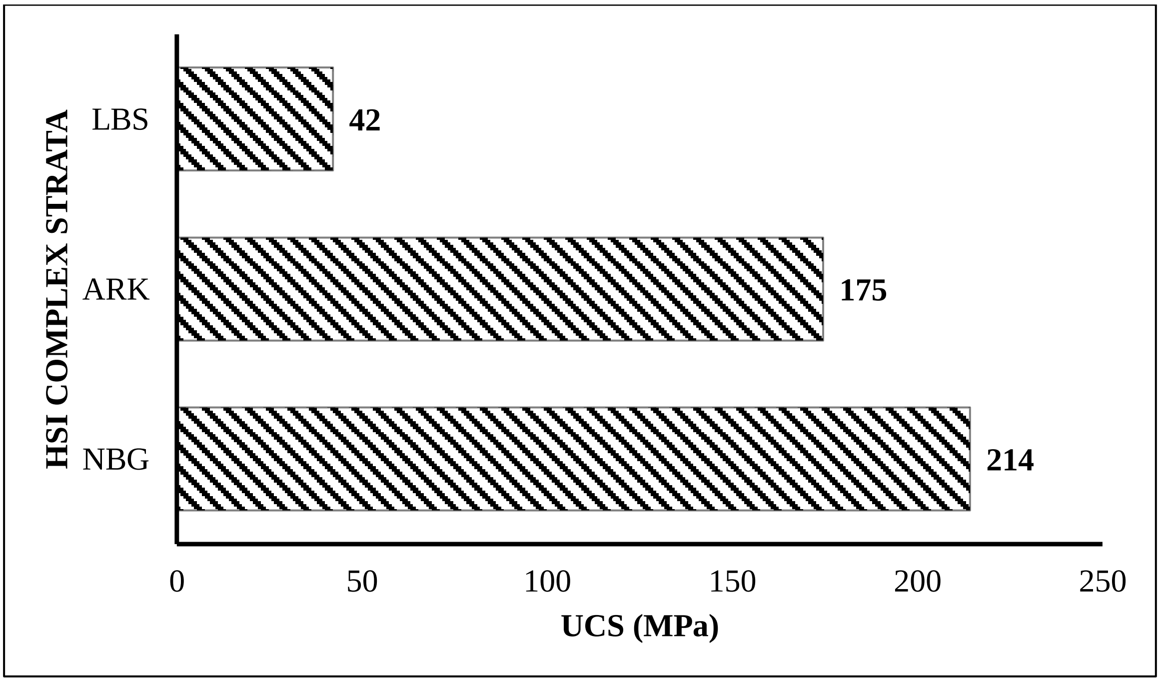

Figure 4.2: UCS values for HSI complex strata

4.3.2 Groundwater inflow results

Following groundwater inflow inspections, it was concluded that although the general conditions in the sub-haulages are “damp”, ground water inflow was less than 10litres per minute for all observations.

4.3.3 Rock Mass Properties

Data for rock mass properties of the HSI complex was collected conducting window mapping of discontinuities along the same sub-haulages chosen for groundwater inflow inspections. Table 4.3 highlights a summary of the rock mass properties for HSI complex strata. RQD results for the strata were collected from a report by Chishimba and Mundike (2014) because core logging could not be done for this study due to unavailability of fresh core samples.

Table 4.2: Rock mass properties for LBS, ARK and NBG

ROCK TYPE	RQD (%)	DISCONTINUITY DATA		
		JOINT SPACING	JOINT CONDITIONS	JOINT ORIENTATIONS
LBS	25 - 35	0.6*m* – 2.0*m*	Slightly rough surfaces, separation <1*mm*	Drive against dip ($45^o – 90^o$)
ARK	65 - 80			
NBG	80 - 100			

4.3.4 Rock Mass Rating Calculations

Data for HSI complex strata shown in Sections 4.3.1 to 4.3.3 were used to calculate the RMR for rock layers as illustrated in Appendix F. Furthermore, where the range of values for parameters of RMR overlaps two distinct rating values, the lowest value was adopted. For example a RQD rating of **13** is accepted for a range of 65% - 85% given that this same range falls in the ratings **13** (for 50% - 75% RQD) and **17** (for 75% - 90% RQD). This was done in line with the conservative approach used in the study to compute the optimal buffer mineral reserves. Figure 4.3 presents the RMR values for NBG, ARK and LBS.

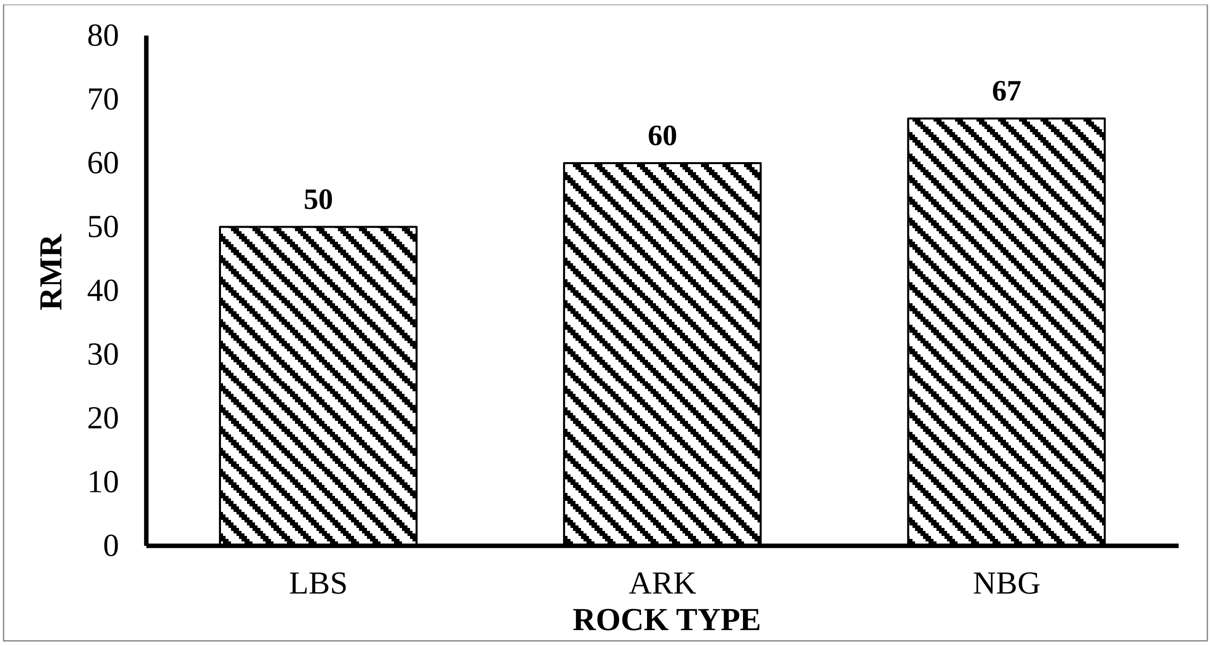

Figure 4.3: RMR values for the HSI complex strata

4.3.5 Q Rating for the HSI Complex

Following underground observations, Table 4.4 presents results which were used to compute rock tunnelling quality indices for the complex.

Table 4.3: Q system data for HSI complex

ROCK TYPE	RQD (%)	J_n	J_r	J_a	J_w	SRF	Q-VALUE
LBS	25 – 35	9	2	4	1	1	1.389
ARK	65 – 80	12	1.5	1	1	1	8.125
NBG	80 – 100	9	1.5	1	1	1	13.333

4.3.6 Rock Mass Classification Based On Stand-Up Time

Secondary developments with the biggest excavation roof span will produce the most conservative stand-up time and this complies with a worst case scenario of pre-mature collapse of the developments. As a result, excavation dimensions of 2.4m x 2.4m (using information from Appendix G) were chosen to determine the shortest active life of secondary developments. Figure 4.4 shows that the minimum stand-up time of 340 days for the secondary developments after Lauffer (1958) and Bieniawski (1989). Additionally, a RMR value of 60 was used because most secondary developments are made in ARK strata.

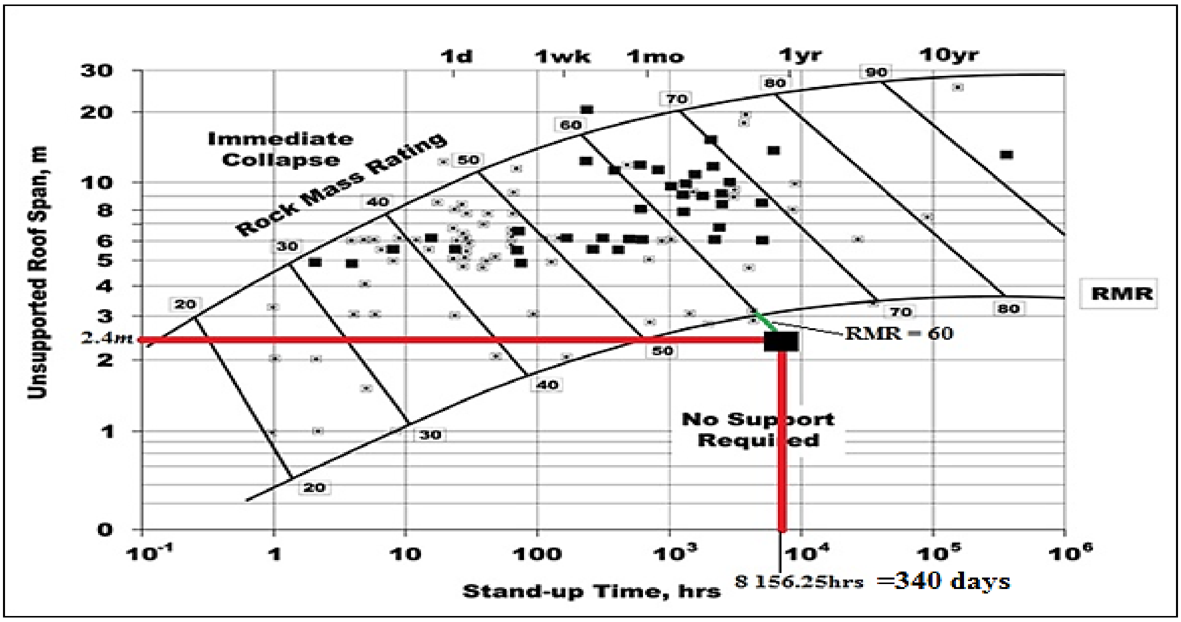

Figure 4.4: Minimum stand-up time for secondary developments (Bieniawski, 1989)

4.3.7 Modified Rock Mass Rating

MRMR by Laubscher (1990) was utilised to assess the in-situ rock mass properties of the HSI complex against the hydraulic radius of trough drives where caving is initiated from. Values generated from assessment of 2720/7EB box (Mundike, 2012) were used. Tables H-1 and H-2 of Appendix H describe the MRMR rating of 45 for ARK in the complex after Laubscher (1990) and Taylor (1980). The hydraulic radius for the trough drives is 23m as illustrated in Figure 4.5.

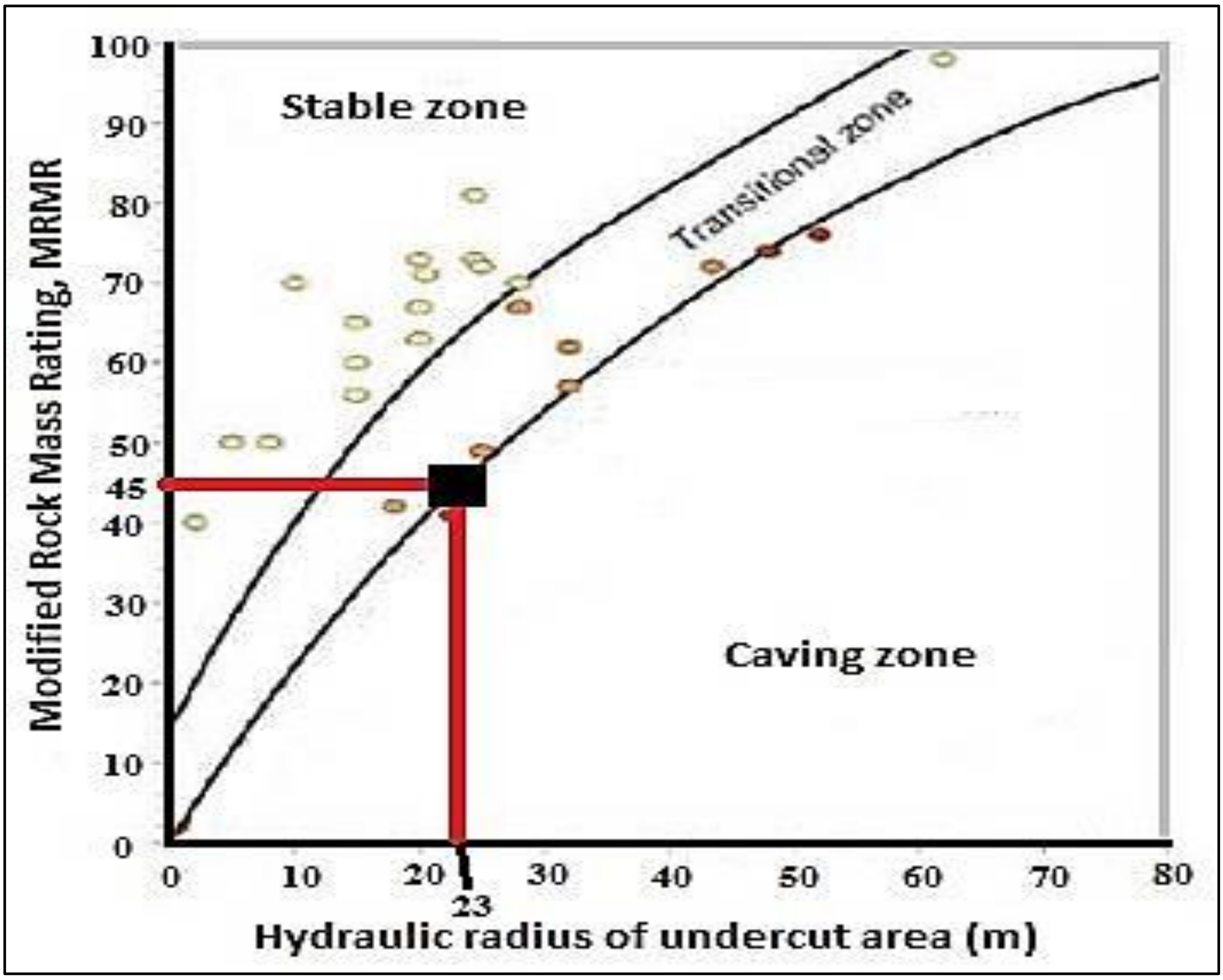

Figure 4.5: Laubscher's Caveability Graph for Arkose rock at NUG (Suorineni et al., 2014)

4.4 Dewatering Scheme

The present phreatic profile is above the HSI complex, accordingly, a dewatering plan has been established so that the caving extraction in the complex is not hindered (KCM, 2016). Table 4.5 presents the specifications of the dewatering system required for the complex.

Table 4.4: Specifications for the dewatering drainage holes

Number of drainage holes per site	3
Metres to be drilled per site	420m per site
Total number of sites	4
Total metres to be drilled	1680m
Unit cost of drilling	$160/m
Total drilling cost	$268,800

4.5 Material Haulage Fleet

Previously, Section 2.7 of Chapter 2 highlighted that ore and waste material is mobilised by dump trucks indicated in the Table 4.6. Each of the trucks has a 12.8m^3 dump box with a gravimetric capacity of 32.65t.

Table 4.5: Current status of dump truck fleet

CALL SIGN	MODEL	STATUS	REMARKS
MT 09	Atlas Copco Wagner MT436B	Non-runner (awaiting engine rebuild and torque converter)	Machine has done its life
MTK 02	Atlas Copco Wagner MT436B	Runner	Machine has done most of its life
MT 13	Atlas Copco Wagner MT436B	Runner	New machine
MT 11	Sandvik EJC 533	Non-runner (awaiting transmission and torque converter)	New machine

Figure 4.6 also confirms the remarks made in the Table 4.6. Each truck has a replacement life of 25,000hrs while the machine overhaul is to be done after 15,000hrs of operation. However, the trucks which have surpassed the machine overhaul threshold have not yet been refurbished.

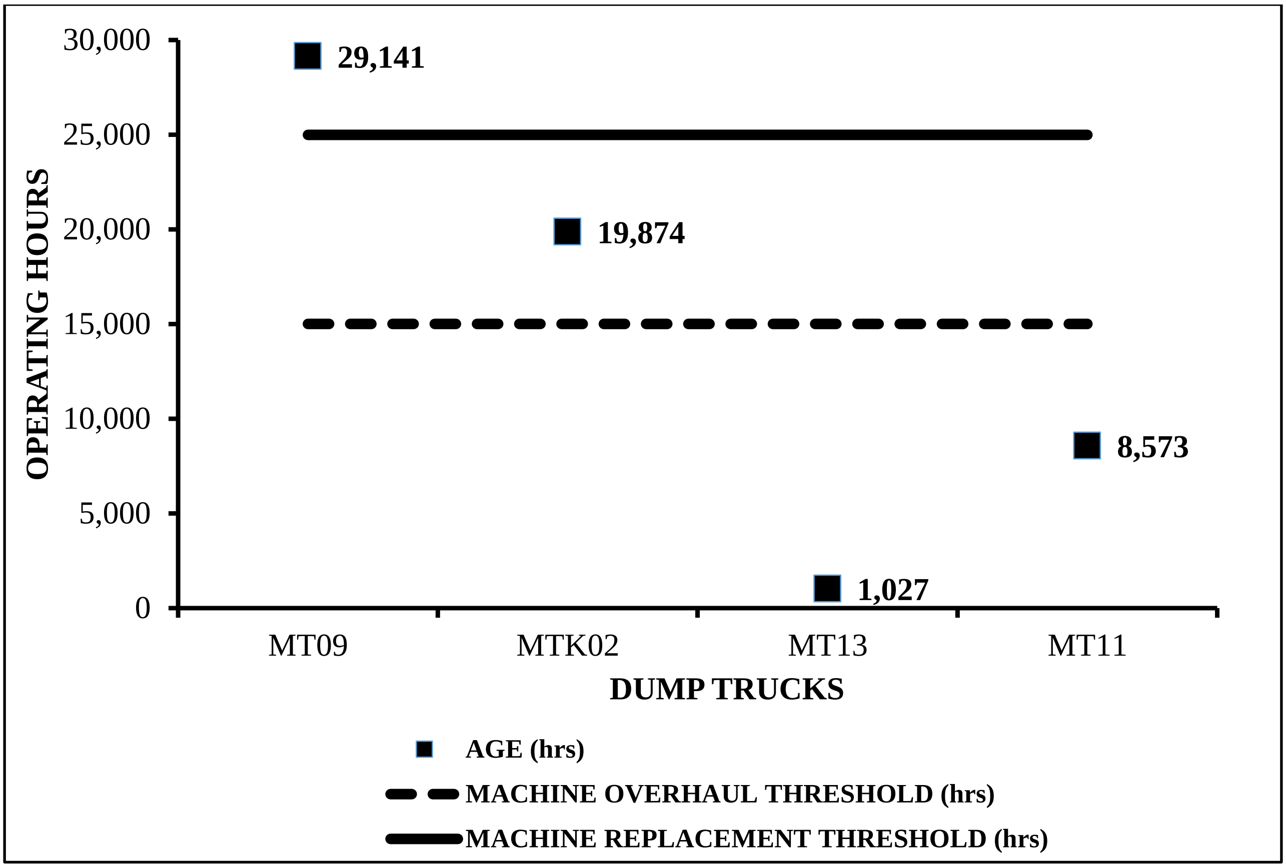

Figure 4.6: Fleet age distribution against machine replacement and overhaul thresholds

4.5.1 Fleet Productive Capacity

Following consultations with NUG mine captains, the maximum truck cycle time from the 3020FT level loading chute to the tipping points and back to the loading point is approximately 30 minutes. This information had to be relied upon since no material haulage by trucks was done during the study period because NUG was under care and maintenance. Figure 4.7 was generated by using Equation 3.6 from Section 3.8.2 of Chapter 3 so as to assess whether or not the rated capacity of the four truck fleet can meet the planned production target. Figure 4.7 evidently shows that NUG fleet production can surpass the planned annual target. Therefore it was identified that it is necessary to evaluate the fleet’s reliabilities and maintainability so that the low fleet availability (as illustrated in Figure 1.4) can be maximised and ultimately the fleet productivity is also increased.

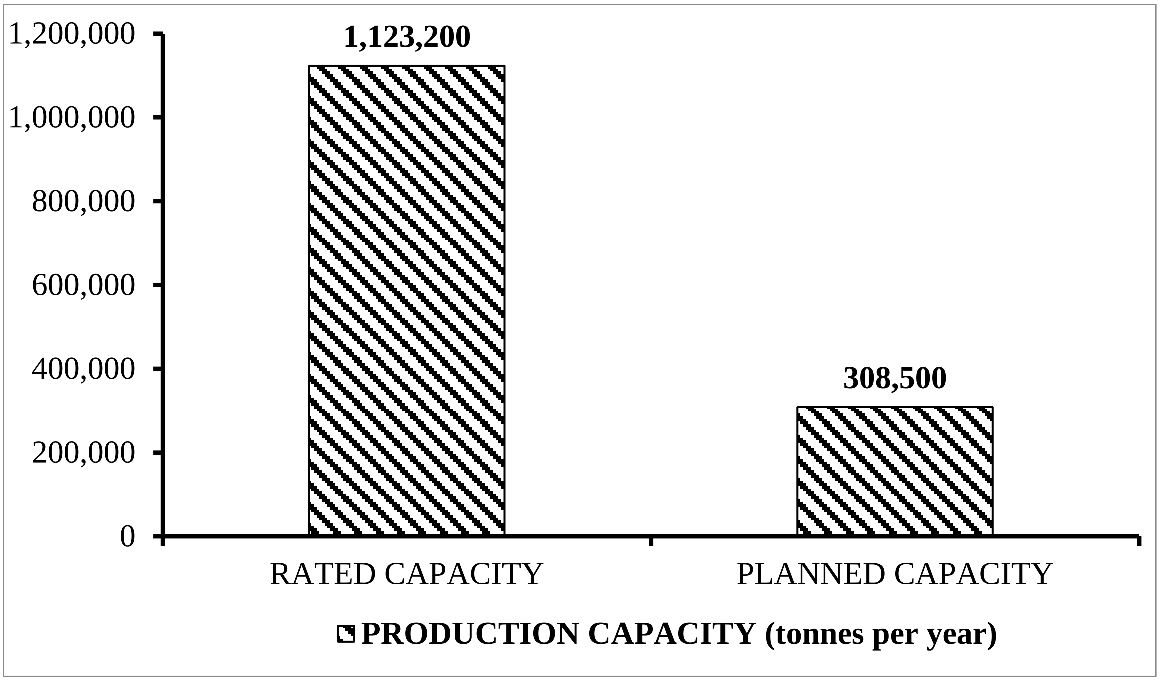

Figure 4.7: Comparison of Rated capacity and Planned capacity of the HSI fleet

4.6 Equipment Failure Data

Information concerning dump truck breakdown durations, failure causes and frequencies was collected from the NUG Mobile Equipment Engineering department for the period between the months of March to August 2015. The dump truck sub systems indicated in section 2.8.3 were used to cluster the failure data into groups. Table 4.7 describes the parts which consist within a given sub system of a truck.

Table 4.6: A description of dump truck sub systems for RAM analysis after Allahkarami et al. (2016) and Samanta et al. (2004)

SUB SYSTEM	COMPONENTS
Engine	Engine body, coolant system, lubrication, fuel, intake and exhaust systems.
Transmission	Gearbox, steering, differential, universal joint/steering box and clutch.
Electrical	Battery, alternator, cable wiring, starter and lights.
Hydraulic	Oil tanks, hoses, pipes, brakes, hoist cylinders, and associated items.
Tyres	Related items.
Body	Dump box, driver cabin, etc.

It must be noted that during the period of evaluation of equipment failure data, MT13 was not yet commissioned for production. MT13 was relocated from a different KCM mine and introduced into NUG operations at a time outside the period of evaluation. Thus, only failure data for three trucks were considered (i.e. MT09, MT11 and MTK02).

4.6.1 Failure and MTTR Data for MT09 Dump Truck

Figure 4.8 illustrates the distribution of rate of failures per sub system and the related MTTR for MT09 Atlas Copco machine. The truck's body took the significantly longest period to repair than any other sub system with a MTTR of 22.875hrs. This is expected since MT09 has already surpassed its service life such that some of its body components are worn out. Although, the "body" sub system took the longest period to repair, it is not a frequent problem as shown by its failure rate which is significantly the lowest of all sub systems. Meanwhile, the "engine" sub system took the second longest period to repair and also it is the most frequent problem as highlighted by its failure rate which is the highest of all the sub systems. For this reason, the "engine" sub system was selected by for further reliability modelling in order to determine the optimum maintenance interval for the sub system.

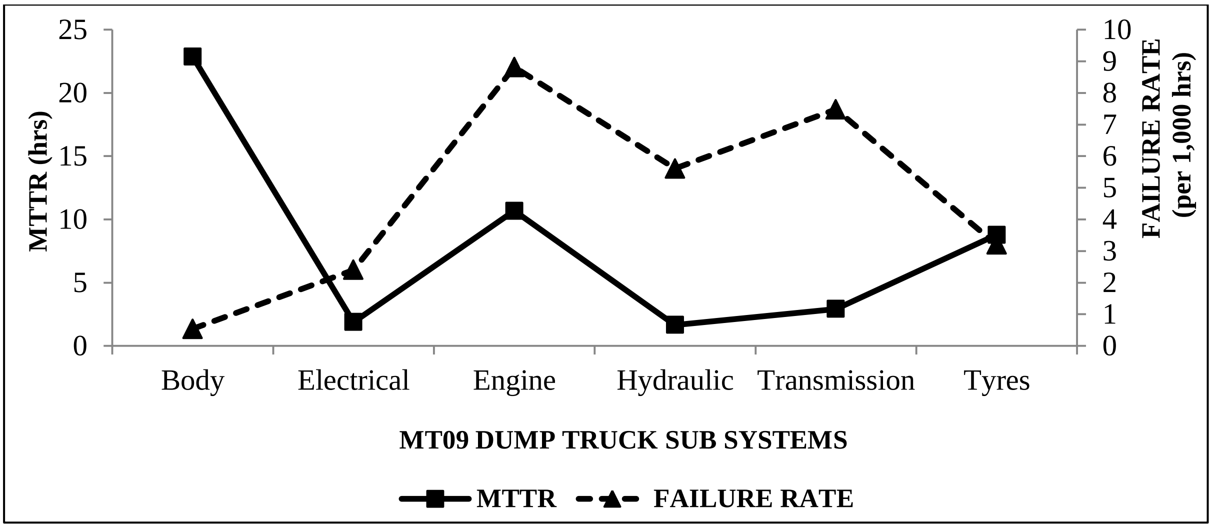

Figure 4.8: Comparison between MTTR and Failure rate for MT09 dump truck

At present, MT09 is awaiting machine overhaul and spares which cost $69 420 to procure as shown in Table 4.8.

Table 4.7: Required spares and their associated costs for MT09 dump truck

SPARES REQUIRED	**PROCUREMENT COSTS**
Engine	$38,000
Torque convertor	$21,420
Centre section	$10,000
TOTAL	**$69,420**

4.6.2 Failure and MTTR Data for MT11 Dump Truck

The distribution of rate of failures per sub system and the related MTTR for MT11 is described in Figure 4.9. Evidently the "transmission" has the most significant impact on MT11's availability because it has both the highest MTTR and failure rate. Therefore, failure data for this sub system was used to compute the optimum maintenance interval using the Reliability Analytics Toolkit (Morris, 2010).

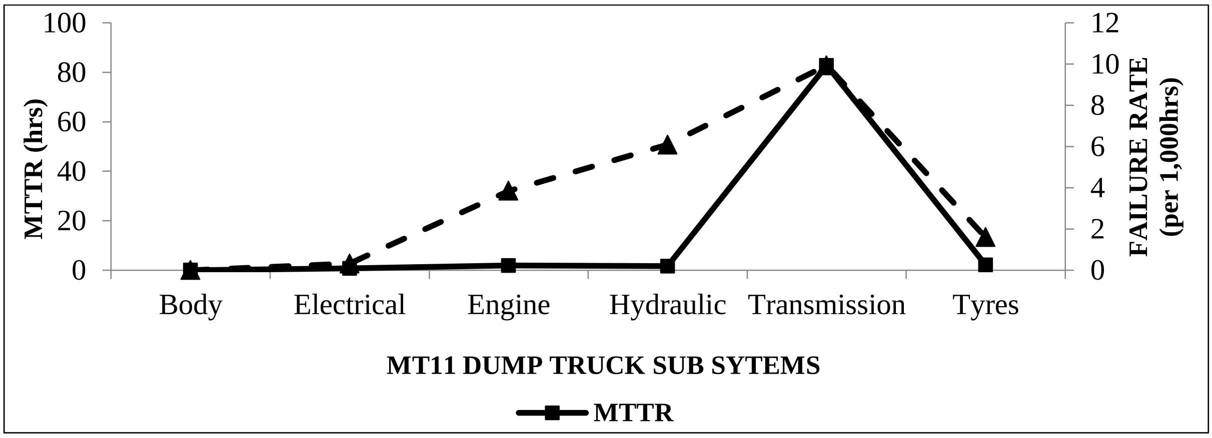

Figure 4.9: Comparison between MTTR and Failure rate for MT11 dump truck

Even though MT11 is a relatively new machine, as shown in Figure 4.8, this truck was decommissioned from operations in August 2015 because of the relatively high failure rates and MTTR of the transmission. Thus, making it more relevant to further process failure data of the transmission sub system and determine appropriate interventions.

4.6.3 Failure and MTTR Data for MTK02 Dump Truck

Figure 4.10 presents a comparison between rate of failure per sub system and MTTR for the MTK02. The distribution of failure rate and MTTR appears to be multifaceted. Therefore the "hydraulics" sub system was selected for reliability modelling because it appears to have the most significant impact on MTK02's availability since it has the 3rd highest MTTR value and also the 3rd highest failure rate.

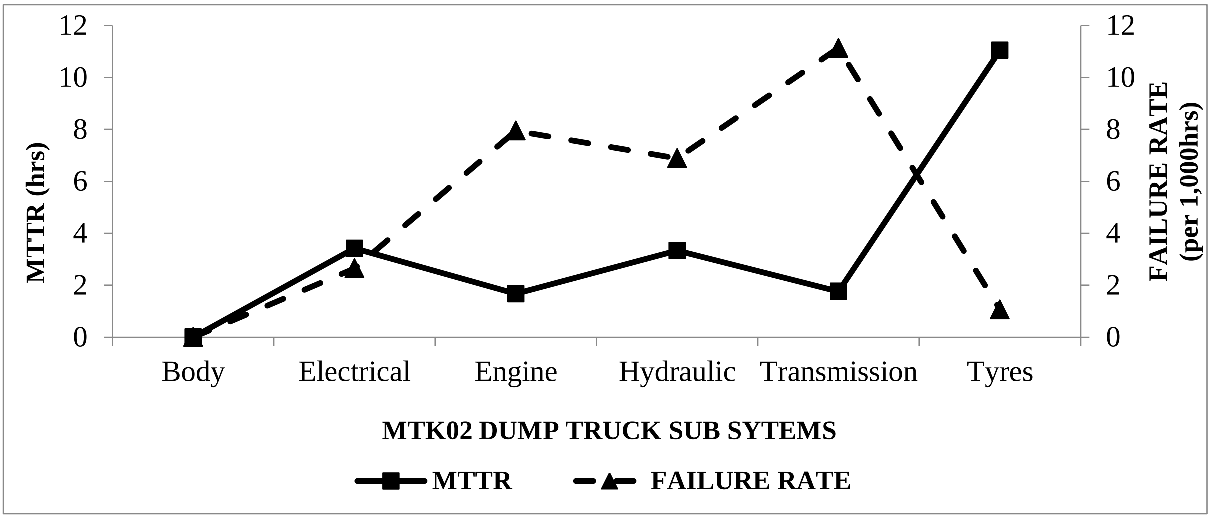

Figure 4.10: Comparison between MTTR and Failure rate for MTK02 dump truck

4.7 Mining Method Selection Data

A preliminary mining method selection process was performed in order to select an appropriate mining method for extraction of future undeveloped reserves by using the online UBC mining method selection tool.

Tables 4.9 to 4.14 describe the properties and information which was used in the selection process as determined by Edumine (1999).

4.7.1 Ore Body Shape

Table 4.9 presents the ore body geometry which describes the mineralisation of the HSI complex. The complex has a platy-tabular shape.

Table 4.8: General ore body shape classification

CATEGORY	DESCRIPTION
Equi-dimensional	Dimensions are of the same order in all directions
Platy-tabular	**Two dimensions are larger than the thickness**
Irregular	Dimensions are not consistent over very short distances

4.7.2 Ore Body Thickness

The thickness of a mineralisation is classified as shown in Table 4.10. The HSI complex ranges from “very narrow” to “narrow”.

Table 4.9: Ore body thickness classification

CATEGORY	THICKNESS
Very narrow	**Less than 3m**
Narrow	**3 to 10m**
Intermediate	10 to 30m
Thick	30 to 100m
Very thick	Greater than 100m

4.7.3 Ore Body Dip

Table 4.11 describes the different categories of ore body dip. The HSI complex’s general dip is 25^{o} therefore it is classified as “intermediate”.

Table 4.10: Ore body dip classification

CATEGORY	DIP
Flat	Less than 20^{o}
Intermediate	**20^{o} to 55^{o}**
Steep	Greater than 55^{o}

4.7.4 Grade Distribution

Table 4.12 indicates the categories which distinguish ore grade distribution. The HSI complex has “gradational” variation of grades.

Table 4.11: Grade distribution categories

CATEGORY	DESCRIPTION
Uniform	There is no significant variation from the mean grade at any point in the ore body.
Gradational	**Grade has a regional characteristic which gradually changes from one zone to another**
Erratic	Extreme grade fluctuations within short distances such that there is no distinctive pattern of grade variation

4.7.5 Ore Body Depth

Depth of a deposit is ranked according to the classifications highlighted in Table 4.13. The HSI complex is considered as a "deep" deposit.

Table 4.12: Classification of ore body depths from the surface

CATEGORY	DEPTH (m)
Shallow	0 to 100m
Intermediate	100 to 600m
Deep	**Greater than 600m**

4.7.6 Geotechnical Properties

The two geotechnical parameters where were considered in the mining method selection process are:

a) Rock Mass Rating (RMR), and
b) Rock Substance Strength (RSS).

The RSS is defined as the ratio of uniaxial compressive strength to major principal stress. Since no in-situ stress measurements have been done at NUG, the overburden confining pressure was considered as the major principal stress (Chishimba & Mundike, 2014). Table 4.14 describes the categories of RSS. The RSS for the hanging wall is "very weak", for the ore zone is "weak" and for the footwall is "medium".

Table 4.13: Categories for Rock Substance Strength

CATEGORY	ROCK SUBSTANCE STRENGTH
Very weak	**Less than 5**
Weak	**5 to 10**
Medium	**10 to 15**
Strong	More than 15

Table 4.15 presents the classification of the ore body based on RMR values. Using data from Appendix F, both the hanging wall and ore zone are considered as "medium" and the footwall is regarded as "strong".

Table 4.14: Categories for ore body depth

CATEGORY	RMR
Very weak	Less than 20
Weak	20 to 40
Medium	**40 to 60**
Strong	**60 to 80**
Very strong	80 to 100

4.8 Summary

This Chapter gave an account of data which was collected for further analysis using Chapter 3 as a guide for the data collection process. Rock mass classification was done after conducting rock sample collection and testing. Rock competency was established to increase from the footwall to the hanging wall. In addition, the shortest active life of secondary developments was computed as 340days. Meanwhile, the rated production capacity of the dump truck fleet was compared with planned production rate. It was identified that the fleet can surpass the planned production target. As a result, failure data of the fleet was evaluated in order to identify truck sub systems which must be further subjected to reliability modelling so that the overall fleet availability is increased. Lastly, mining method selection data was collected so that it is used as input data on the online UBC mining method selection tool.

CHAPTER 5: DATA ANALYSES AND RESULTS DISCUSSIONS

5.1 Introduction

Investigations were carried to query, collate and process the collected data so as to draw consequential findings from this study. Furthermore, scholarly deliberations were accomplished, at the researcher's discretion, such that the research questions postulated in Section 1.5 of Chapter 1 are meticulously and adequately answered. This Chapter also served to validate the data which was gathered and presented in the Chapter 4.

5.2 Production and Development Control

A number of calculations for angle of draw, interactive draw point spacing, rate of development and undercut dimensions were done after considering the inherent geotechnical conditions of the HSI complex.

5.2.1 Undercut Design

The undercut dimensions were determined using Equation 5.1, taking into consideration that the MRMR for the ore zone is 45 and the associated hydraulic radius being 23m, as highlighted in Section 4.3.7 of Chapter 4. In addition, the undercut has a length of 64m (Hakakwale, 2013):

$$Hydraulic\ radius = \frac{Area}{Perimeter} = \frac{L \times W}{2(L+W)} \qquad [5.1]$$

Since hydraulic radius is 19m and the undercut length is 64m, therefore minimum undercut width is:

$$Width = \frac{-2 \times 23 \times 64}{(2 \times 23) - 64} = 163.6m$$

Considering the current NUG mining layout and ore body geometry in the HSI complex, it is not feasible to induce caving by undercutting using the dimensions 64m × 163.6m. This is a clear indication that block caving is not suitable to exploit the HSI complex using the NUG development configuration. As a result, an alternative method was suggested in the later sections of this Chapter which can best extract this deposit.

Despite this assertion, block caving developments have already been excavated beyond the 6E position for 2720FT, 2870FT and 3020FT levels. NUG planning department resolved to conduct inclined undercutting as illustrated in Figure 5.1. Instead of undercutting from both trough drives, fan drilling and low charge blasting operations are done only in the southern trough drive. However, the blast holes are drilled such that they also cover the undercut region of the northern trough drive. The roof of the northern trough drive is enlarged prior to blasting from the southern trough as shown in Figure 5.1. Spacing of draw points were calculated and recommended for the inclined undercutting technique, even though the effectiveness of this undercutting method could not be validated due to unavailability of software resources (e.g. PFC 2D, PFC 3D, etc.). The total undercutting width is 10.4m as shown in Figure B-2 of Appendix B.

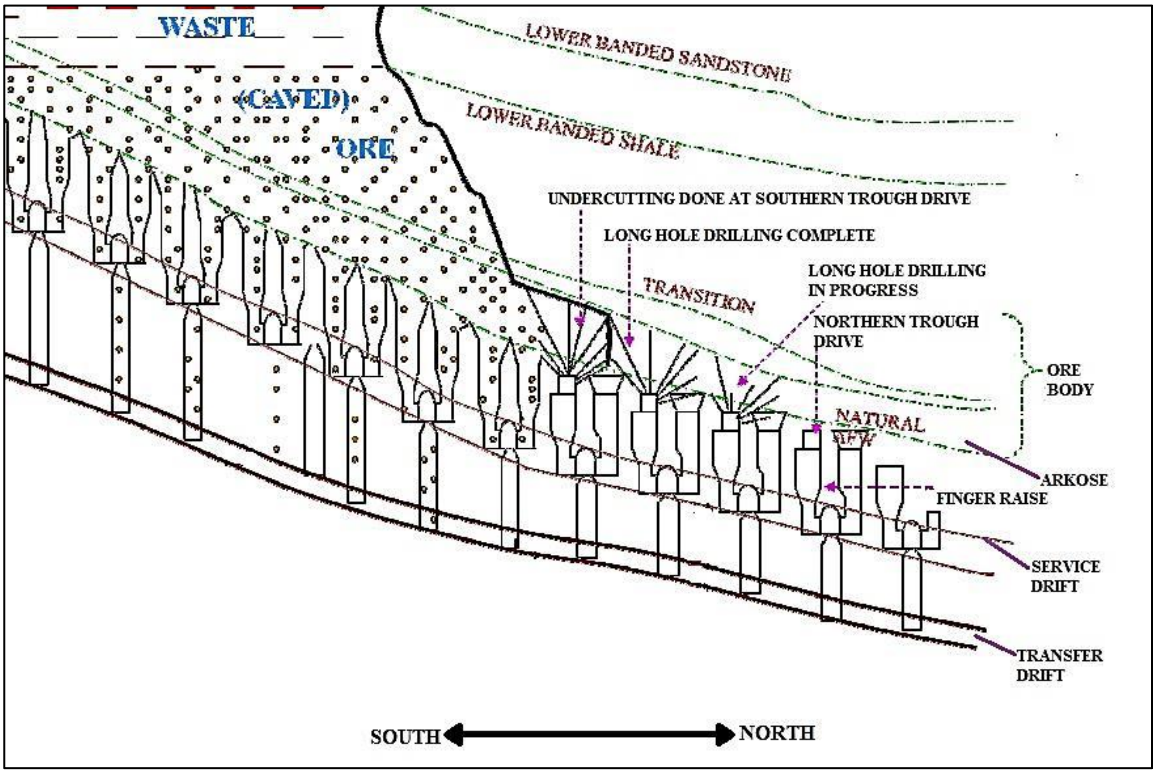

Figure 5.1: Proposed inclined undercutting technique for the HSI complex (KCM, 2014)

5.2.2 Interactive Draw Design

The vertical distance from undercut roof to hanging wall of the ore body for each block was considered as the height of interaction zone (HIZ), and the undercut face width as 10.4m, so that dilution entry into the scraper drifts is delayed as long as possible. Chishimba & Mundike (2014) determined that the angle of internal friction for Arkose to be 37^o, therefore, the angle of draw is 63.5^o by using Equation 2.11 highlighted in Section 2.5 of Chapter 2. The calculation of angle of draw is presented below.

$$\alpha = \frac{37}{2} + 45 = 63.5^o$$

After taking into account HIZ, angle of draw and undercut face width, the draw point spacing for each block was computed using Equation 2.10 which was also presented Section 2.5 of Chapter 2. Figure 5.2 illustrates a sketch that was used to determine the vertical distance from undercut roof to assay hanging wall of the ore body. HIZ was determined by summing up block thickness and vertical distance from undercut roof to natural footwall.

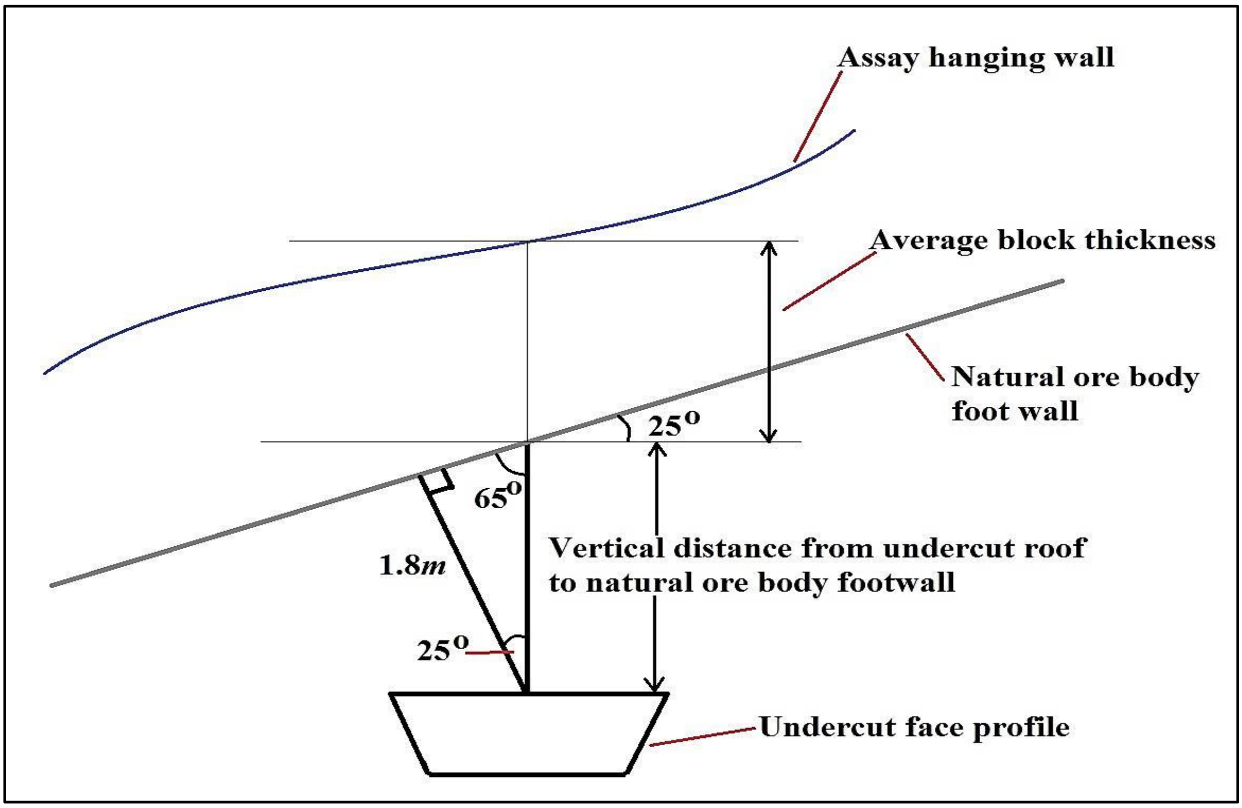

Figure 5.2: Sketch illustration of HIZ for any particular HSI complex block

Subsequently, Figure 5.3 indicates the distribution of draw point spacing for all the HSI complex blocks such that mode of draw becomes interactive and not isolated or isolated-interactive. It must be noted that calculation of draw point spacing for 2870/7EC block was not done since it was shown earlier in Section 4.2 of Chapter 4 that blending the block with the high grade blocks yields a low tonnage of contained Cu which is not beneficial to KCM.

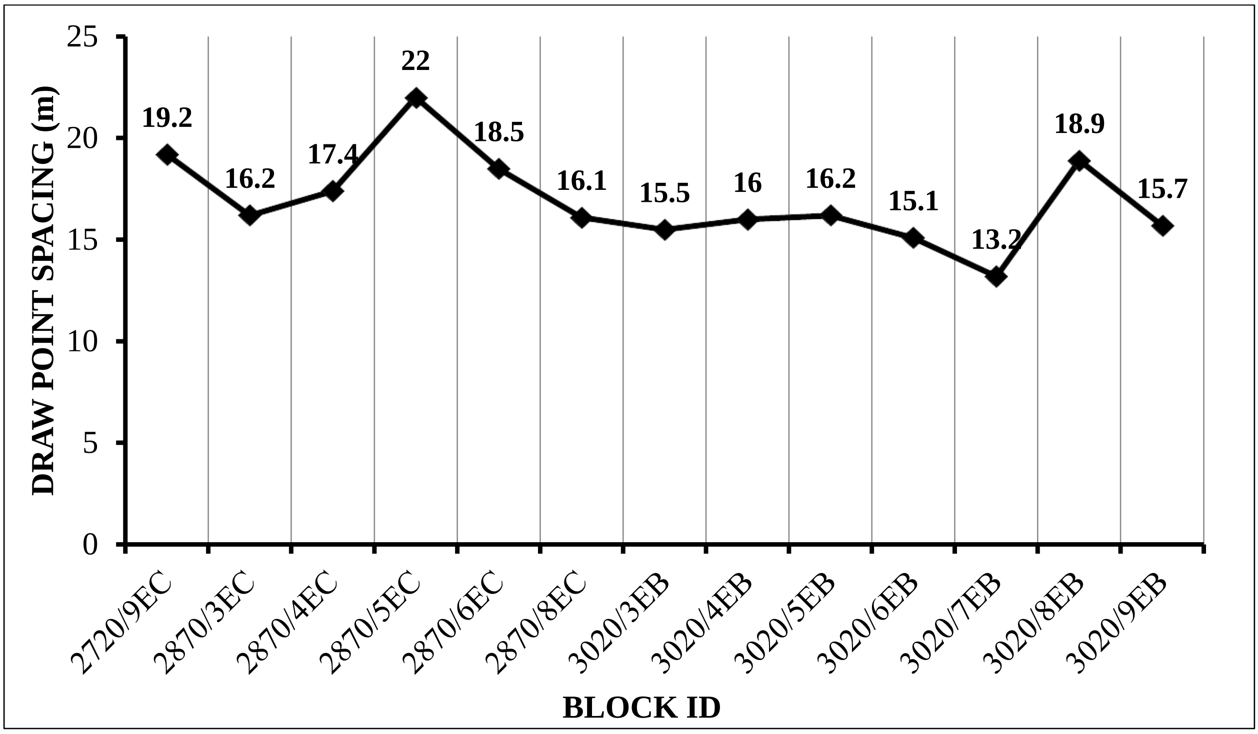

Figure 5.3: Distribution of recommended draw point spacing for interactive drawing

5.2.2 Dilution Entry in the Draw Zones

Equation 2.2 from Section 2.4.4 of Chapter 2 was used to estimate the stage when dilution begins to report to the scraper drifts provided that drawing operations are producing interactive zones. Figure 5.4 illustrates the tonnages drawn at DEP for all the blocks considering that height of the draw zone is equated to vertical distance between production levels and also that the DCF is unity. DCF was assigned the value of 1 with the intention of computing draw parameters which delay dilution entry as long as possible (i.e. maximised DEP values). Correspondingly, swell factor was assumed to be 1.12 as suggested by Laubscher (1994) for medium fragmentation of the caved mass.

Once tonnages at DEP have been drawn for any particular block, meticulous sampling and assaying must be done periodically to monitor the discharge of dilution into scraper drifts up to the point when drawn grade has fallen below the cut-off grade.

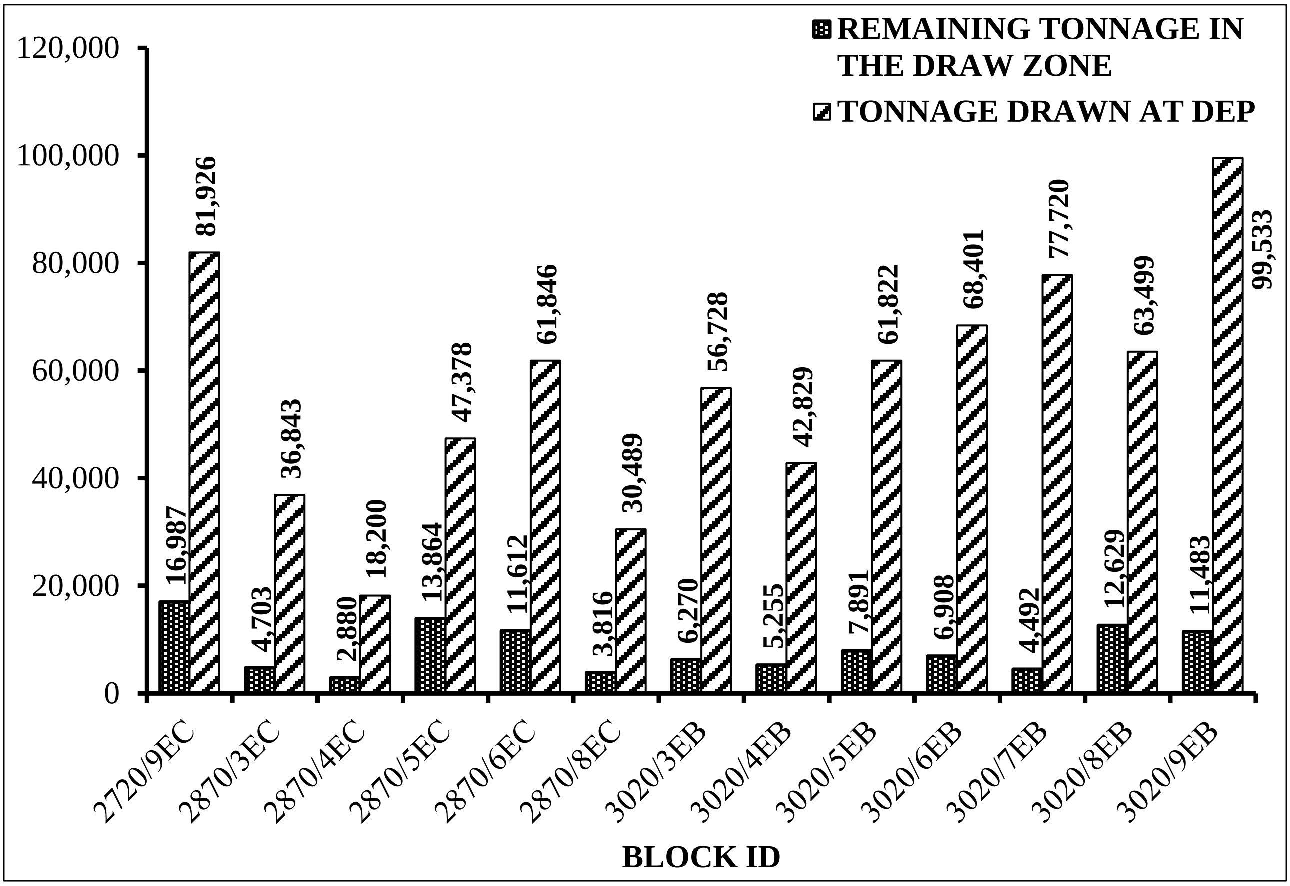

Figure 5.4: Tonnages at DEP and remaining tonnages for the HSI complex blocks

5.2.3 Optimal Buffer Mineral Reserves

Conventional practice in the management of mineral reserves involves maintaining the largest possible inventory of reserves so that the time between development and production is as long as possible. This time lag is essentially the maximum period over which a mine can continue to produce at a given production rate provided that all development operations cease immediately.

However there are a number of dynamics to this conventional practice of mineral reserves management. One important aspect of these dynamics is that maintaining a large mineral reserve inventory depends on existing costs of development. Logically it is unjustifiable to perpetuate the large mineral reserve inventory "philosophy" in a situation where the costs of development are significantly high.

Although the converse is true, it must also be noted that there is another important aspect to the dynamics of the traditional practice of mineral reserves management. This aspect involves limiting the development of mineral reserves in unstable ground because some development ends may require to be re-mined, once or more, as a result of partial or complete closure of the excavations between the time they are mined and the time they are utilised. One approach to resolve this ordeal involves increasing support density of development headings. NUG has adopted this approach and a total cost of $173,231.46 has been incurred in supporting secondary developments in the HSI complex (KCM, 2016). This approach adversely results in incurrence of support costs for developments which are not yet being utilised. Therefore, with the aim of reducing this support cost, an alternative approach was suggested whereby developments are made available and also utilised before the end of their duty life.

Optimal buffer mineral reserves (OBMR) are defined as the maximum reserves which can be developed and exploited before lapsing of the developments' stand-up time. The OBMR present the opportunity to provide an alternative to increasing support density in the developments so as to avoid pre-mature collapse of developments. Section B of Table 3.1 in Chapter 3 and Equation 2.9 highlight the parameters which were used to calculate OBMR. In addition, previous KCM cave production records for the LOB blocks have shown that the highest mining block recovery factor achieved is 1.49 (i.e. 149%). This value was used to calculate the most conservative tonnage of OBMR.

Bearing in mind that the production rate for the HSI complex is 308,500t per year (KCM: 18 month production plan, 2014) and the shortest stand-up time of secondary developments is 340 days (i.e 0.93years), therefore the OBMR is:

$$OBMR = \frac{308\ 500t\ per\ year \times 0.93\ years}{1.49} = 192\ 553t$$

5.2.3.1 Empirical Support Design For OBMR

The traditional empirical support design method by Barton (1971) was employed for application in the optimal BMR. Table 4.4 of Chapter 4 showed a Q-rating of 8.125 for ARK. The technical guidelines for the support design are specified in Table 5.1.

Table 5.1: Technical guidelines for empirical support design (Barton, 1971)

	PERMANENT SUPPORT	**TEMPORARY SUPPORT**
ROOF	ESR is not changed Q is not changed	Increase ESR to 1.5 ESR Q is increased to $5Q$
WALLS	For $Q > 10$: $Q_w = 5Q$ For $0.1 < Q < 10$: $Q_w = 2.5Q$ For $Q < 0.1$: $Q_w = 1.0\ Q$	Increase ESR to 1.5 ESR $Q_w = 5Q_w$

An excavation to support ratio (ESR) of **3** was used since the secondary developments will be temporary openings until the end of their stand-up time.

The equivalent dimension (D_e) and rock mass quality (Q) were calculated as shown in Table 5.2. The biggest dimensions of all secondary developments in ARK were used as this produces the worst case scenario in terms of support design. The excavation dimensions which were used are 2.4m x 2.4m as shown in Table G-1 of Appendix G.

Table 5.2: Empirical support specifics for secondary developments in Arkose rock (after Barton, 1971)

<table>
<tr><th colspan="2"></th><th>PERMANENT SUPPORT</th><th>TEMPORARY SUPPORT</th></tr>
<tr><td rowspan="2">ROOF</td><td>D_e</td><td>$D_e = \frac{Excavation\ span}{ESR} = \frac{2.4}{3} = 0.800$</td><td>$D_e = \frac{Excavation\ span}{1.5 \times ESR} = \frac{2.4}{1.5 \times 3} = 0.533$</td></tr>
<tr><td>Q</td><td>$Q = 8.125$</td><td>$Q = 5 \times 8.125 = 40.625$</td></tr>
<tr><td rowspan="2">WALLS</td><td>D_e</td><td>$D_e = \frac{Excavation\ height}{ESR} = \frac{2.4}{3} = 0.800$</td><td>$D_e = \frac{Excavation\ height}{1.5 \times ESR} = \frac{2.4}{1.5 \times 3} = 0.533$</td></tr>
<tr><td>Q</td><td>$Q_w = 2.5 \times 8.125 = 20.313$</td><td>$Q_w = 5 \times 20.313 = 101.565$</td></tr>
</table>

The permanent and temporary support categories for secondary developments made in ARK are indicated in the empirical chart shown in Figure 5.5.

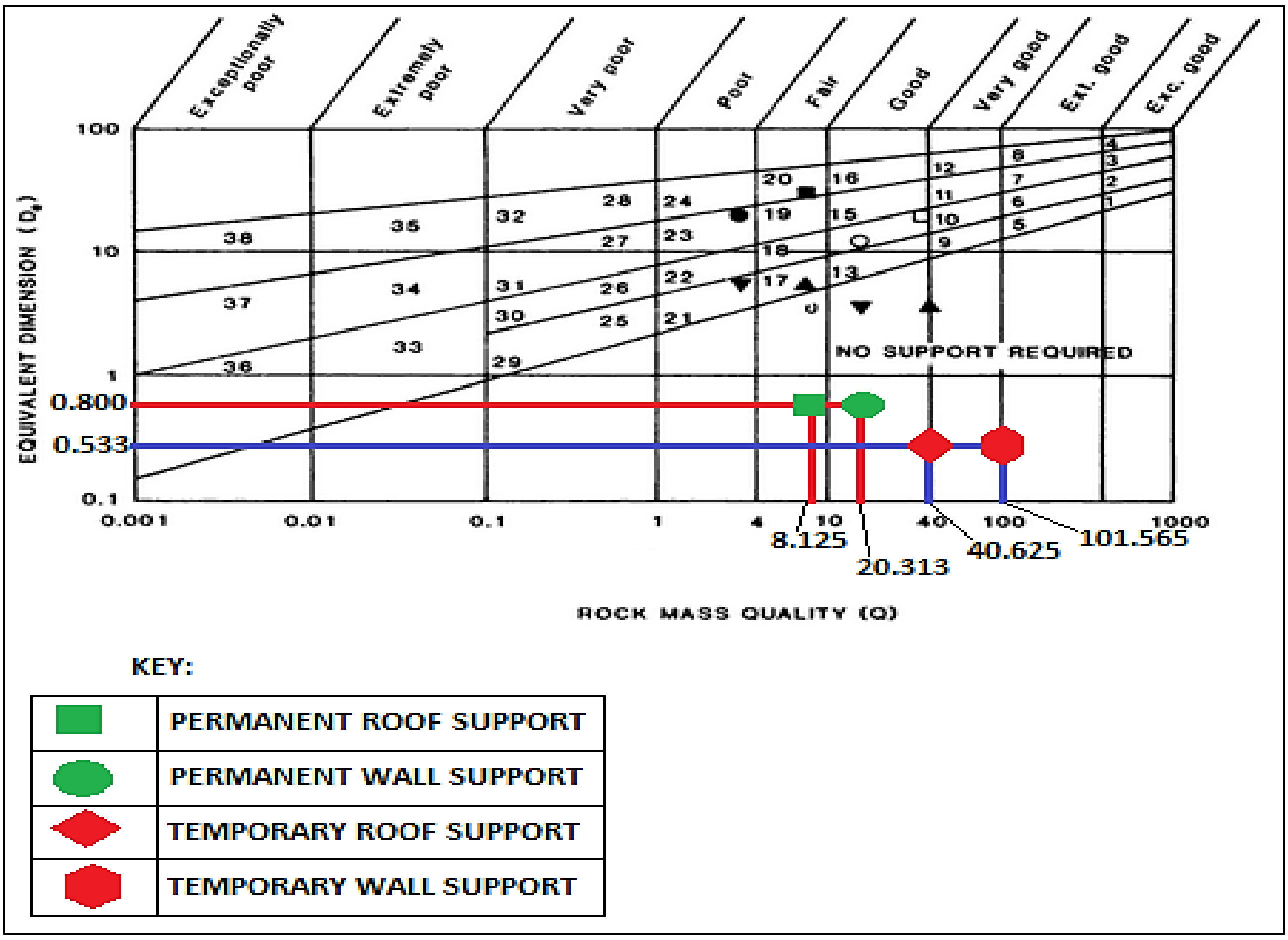

Figure 5.5: Empirical support for secondary developments in Arkose strata (Barton, 1974 and Afrouz, 2000)

As shown in Figure 5.5, both temporary and permanent support empirical design for secondary developments in ARK fall in the **"NO SUPPORT REQUIRED"** region of the empirical graph. This result also concurs with the result shown in Figure 4.6 in Section 4.3.6 of Chapter 4. Therefore, bolt and anchor lengths were computed which are meant to mitigate potential fall of ground in areas where unwanted geotechnical conditions like roof spalling and key blocks are observed.

5.2.3.1.1 Recommended bolt and anchor lengths

The bolt and anchor lengths computed in this Section can be utilised to abate undesirable ground conditions resulting from overstress regime along secondary developments (e.g. key blocks, spalling, slabbing, yielding, fracturing or rock acoustics).

For roof:

$$Bolt\ length = 2 + \frac{0.15 \times Roof\ span}{ESR} = 2 + \frac{0.15 \times 2.4}{3} = 2.12m$$

$$Anchor\ length = \frac{0.40 \times Roof\ span}{ESR} = \frac{0.40 \times 2.4}{3} = 0.32m$$

For walls:

$$Bolt\ length = 2 + \frac{0.15 \times Height}{ESR} = 2 + \frac{0.15 \times 2.4}{3} = 2.12m$$

$$Anchor\ length = \frac{0.35 \times Height}{ESR} = \frac{0.35 \times 2.4}{3} = 0.28m$$

5.2.3.2 Cost-Benefit Implication of OBMR

Two utility options for mineral reserves management were considered:

A) Sustaining the longest possible period between development and production; and
B) Providing reserves when they are needed such that they are extracted just-in-time before expiration of their stand-up times.

Figure 5.6 describes the similarities and contrasts of both options. Option A will result in the incurrence of $173,231.46 for supporting developments while no support is required for Option B. Therefore, Option B results in development support cost savings.

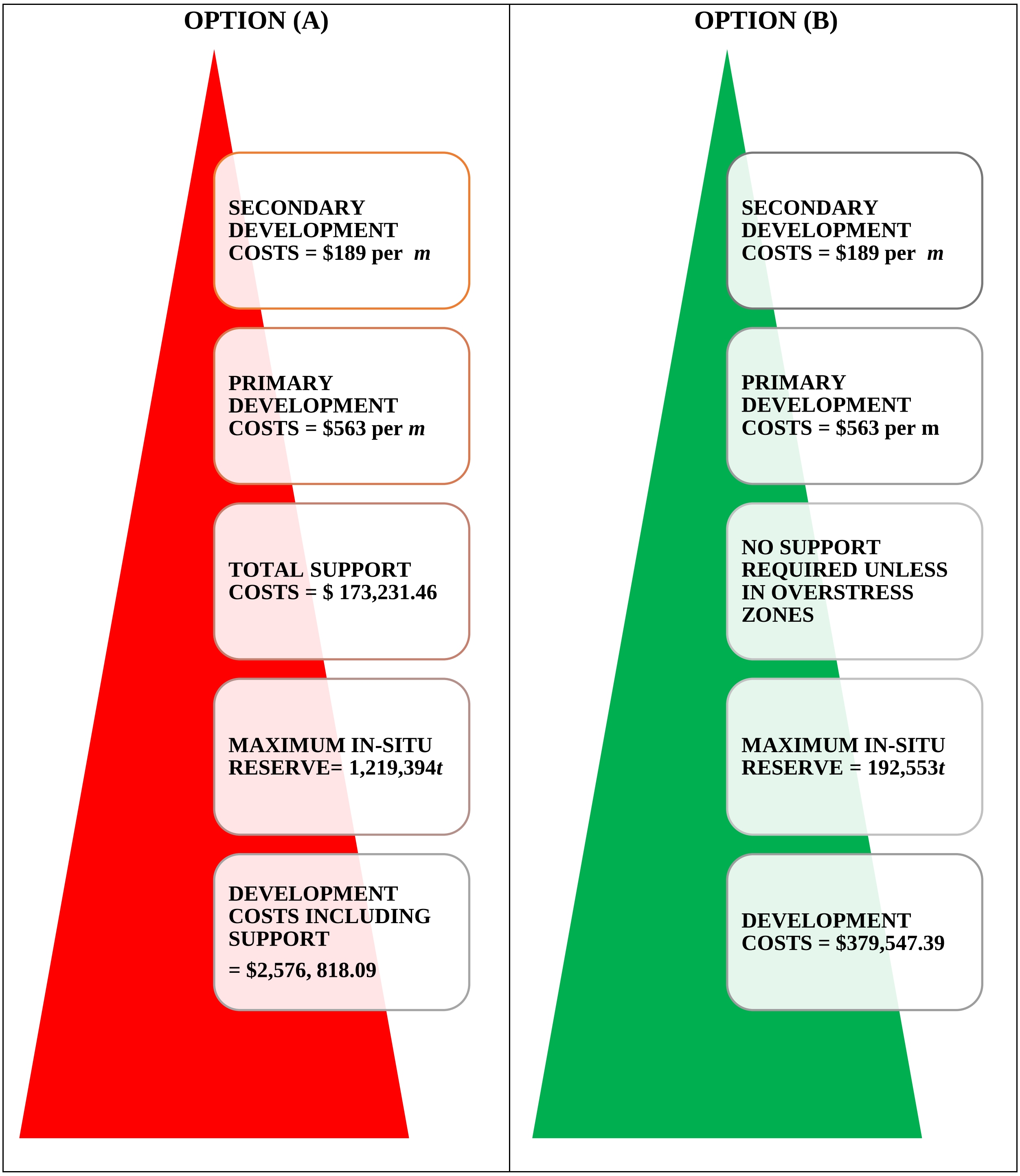

Figure 5.6: Contrasts and similarities between the two options for mineral reserve management

5.3 RAM analysis of NUG fleet

The evaluation of failure data for NUG dump truck fleet, in Section 4.5 of Chapter 4, facilitated the identification of dump truck sub systems with the most impact on machine availability. The data for cumulative time-between-failures (TBF) of the identified sub systems were input in the Reliability Analytics Toolkit. Consequently, reliability modelling was performed at 95% confidence intervals so that an appropriate maintenance interval for the chosen sub system is recommended. For all the selected maintenance intervals, a target reliability of 75% was chosen since it coincides with the planned machine availabilities of 75% at NUG.

5.3.1 Reliability assessment for MT09 engine sub system

The reliability of the engine sub system for the MT09 truck was modelled and an appropriate maintenance interval was recommended even though the truck is awaiting overhaul and engine rebuild. However, this suggested interval must be cancelled once machine overhaul has been performed. Figure 5.7 illustrates the computed reliability curve for MT09 engine using the Reliability Analytics Toolkit.

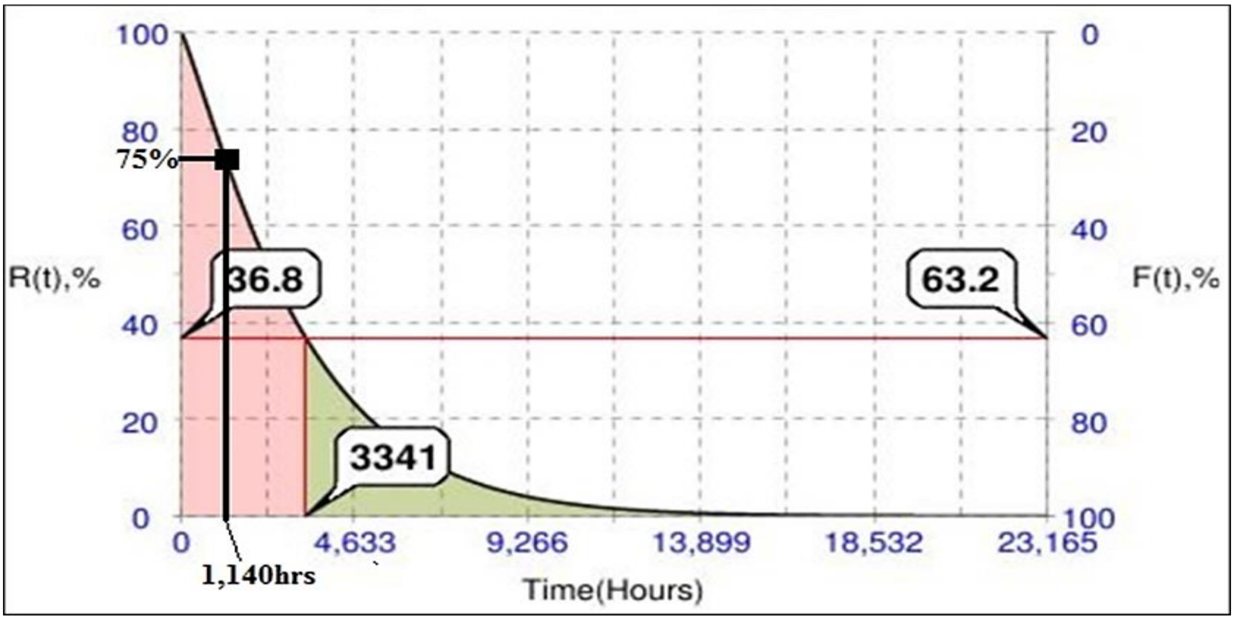

Figure 5.7: Reliability curve for MT09 engine sub system

The displayed points on the graph merely indicate a position on the curve where reliability is at 36.8%. Despite this, time associated with 75% reliability was determined from the reliability modelling output displayed in Table I-1 of Appendix I. Hence the maintenance interval for the engine sub system which results in 75% reliability is **1,140*hrs***.

5.3.2 Reliability Assessment for MT11 transmission sub system

It was observed that the transmission sub system MTTR for the MT11 truck was significantly higher than the MTTR for MT09 and MTK02. This comparison is illustrated in Figure 5.8. Furthermore, it was inferred that the MTTR disparity illustrated in Figure 5.8 is a result of low manpower proficiency in diagnosis, debugging and servicing of MT11 transmission since MT11 is relatively new. Henceforth, KCM must send a number of artisans to Sandvik for training on diagnosis, debugging and servicing of the transmission for the Sandvik EJC533 dump truck. This will increase the artisans' proficiency to repair transmission failures timeously and ultimately increase the MT11 dump truck availability.

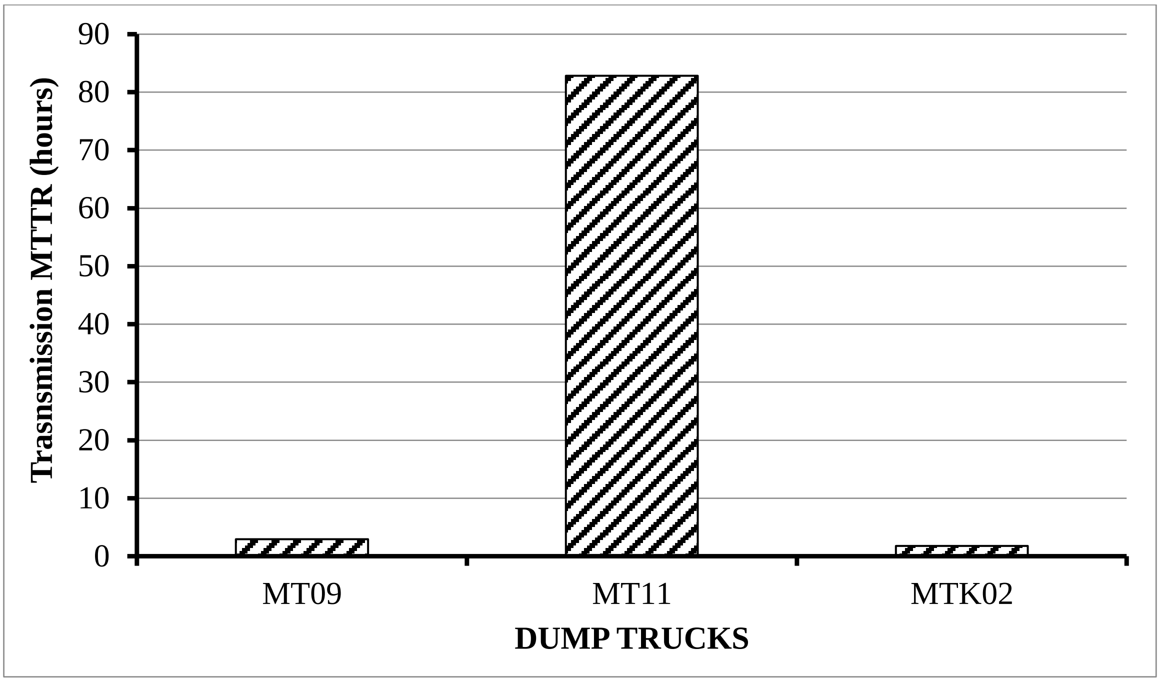

Figure 5.8: Comparison of transmission MTTR for NUG dump trucks

Figure 5.9 illustrates the reliability curve for MT11 transmission sub system. Using, information processed by the Reliability Analytics Toolkit, as shown in Table I-2 of Appendix I, the suggested maintenance interval for MT11 transmission is **2,833*hrs***.

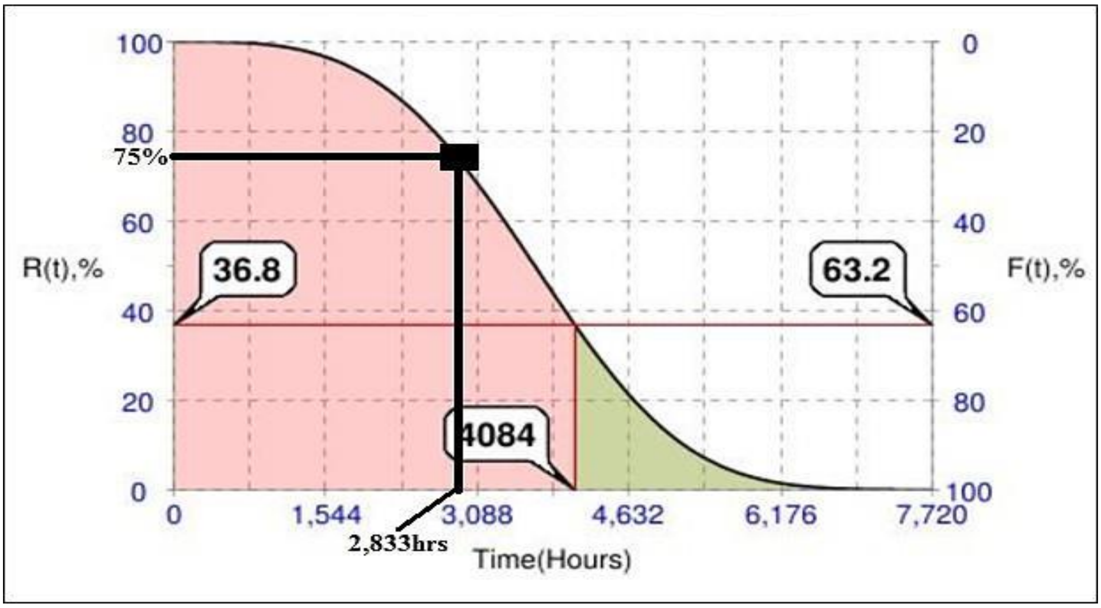

Figure 5.9: Reliability curve for MT11 transmission sub system

5.3.3 Reliability assessment for MTK02 hydraulics sub system

Figure 5.10 indicates the reliability curve for the MTK02 hydraulics sub system. The maintenance interval which coincides with 75% reliability is **924*hrs***, as shown in Table I-3 of Appendix I.

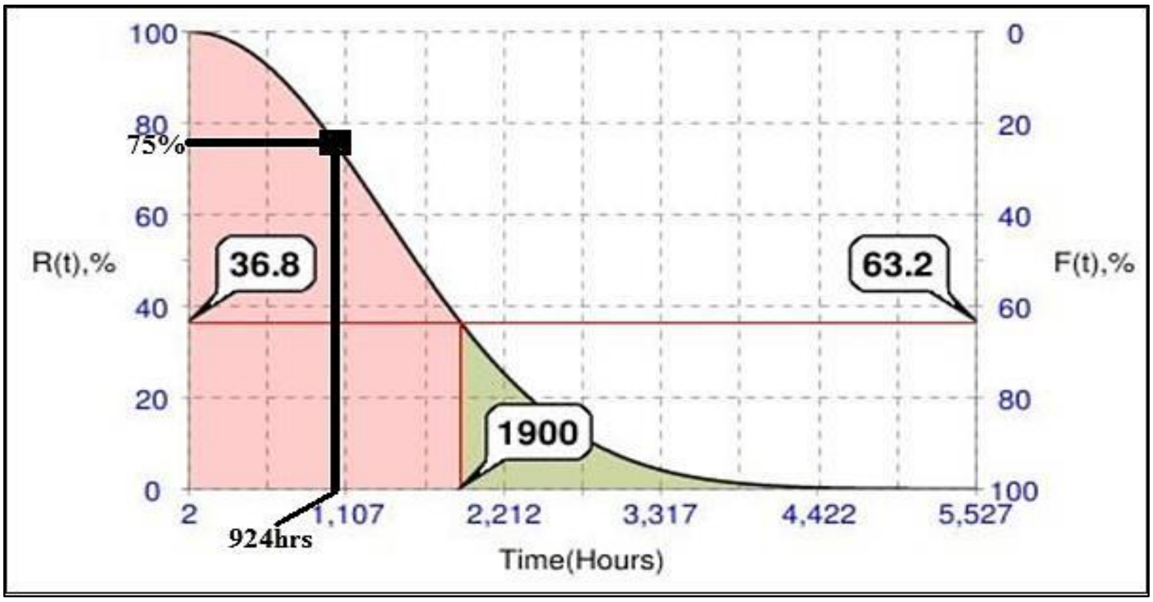

Figure 5.10: Reliability curve for MTK02 hydraulics sub system

5.4 Mining Method Selection

Section 4.7 of the Chapter 4 indicated data which was used to select the mining method using the online UBC mining method selection tool. Figure 5.11 illustrates the rankings of different mining methods with correspondence to the geotechnical characteristics, geometry and grade distribution of the HSI complex. Cut and Fill stoping, and also, Longwall mining methods were established as the two most technically superior methods to extract the complex. Figure 5.11 also illustrates that block caving is the least technically feasible mining method to exploit the complex. Hence, there is an urgent need to re-adapt the current method to another one more suited to the deposit.

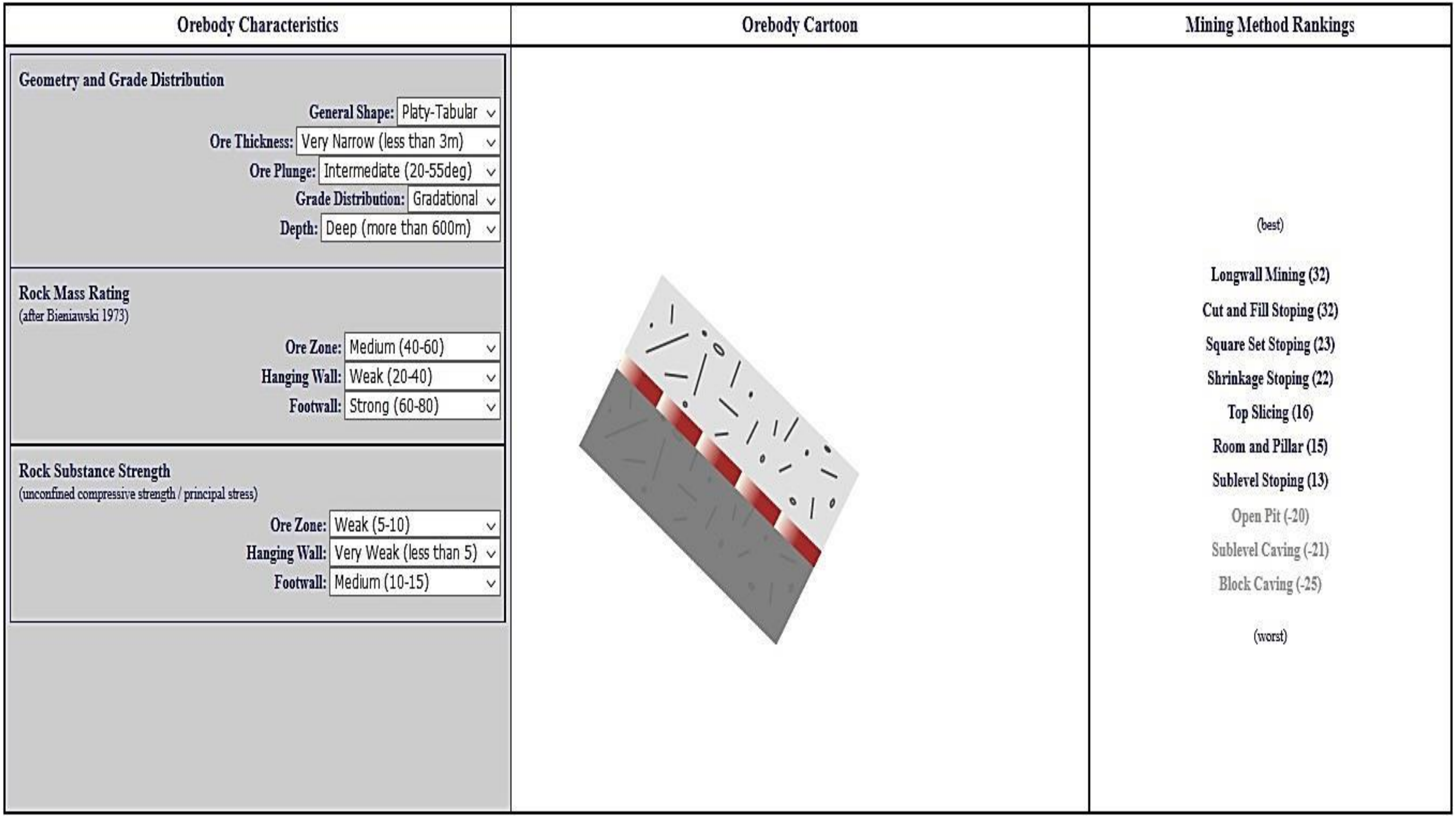

Figure 5.11: Rankings of mining methods after using the UBC tool

5.4.1 Evaluation of the two most technically superior methods

The documented benefits and drawbacks of the two methods were reviewed in order to identify the best method. Table 5.3 describes a comparison of the two selected methods. Since the HSI complex is thin and rich, the key parameters which were considered are:

i. Mining productivity; and
ii. Operating costs.

Table 5.3: Relative cross-comparison of the two selected mining methods

	LONGWALL MINING	CUT AND FILL STOPING
BENEFITS	• Amenable to mechanisation therefore minimised stope turn-around time. • Allows a degree of selectivity for thickness greater than 4m because multiple lifts can be done. • The roof can collapse easily at greater depths, hence, minimum risk of air blasts. • Down-dip extraction provides gravity assist. • Relatively higher mining productivity per man shift due to larger production face dimensions and lower amount of non-productive work like filling. • It is less difficult to standardise operations because of relatively lower amount of non-productive operations required for extraction. • Relatively lower operating cost due to fewer non-productive operations.	• Relatively lower dilution because it allows selective stope development. • Adaptable to variations of grade and rock mass conditions. • Relatively higher gravity assist potential due to flexibility of the method. • Allows extensive sampling for each mining cycle due to flexible and selective operations. • Low occurrences of large-scale uncontrolled ground movement due to small openings. • Requires relatively minor equipment investment.
DRAWBACKS	• Requires a significant amount of pre-production investment. • Requires perpetual assessment of stress regime so as to mitigate undesirable geotechnical conditions. • Higher dilution can occur for thickness less than 1m.	• Lower stope productivity due to limited production face dimensions. • Greater costs of operation because of higher amount of non-productive work required for extraction (e.g. backfilling). • Difficult to standardise non-production work due to alternating stope sequencing. • Higher safety risks due to potential of ground stability because of fill which can settle improperly. • Lower productivity per man shift due to larger labour force required for production.

From the comparison Table 5.3, both methods can provide high recovery-low dilution extraction. Despite this, the suggested method is Longwall mining because it provides relatively higher productivity per man shift such that early capital recoupment is realised. In addition, operating costs are relatively lower than those for Cut and Fill stoping due to lesser amount of auxiliary operations required for production. The relatively high pre-production capital investment required for Longwall mining can be offset by relatively lower operating costs. Ultimately, at mine closure or project decommissioning the capital invested (e.g. production equipment) will still hold a salvage value for potential re-sale or re-allocation to other mine sites. However, it is acknowledged that in-depth evaluation of net present values for access and ventilation developments is needed for one to arrive at a more conclusive decision. This process falls outside the scope of this study, as a result it is recommended as further research work to be done.

5.5 Economic Evaluation

Calculations of Earnings before Interests, Taxes, Depreciation and Amortisation (EBITDA) were done as shown in Appendix J. Table 5.4 presents the operating cost parameters used in these calculations. Implementation of the computed interactive draw and machine reliability parameters, proposed in Section 5.2 and 5.3 of this Chapter, yields a net discounted EBITDA of $63,006,898.32 with an associated life-of-mine of at least 2.42 years considering only tonnages at DEP.

Table 5.4: Operating cost elements which were used for EBITDA calculations

COST ELEMENT	UNIT	AMOUNT
MINING	$/t	33.95
CONCENTRATING	$/t	307.06
TAILINGS LEACH PLANT	$/t	1,785.75
SMELTER	$/t	524.04
ADMINSTRATION AND ENGINEERING	$/t	724.45
TOTAL	**$/t**	**3,375.25**

5.6 Summary

Inducing caving by employing the traditional design by Laubscher (2000) is not achievable due to the present NUG development configuration since the hydraulic radius for Arkose of 19m requires a mining caving area with dimensions 64m $\times$ 163.6m. Despite this a unconventional inclined undercutting technique was proposed which must be validated by trial mining before full scale implementation. Interactive draw parameters were defined per block. In addition, an analysis of the NUG dump truck fleet identified that the transmission MTTR for MT11 is significantly higher than that for MTK02 and MT09. Lastly, the current block caving was shown to be the least technically favoured method for extracting future deposits of the HSI complex. Cut and Fill stoping, and also, Longwall mining have been established as the technically superior mining methods. Following a comparison of the two methods, Longwall mining was identified as the best method.

CHAPTER 6: CONCLUSIONS AND RECOMMENDATIONS

6.1 Conclusions

The sub-objectives stated in Section 1.3.2 of Chapter 1 were linked to the deduced study conclusions.

- NUG mine documentation was evaluated thoroughly as well as scholarly knowledge on caved mass flow in block caving, rock mass classification systems, mining method selection techniques and RAM modelling for dump trucks. This review process enabled the researcher to gain intimate knowledge of all the study variables such that a sufficient research design was formulated in Chapter 3. The whole of Chapter 2 is a description of the literature which was reviewed and utilised in the study.
- The 2820/7EC block must not be considered for blending purposes because it was shown that if blended with high grade blocks, the overall yield of contained Cu is lower than the alternative of just regarding the block as waste. The traditional undercut design based on Laubscher (2000) is not feasible since the present developments do not allow inducing caving by undercutting 64m $\times$ 163.6m dimensions. However, NUG has proposed an inclined undercutting technique illustrated in Figure 5.1. This technique requires validation by either sandbox modelling and/or trial mining using the stipulated draw point spacing indicated in Figure 5.3 for each block. In addition, the angle of draw must be restricted to 63.5^{o} so as to further aid in interactive draw operations. The specified draw parameters will result in extracting DEP tonnages shown in Figure 5.4 as per given block. Sampling and assaying should be intensified after the DEP tonnages have been drawn so as to monitor the diluted grades being discharged into the scraper drifts. The net discounted EBITDA associated with extracting the HSI complex is $63,006,898.32 over a life of mine of 2.42 years after considering DEP tonnages only.
- The buffer reserves available for production at any given time must not exceed 192,553t since the annual production rate is 308,500 tonnes per year and the minimum stand-up time of secondary developments is 340 days. This will save KCM $173,231.46 for supporting secondary developments which are yet to be utilised. The developments made in the buffer reserves were determined to fall in the “NO

SUPPORT REQUIRED" of the empirical graphs by Barton (1971) and Bieniawski (1989). However, in cases where undesirable geotechnical conditions are observed in these reserves, recommended bolt and anchor lengths for the roof are 2.12m and 0.32m respectively. While, proposed bolt and anchor lengths for the walls are 2.12m and 0.28m respectively.

- MT11 dump truck's transmission sub system will attain the budget 75% reliability if it is serviced after 2,833*hrs* of operation. MTK02 dump truck's hydraulics sub system will also reach the same reliability if it is serviced after 924*hrs* of utilisation. Lastly, MT09 dump truck's engine will reach 75% availability if serviced after 1,140*hrs*. Table 4.7 defines the transmission, hydraulics and engine sub systems for MT11, MTK02 and MT09 dump trucks. Despite this, MT09 is due for overhaul and engine re-build which costs $69,420. In addition, NUG mobile equipment artisans must be sent to Sandvik for diagnosis and debugging training of the transmission for the Sandvik EJC533 dump truck in order to improve their maintenance and repairing proficiency of the MT11 truck.
- The current block caving mining method is not the best technique for the HSI complex as evidently shown by the results from the UBC tool by Edumine (Figure 5.11). Block caving is the least suitable method as indicated by this tool. Furthermore, minimum caving undercut dimensions are too big for NUG mine layout, from 1 central up to 6E position, on all HSI complex production levels. As a result, adaptation of the current mining method to Longwall mining technique is essential for exploitation of future HSI complex reserves.

6.2 Recommendations

- ➢ The proposed undercutting technique by NUG planning department must first be validated by either trial mining or a sand box model on a scale of 1:30 and/or computer simulations with specialised software like Particle Flow Code (PFC) 2D, PFC 3D, Abaqus 3D.
- ➢ Extraction of the complex must be carried out using the stated drawing rates indicated in Table 2.1 and the specified interactive draw parameters (i.e. Figure 5.3 for draw point spacing and 63.5^{o} angle of draw).
- ➢ Stand-up time of secondary must govern buffer mineral reserves such that support costs are reduced.

- Tyre stock levels, underground, must be computed based on economic order quantities for the NUG truck fleet such that tyre MTTR for trucks is reduced by avoiding long delays of moving tyres from the surface to underground.
- The calculated maintenance intervals for the chosen dump truck sub systems must be adhered to such that truck availabilities are increased, and ultimately the actual tonnages are maximised. In addition, NUG artisans must be sent to Sandvik for training on transmission debugging and servicing of the EJC533 dump truck such that MTTR of transmission is reduced.
- Redundancy of the NUG fleet must be analysed for optimum allocation of equipment since the rated capacity of the trucks significantly surpasses the planned production targets.
- Evaluation of net present values of development costs for the Longwall and Cut-and-fill methods must be done to further refine the mining method decision since it is highly critical and irreversible decision once it has been implemented. Computer modelling using softwares like Datamine, Surpac or Vulcan will aid in this process.

REFERENCES

Afrouz, A.A., 2000. *Practical Handbook of Rock Mass Classification Systems and Modes of Ground Failure*. Boca Raton, Florida: CRC Press.

Allahkarami, Z., Sayadi, A.R. & Lanke, A., 2016. Reliability analysis of motor system of dump truck for maintenance management. In U. Kumar, A. Ahmadi, A.K. Verma & P. Varde, eds. *Current Trends in Reliability, Availability, Maintainability and Safety*. Springer International Publishing. pp.681-88.

Azadeh, A., Osanloo, M. & Ataei, M., 2010. A new approach to mining method selection based on modifying the Nicholas technique. *Applied Soft Computing*, 10, pp.1040-61.

Bartlett, P.J., 1992. The design and operation of a mechannized cave at Premier Diamond Mine. In *Massmin 2000*. Brisbane, 1992. AusIMM.

Barton, N.R., 1971. *A model study of the behaviour of excavated slopes*. University of London, Imperial College of Science and Technology: Ph.D. Thesis.

Barton, N.R., 1974. A review of the shear strength of filled discontinuities in rock. In *Norwegian Geotechnical Institute*. Lisbon, 1974. Oslo: Norwegian Geotech Inst.

Bieniawski, Z.T., 1976. Rock mass classification in rock engineering. In *Exploration for rock engineering proc. of the symp.* Cape Town, 1976.

Bieniawski, Z.T., 1989. *Engineering rock mass classifications*. New York: Wiley.

Birolini, A., 2007. *Reliability Engineering, Theory and Practice*. 5th ed. Springer International Press.

Boshkov, S.H. & Wright, F.D., 1973. Underground mining systems and equipment. In B. Cummins & A. Given, eds. *SME Mining Engineering Handbook*. New York: SME-AIME.

Carter, P.G., 2011. Selection process for hard-rock mining. In P. Darling, ed. *SME Mining Engineering Handbook*. Colorado: Society for Mining, Metallurgy and Exploration Inc. pp.357-76.

Castro, R.L. & Parades, P.S., 2014. Empirical observations of dilution in panel caving. *Journal of the Southern African Institute of Mining and Metallurgy*, 114, pp.455-62.

Castro, R.L., Vargas, R. & de la Huerta, W., 2012. Determination of draw point spacing in panel caving: A case study at the El Teniente Mine. *Journal of the Southern African Institute of Mining and Metallurgy*, 112, pp.871-76.

Chishimba, D. & Mundike, S., 2014. *Ground Control Management Plan Revision No. 2*. KCM Standard Operating Procedures. Chingola: Unpublished Reports Konkola Copper Mines.

Cokayne, E.W., 1998. Sublevel Caving: An Introduction. In R.E. Gertsch & R.L. Bullock, eds. *Techniques in Underground Mining*. 1st ed. Littleton: Society for Mining, Metallurgy and Exploration, Inc. pp.616-17.

Deere, D.U., 1989. *Rock quality designation (RQD) after 20 years*. Vicksburg: MS: Waterways Experimental Station U.S. Army Corps Engrs Contract Report GL-89-1.

Deere, D.U., Hendron, A.J., Patton, F.D. & Cording, E.J., 1967. Design of surface and near surface construction in rock. In Fairhurst, C., ed. *Failure and breakage of rock, proc. 8th U.S. symp. rock mech.* New York, 1967. Soc. Min. Engrs. Am. Inst. Min. Metall. Petrolm. Engrs.

Dhillion, B.S., 2008. *Mining Equipment Reliability, Maintainability and Safety*. Springer International Press.

Diering, T., 2007. Template Mixing: A depletion engine for block cave scheduling. In *Proceedings APCOM 2007*. Santiago, 2007.

Diering, J.A.C. & Laubscher, D.H., 1987. Practical approach to the numerical stress analysis of mass mining. *Trans. Instituitio of Mining and Metallurgy*, pp.A179-88.

Edumine, 1999. *Mining method selection*. [Online] Available at: http://www.edumine.com/xtoolkit/xmethod/miningmethodgraphic.htm [Accessed 27 September 2016].

Hakakwale, B., 2013. *Examination of the geological set up and rock mass characteristics of Nchanga Underground Mine in order to optimise draw of "The Feldspathic-Quartzite" ore in the caved areas*. MMinSc. Dissertation. Lusaka, Zambia: University of Zambia Mining Engineering Department, School of Mines.

Halim, A.E., 2004. 3D large scale physical modelling for studying interactive drawing and drawpoint spacing in block caving mines. *JKMRC International Student conference*.

Hartman, H.L., 1987. *Introductory Mining Engineering*. 1st ed. New York: Wiley & Sons.

Heslop, T.G. & Laubscher, D., 1981. Draw control in caving operations on Southern African chrysollite asbestos mines. In D. Stewart, ed. *Design and operation of caving and sublevel stoping mines*. New York: Society of Mining Engineers - AIME. pp.755-74.

Hoek, E., 2007. *Practical Rock Engineering Course Notes*. [Online] Available at: https://www.rocscience.com/documents/hoek/corner/Practical-Rock-Engineering-Full-Text.pdf [Accessed 09 December 2016].

Hustrulid, W., 2000. Method selection for large-scale underground mining. In *Proceedings of MassMin 2000*. Brisbane, 2000. The Australian Institute of Mining and Metallurgy.

Julin, D., 1992. Block Caving. In H. Hartman, ed. *SME Mining Engineering Handbook*. Littleton, Colorado: Society for Mining, Metallurgy and Exploration. pp.1815-36.

KCM, 2000. *Nchanga Underground Training Manual*. Chingola: (Unpublished Reports) Konkola Copper Mines.

KCM, 2014. *Cave Control Manual*. KCM Standard Operating Procedures. Chingola: Unpublished Reports Konkola Copper Mines.

KCM, 2014. *KCM: 18 month production plan for the HSI complex*. Medium Term NUG Mine Plan. Chingola, Zambia: Unpublished Report Konkola Copper Mines.

KCM, 2016. *Technical review of the areas in the HSI and LOB with a view to optimise NUG operations*. KCM Mine Planning Report. Chingola, Zambia: Unpublished reports Konkola Copper Mines.

Khoshalan, A.H., Torabi, S.R., Hoseinie, S.H. & Ghodrati, B., 2014. An introduction to RAM analysis of Earth Pressure Balance (EPB) tunnel boring machine. *Scientific Journal of Pure and Applied Sciences*, 3(3), pp.1-8.

Kvapil, R., 1998. The mechanics and design of sublevel caving systems. In W.A. Hustrulid, ed. *Underground Mining Methods Handbook*. New York: SME-AIME. pp.880-97.

Kvapil, R., 2004. Gravity flow in sublevel and block caving: a common sense approach. In *Proceedings of MassMin 2004*. Lulea, Sweden, 2004. Lulea University of Technology Press.

Laubscher , D.H., 1981. Selection of mass underground mining methods. In D. Stewart, ed. *Design and Operation of Caving and Sublevel Stoping Mines*. New York: SME-AIME. pp.23-38.

Laubscher , D.H. & Page, C.H., 1990. The design of rock support in high stress or weak rock environments. In *Proc. 92nd Can. Inst. Min. Metall. AGM*. Ottawa, 1990.

Laubscher, D.H., 1977. Geomechanics classification of jointed rock masses - mining applications. *Trans Instn. Min. Metall.*, pp.A1-8.

Laubscher, D.H., 1984. Design aspects and effectiveness of suport systems in different mining conditions. *Trans Instn. Min. Metall.*, pp.A70-82.

Laubscher, H., 1994. Cave Mining - The state of the art. *Journal of the South African Institute of Mining and Metallurgy*, pp.279-93.

Laubscher, D.H., 2000. *Block Caving Manual*. University of Queensland, Australia: Prepared for the International Caving Study Phase 1.

Laubscher, D.H. & Taylor, H.W., 1976. The importance of geomechanics classification of jointed rock masses in mining operations. In Bieniawski, Z.T., ed. *Exploration for rock engineering*. Cape Town: Balkema, 1976.

Lauffer, H., 1958. Rock classification for tunnel construction. *Geology Bauwesen*, 1(24), pp.46-51.

Leonardi, C.R., Owen, D.R.J. & Feng, Y.T., 2011. Simulation of fines migration using a non-Newtonian lattice Boltzmann-discrete element model (Part I: 2D Implementation Aspects). *Emerald Insight*, 29(4), pp.366-91.

Marano, G., 1980. The interaction betweeen adjoining draw points in free flowing materials and its application in mining. *Zimbabwe Chamber of Mines Journal*, pp.25-32.

Mohammadi, M., Rai, P. & Gupta , S., 2015. Performance measurement of mining equipment. *International Journal of Emerging Technology and Advanced Engineering*, 5(7), pp.240-48.

Morris, S., 2010. *Reliability Analytics Toolkit*. [Online] Available at: http://reliabilityanalyticstoolkit.appspot.com/weibull_analysis [Accessed 18 December 2016].

Morrison, R.G.K., 1976. *A philosophy of ground control*. Montreal, Canada: McGill University.

Mundike, S., 2012. *Rock Mass Classification Values for Nchanga Underground Mine*. Geotechnical report. Chingola: Unpublished reports Konkola Copper Mines.

Munro, D.D., 2013. Inclined caving as a mass mining method. *Journal of the Southern African Institute of Mining and Metallurgy*, 113(7), pp.117-32.

Musingwini, C., Minnitt, R.C.A., Phuti, D. & Makwara, F., 2003. Just-in-time development model for a sub-level caving underground mine in Zimbabwe. *Journal of the Southern African Institue for Mining and Metallurgy*, pp.187-91.

Nicholas, D.E., 1981. Mining Method Selection - A Numerical Approach. In D. Stewart, ed. *Design and Operation of Caving and Sublevel Stoping Mines*. New York: SME-AIME. pp.39-53.

Pacher, F., Rabcewicz, L. & Golser, J., 1974. derGebirgsklassifizierung Stand-up time in tunnels (Translated from Austrian). *Proc. XXII Geomech. colloq. Salzburg*, pp.51-58.

Palmstrom, A., 1982. The volumetric joint count - A useful and simple measure of the degree of rock jointing. In *Proc. 4th congr. Int. Assn Engrng Geol*. Delhi, 1982.

Pearson, N.B., 1981. The development and control of block caving at the Chingola division of Nchanga Consolidated Copper Mines Limited, Zambia. In D. Stewart, ed. *Design and operation of caving and sub level stoping mines*. Society of Mining Engineers of the American Institute of Mining, Metallurgical, and Petroleum Engineers. pp.211-22.

Peskens, T.W., 2013. *Underground mining method selection and preliminary techo-economic mine design for Wombat ore body, Kylylahti deposit, Finland*. M.Sc. Thesis. Finland: Delft University of Technology Department of Geoscience and Engineering.

Rubio, E., 2002. *Long Term Planning Of Block Caving Operations Using Mathematical Programming Tools*. MSc. Thesis. Vancouver: University of British Columbia.

Samanta, B., Sarkar, B. & Mukherjee, S.K., 2001a. An application of Weibull distribution for reliability study of shovel machine used in a coal mine. *MGMI, Transactions*, 97, pp.77-86.

Samanta, B., Sarkar, B. & Mukherjee, S.K., 2001b. Reliability analysis of shovel machines used in an open cast coal mine. *Mineral Resource Engineering*, 10, pp.219-31.

Samanta, B., Sarkar, B. & Mukherjee, S.K., 2004. Reliability modelling and performance analyses of an LHD system in mining. *Journal of the Southern African Institute of Mining and Metallurgy*, pp.1-8.

Silverman, B.W., 1986. *Density estimation and data analysis*. 26th ed. CRC Press.

Suorineni, F.T., Hebblewhite, B. & Saydam, S., 2014. Geomechanics challenges of contemporary deep mining: A suggested model for increasing future mining safety and productivity. *The Southern African Institute of Mining and Metallurgy*, 114, pp.1023-32.

Susaeta, A., 2004. Theory of gravity flow (part 1). *Proceedings of MassMin*, pp.167-72.

Susaeta, A., Rubio, E. & Pais, G., 2008. Dilution behaviour at Codelco panel cave mines. In Schunnesson, H. & Nordlung, E., eds. *Proceedings of the 5th International Conference and Exhibition on Mass Mining, MassMin 2008*. Lulea, Sweden, 2008. Lulea University of Technology Press.

Taylor, H.W., 1980. *A geomechanics classification applied to mining problems at Shabanie and King mines, Zimbabwe*. M.Phil. Thesis. Harare: Univeristy of Rhodesia.

Wickham, G.E., Tiedemann, H.R. & Skinner, E.H., 1972. Support determination based on geologic predictions. In Lane, K.S. & Garfield, L.A., eds. *Proc. North American rapid excav. tunneling conf., Chicago*. New York, 1972. Soc. Min. Engrs, Am. Inst. Min. Metall. Petrolm Engrs.

APPENDICES

Appendix A: Nchanga Underground Phreatic Profile

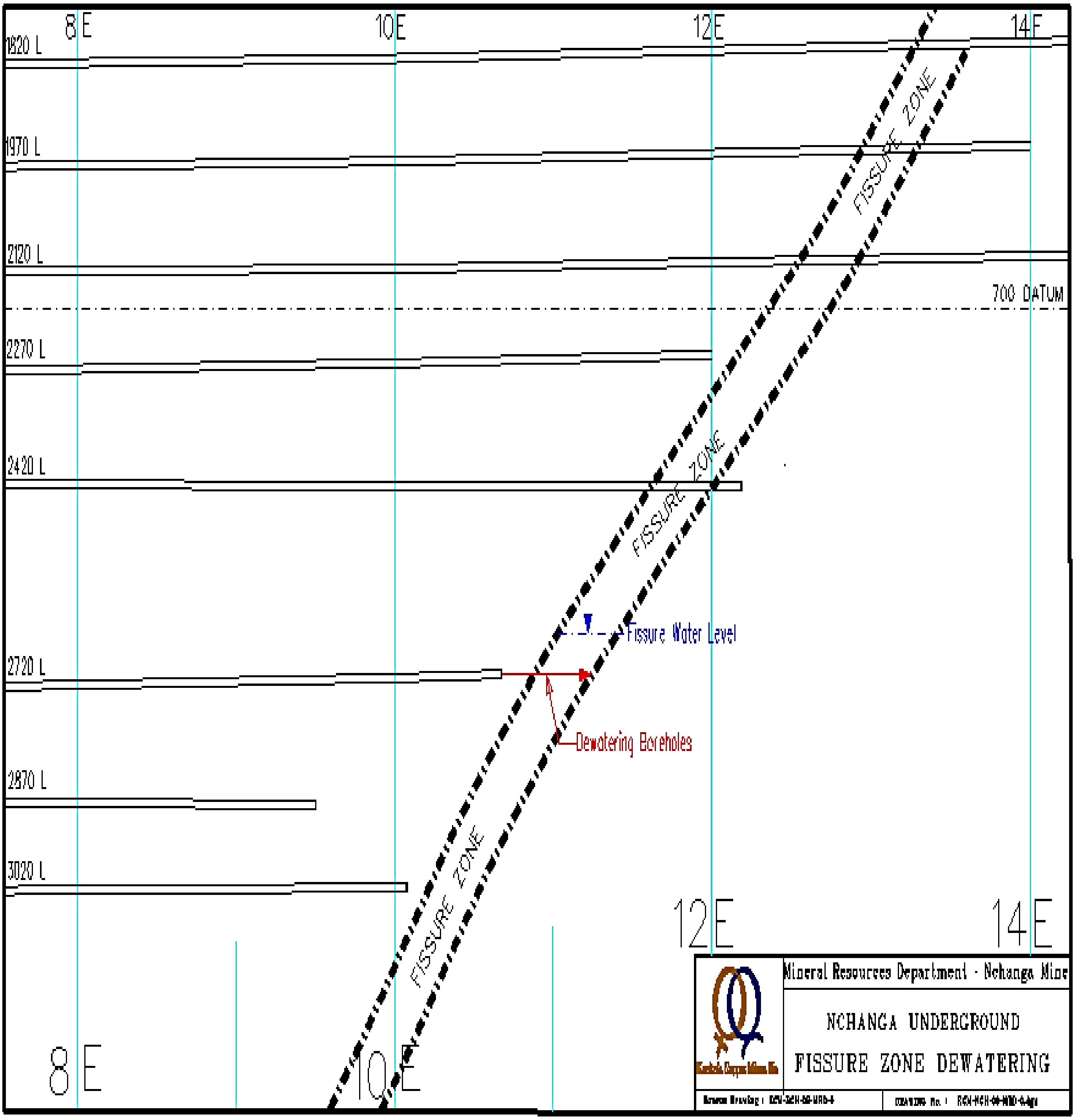

Appendix B: NUG Draw Point Geometry

Appendix B-1: Aspect View of Scraper Drift Dimensions

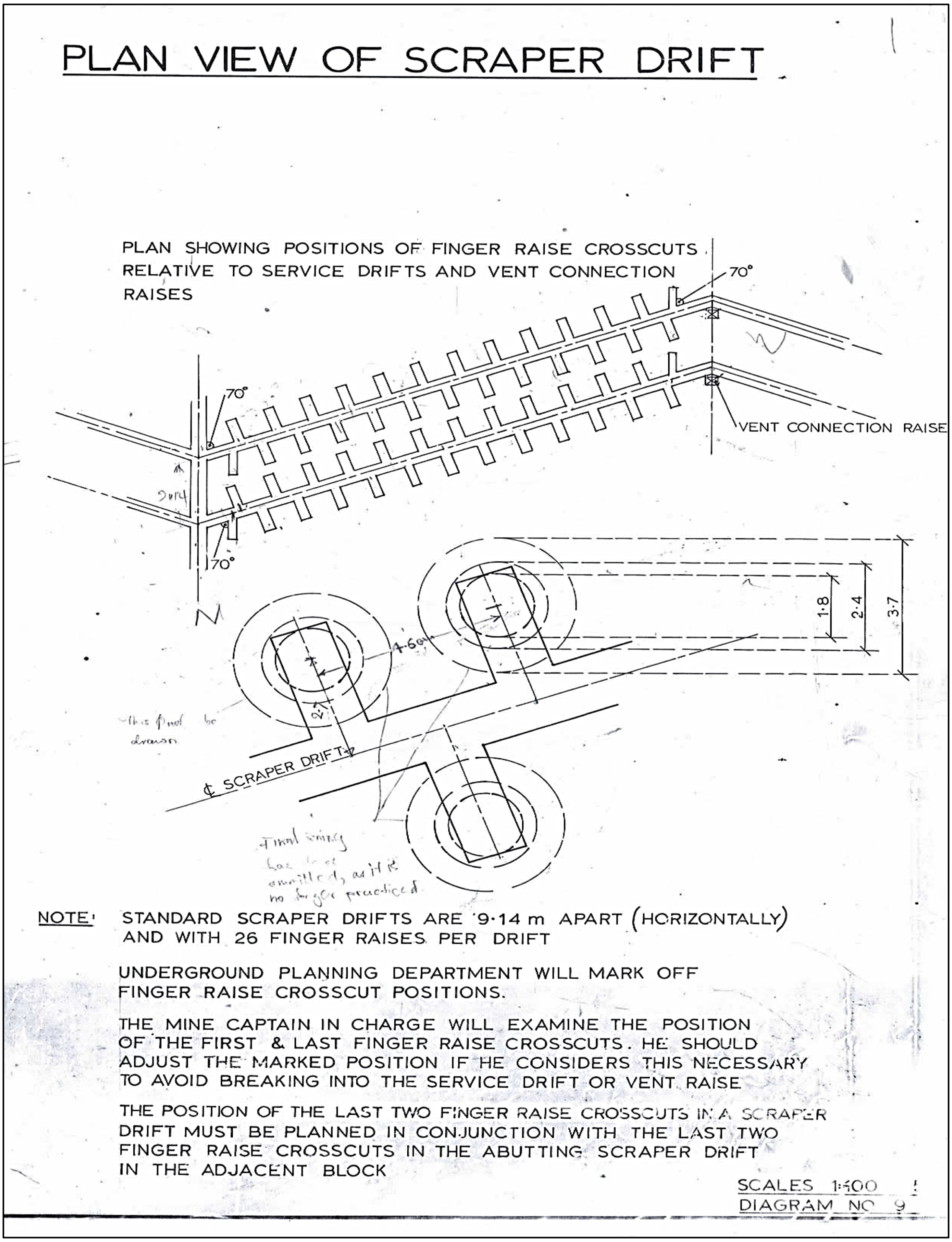

Appendix B-2: Draw Point Dimensions

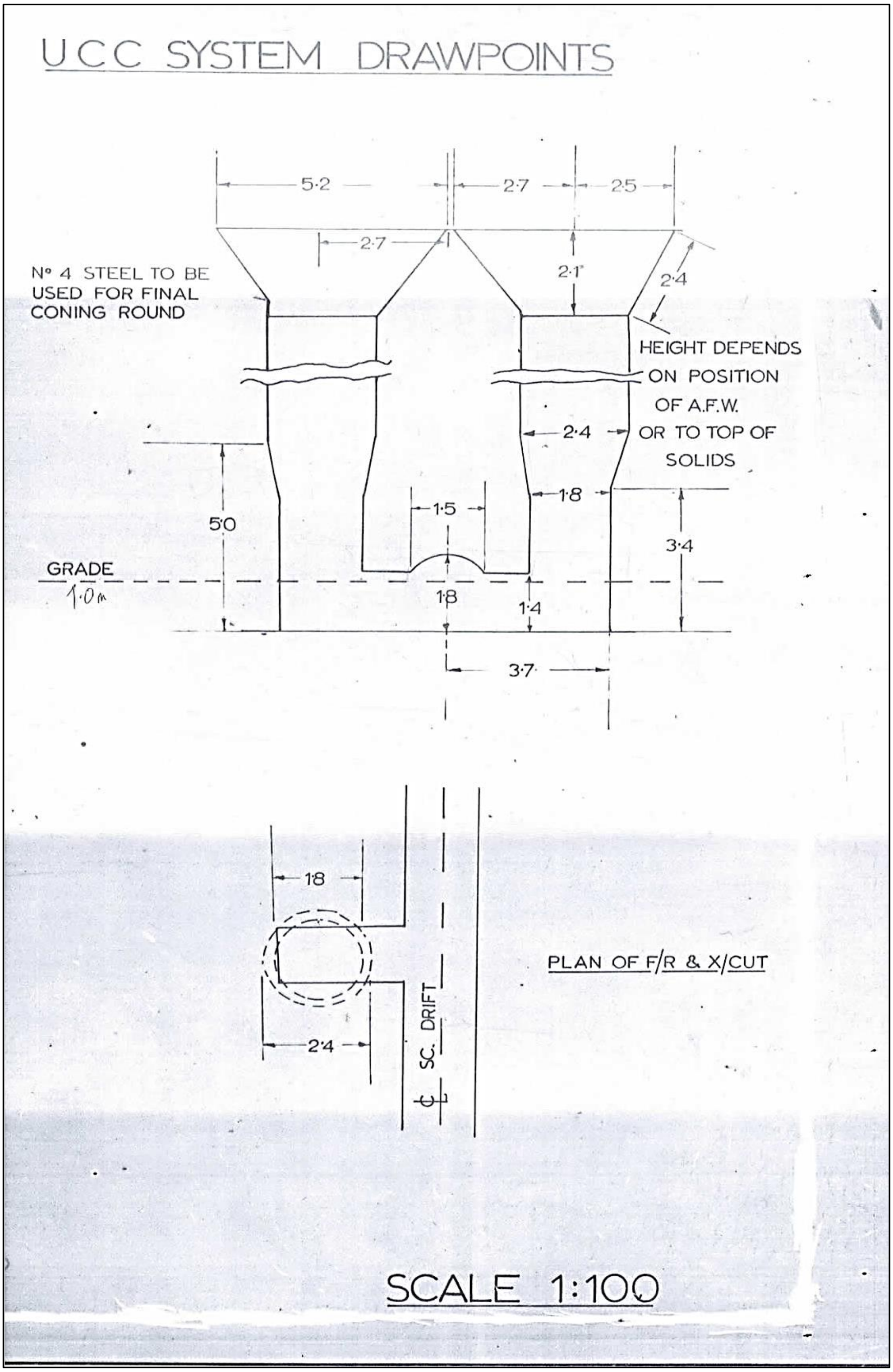

Appendix C: Data Collection Checklist

Table C-1: Rock Mass Geological Data

Discontinuities		
Joint set number	**Collected**	✓
	Not Collected	
Joint roughness number	**Collected**	✓
	Not Collected	
Joint alteration number	**Collected**	✓
	Not Collected	
Joint spacing	**Collected**	✓
	Not Collected	
Joint surface conditions	**Collected**	✓
	Not Collected	
Joint strike and dip orientations	**Collected**	✓
	Not Collected	
Joint water reduction factor	**Collected**	✓
	Not Collected	

Stress Regime		
Stress reduction factor	**Collected**	✓
	Not Collected	
Major principal stress	**Collected**	
	Not Collected	✓
HSI Complex Ore Body		
General ore body shape	**Collected**	✓
	Not Collected	
Ore body thickness	**Collected**	✓
	Not Collected	
Deposit plunge	**Collected**	✓
	Not Collected	
Grade distribution	**Collected**	✓
	Not Collected	
Depth from surface	**Collected**	✓
	Not Collected	

Table C-2: Cash Flow Components

Net Smelter Return	**Collected**	✓	Smelting costs	**Collected**	✓
	Not Collected			**Not Collected**	
Mining costs	**Collected**	✓	Concentrating costs	**Collected**	✓
	Not Collected			**Not Collected**	
Returns from TLP Primary Cu	**Collected**	✓	Fixed costs	**Collected**	✓
	Not Collected			**Not Collected**	

Table C-3: Mining System Parameters

Development and Production end dimensions	**Collected**	✓	Discount rate	**Collected**	✓
	Not Collected			**Not Collected**	
HSI Production target	**Collected**	✓	Capacity of box raise on 2675FT level	**Collected**	
	Not Collected			**Not Collected**	✓
Monthly production rate	**Collected**	✓	Capacities of trackless equipment	**Collected**	✓
	Not Collected			**Not Collected**	
Production Period (*T*)	**Collected**	✓	Mining capacity	**Collected**	✓
	Not Collected			**Not Collected**	
Tonnage mined over *T*	**Collected**	✓	Concentrating capacity	**Collected**	✓
	Not Collected			**Not Collected**	
Tonnage produced at the smelter over *T*	**Collected**	✓	Smelting capacity	**Collected**	
	Not Collected			**Not Collected**	✓
Tonnage produced at the concentrator over *T*	**Collected**	✓			
	Not Collected				

Table C-4: Index Properties Of Rock

UCS of ore zone, hanging wall and foot wall	**Collected**	✓	Friction angle	**Collected**	✓
	Not Collected			**Not Collected**	
Point-load strength index of ore zone, hanging and foot walls	**Collected**	✓	Particle and bulk densities	**Collected**	✓
	Not Collected			**Not Collected**	
RQD of ore zone, hanging wall, foot wall	**Collected**	✓	Moisture content	**Collected**	✓
	Not Collected			**Not Collected**	
Cohesion	**Collected**	✓	Abrasion	**Collected**	
	Not Collected			**Not Collected**	✓
			Maximum rock lump size and angle of repose	**Collected**	✓
				Not Collected	

Table C-5: Ore And Waste Mobilisation System

Annual Calendar shifts	**Collected**	✓	Hauling distances	**Collected**	✓
	Not Collected			**Not Collected**	
Planned production duration per shift	**Collected**	✓	Required spares for the fleet	**Collected**	✓
	Not Collected			**Not Collected**	
Fleet size	**Collected**	✓	Utilised lives of the fleet	**Collected**	✓
	Not Collected			**Not Collected**	
Failure data of the fleet	**Collected**	✓	Bucket fill factor	**Collected**	✓
	Not Collected			**Not Collected**	
			Planned availability and utilisation	**Collected**	✓
				Not Collected	

Appendix D: Exploration Data for HSI Complex Blocks

BLOCK ID	IN SITU TONNAGE	BLOCK GRADE (%TCu)	THICKNESS (m)	%ASCu	%AICu	WASTE TO ORE GRADE RATIO	ORE TONNAGE TO BE DRAWN	CONTAINED Cu TONNAGE
2720/9EC	116,576	6.6	6.8	2.15	4.45	0.15	98,912.97	6,528.26
2870/3EC	54,611	4.18	3.8	1.96	2.22	0.24	41,546.17	1,736.63
2870/4EC	35,718	2.44	5.0	1.39	1.05	0.41	21,079.48	514.34
2870/5EC	119,018	2.06	9.6	0.91	1.15	0.49	61,242.27	1,261.59
2870/6EC	103,442	3.45	6.1	0.87	2.58	0.29	73,458.81	2,534.33
2870/7EC	48,601	0.18	2.7	0.09	0.09	5.56	-	-
2870/8EC	49,970	3.19	3.7	1.48	1.71	0.31	34,305.42	1,094.34
3020/3EB	82,685	4.2	3.1	1.96	2.24	0.24	62,998.10	2,645.92
3020/4EB	67,791	3.44	3.6	1.03	2.41	0.29	48,084.31	1,654.10
3020/5EB	89,746	4.48	3.8	0.58	3.9	0.22	69,713.41	3,123.16
3020/6EB	86,667	7.63	2.7	1.03	6.6	0.13	75,308.28	5,746.02
3020/7EB	85,818	23.8	0.8	1.3	22.5	0.04	82,212.20	19,566.50
3020/8EB	127,220	2.49	6.5	1.39	1.1	0.4	76,127.63	1,895.58
3020/9EB	151,532	3.74	3.3	2.04	1.7	0.27	111,015.42	4,151.98
						TOTALS	**856,005**	**52,452.75**

Appendix E: Point Load Test Results for Irregular Lumps

Table E-1: Results for Nchanga Basement Granite

SAMPLED AREA: HSI COMPLEX- NUG							CLIENT NAME:		ROBERT NYIRENDA		
SAMPLED MATERIAL: NCHANGA BASEMENT GRANITE											
SAMPLE No.	W_1(*mm*)	W_2(*mm*)	W(*mm*)	D(*mm*)	P(*kN*)	D_e(*mm*)	D_e^2(mm^2)	Is(*MPa*)	Size Factor *F*	$I_s(50)$ (*MPa*)	UCS (*MPa*)
1	33	40	36.5	15	8.357	26.401	697.008	11.990	0.750	8.995	215.882
2	25	36	30.5	16	8.079	24.925	621.260	13.004	0.731	9.507	228.163
3	48	57	52.5	24	15.561	40.051	1604.074	9.701	0.905	8.779	210.699
4	52	71	61.5	27	20.912	45.978	2113.940	9.892	0.963	9.526	228.625
5	34	38	36	15	8.627	26.219	687.460	12.549	0.748	9.385	225.251
6	29	35	32	24	9.846	31.269	977.721	10.070	0.810	8.153	195.667
7	48	73	60.5	30	18.460	48.069	2310.630	7.989	0.982	7.849	188.372
8	30	39	34.5	24	12.658	32.467	1054.106	12.008	0.823	9.888	237.304
9	24	37	30.5	20	9.916	27.867	776.575	12.769	0.769	9.815	235.569
10	32	36	34	27	11.257	34.186	1168.682	9.632	0.843	8.117	194.820
11	26	38	32	22	9.485	29.937	896.244	10.583	0.794	8.402	201.642
12	37	45	41	23	12.661	34.648	1200.509	10.546	0.848	8.942	214.602
13	20	33	26.5	22	9.709	27.243	742.202	13.081	0.761	9.954	238.888
14	42	48	45	25	13.855	37.845	1432.209	9.674	0.882	8.534	204.822
15	29	37	33	22	10.522	30.402	924.252	11.384	0.799	9.101	218.417
16	35	42	38.5	25	12.864	35.005	1225.334	10.498	0.852	8.942	214.612
17	27	35	31	20	9.481	28.095	789.306	12.012	0.772	9.267	222.415
18	30	42	36	20	10.166	30.276	916.614	11.091	0.798	8.850	212.388
19	24	39	31.5	26	9.584	32.290	1042.648	9.192	0.821	7.550	181.203

Table E-2: Results for Arkose

SAMPLED AREA: HSI COMPLEX- NUG							CLIENT NAME:		ROBERT NYIRENDA		
SAMPLED MATERIAL: ARKOSE											
SAMPLE No.	W_1(*mm*)	W_2(*mm*)	W(*mm*)	D(*mm*)	P(*kN*)	D_e(*mm*)	D_e^2(mm^2)	Is(*MPa*)	Size Factor *F*	I_s(50) (*MPa*)	UCS (*MPa*)
1	15	19	17	17	4.157	19.181	367.919	11.299	0.625	7.065	169.572
2	33	40	36.5	15	7.070	26.401	697.008	10.143	0.731	7.418	178.029
3	26	33	29.5	19	7.098	26.713	713.558	9.947	0.736	7.316	175.595
4	38	46	42	18	8.580	31.023	962.444	8.915	0.791	7.056	169.338
5	16	20	18	17	4.610	19.737	389.561	11.834	0.634	7.504	180.108
6	26	32	29	26	8.343	30.982	959.898	8.692	0.791	6.875	164.990
7	34	41	37.5	23	9.460	33.136	1098.027	8.615	0.817	7.043	169.022
8	46	57	51.5	33	16.658	46.514	2163.590	7.699	0.965	7.431	178.354
9	37	47	42	38	14.902	45.076	2031.827	7.334	0.950	6.971	167.304
10	46	57	51.5	25	13.257	40.486	1639.083	8.088	0.902	7.293	175.040
11	34	41	37.5	23	9.709	33.136	1098.027	8.842	0.817	7.228	173.471
12	39	50	44.5	16	8.855	30.107	906.429	9.769	0.780	7.619	182.859
13	37	48	42.5	38	16.522	45.343	2056.015	8.036	0.953	7.660	183.842
14	23	28	25.5	25	7.864	28.488	811.585	9.690	0.759	7.355	176.527
15	20	26	23	18	5.481	22.958	527.053	10.399	0.683	7.102	170.442
16	31	40	35.5	22	9.166	31.532	994.271	9.219	0.798	7.355	176.514
17	34	42	38	20	8.584	31.105	967.537	8.872	0.792	7.031	168.743
18	48	59	53.5	26	14.236	42.081	1770.847	8.039	0.919	7.388	177.308
19	26	33	29.5	18	7.032	26.000	676.003	10.402	0.726	7.550	181.211
20	41	50	45.5	31	14.226	42.375	1795.672	7.922	0.922	7.305	175.330
21	44	56	50	35	16.383	47.200	2227.880	7.354	0.972	7.149	171.574

Table E-3: Results for Lower Banded Shale

SAMPLED AREA: HSI COMPLEX- NUG							CLIENT NAME:		ROBERT NYIRENDA		
SAMPLED MATERIAL: LOWER BANDED SHALE											
SAMPLE No.	W_1(*mm*)	W_2(*mm*)	W(*mm*)	D(*mm*)	P(*kN*)	D_e(*mm*)	D_e^2(mm^2)	Is(*MPa*)	Size Factor *F*	$I_s(50)$ (*MPa*)	UCS (*MPa*)
1	17	22	19.5	17	1.157	20.543	422.024	2.742	0.647	1.773	42.552
2	30	37	33.5	31	2.570	36.361	1322.088	1.944	0.855	1.663	39.911
3	52	68	60	40	4.998	55.275	3055.379	1.636	1.050	1.718	41.237
4	35	45	40	24	2.580	34.959	1222.151	2.111	0.839	1.772	42.516
5	20	26	23	17	1.310	22.311	497.772	2.632	0.673	1.772	42.533
6	51	66	58.5	20	2.943	38.594	1489.497	1.976	0.881	1.740	41.770
7	54	74	64	31	4.460	50.257	2525.780	1.766	1.003	1.770	42.486
8	15	21	18	15	0.958	18.540	343.730	2.787	0.615	1.714	41.137
9	25	34	29.5	25	2.052	30.641	938.892	2.186	0.787	1.719	41.264
10	51	65	58	35	4.557	50.836	2584.341	1.763	1.008	1.778	42.665
11	24	29	26.5	22	1.808	27.243	742.202	2.436	0.743	1.809	43.418
12	37	48	42.5	35	3.697	43.517	1893.698	1.952	0.934	1.824	43.772
13	36	49	42.5	35	3.709	43.517	1893.698	1.959	0.934	1.830	43.914
14	19	25	22	15	1.155	20.497	420.115	2.749	0.646	1.776	42.624
15	32	40	36	30	2.722	37.080	1374.920	1.980	0.864	1.710	41.040
16	27	34	30.5	27	2.294	32.379	1048.377	2.188	0.808	1.769	42.444
17	21	28	24.5	25	1.881	27.924	779.758	2.412	0.752	1.813	43.519
18	55	73	64	42	5.466	58.498	3422.024	1.597	1.080	1.725	41.400
19	16	21	18.5	17	1.084	20.010	400.382	2.707	0.638	1.728	41.484
20	15	21	18	15	0.936	18.540	343.730	2.723	0.615	1.675	40.193
21	45	57	51	55	5.732	59.758	3570.974	1.605	1.091	1.752	42.041
22	21	29	25	23	1.766	27.056	732.018	2.413	0.740	1.786	42.854

Appendix F: RMR Data Calculation Sheet

Table F-1: RMR for Lower Banded Shale

<table>
<tr><th colspan="3">PARAMETER</th><th>VALUES</th></tr>
<tr><td rowspan="2">1.</td><td rowspan="2">STRENGTH OF INTACT ROCK MATERIAL</td><td>POINT-LOAD STRENGTH INDEX</td><td>2.194 MPa</td></tr>
<tr><td>RATING</td><td>7</td></tr>
<tr><td rowspan="2">2.</td><td rowspan="2">DRILL CORE QUALITY (RQD)</td><td></td><td>25 – 35%</td></tr>
<tr><td>RATING</td><td>8</td></tr>
<tr><td rowspan="2">3.</td><td rowspan="2">JOINT SPACING</td><td></td><td>0.6m – 2.0m</td></tr>
<tr><td>RATING</td><td>15</td></tr>
<tr><td rowspan="2">4.</td><td rowspan="2">JOINT CONDITIONS</td><td></td><td>Slightly rough surfaces, separation <1<i>mm</i></td></tr>
<tr><td>RATING</td><td>15</td></tr>
<tr><td rowspan="2">5.</td><td rowspan="2">GROUNDWATER CONDITIONS</td><td></td><td><10<i>l</i> per minute inflow, damp conditions</td></tr>
<tr><td>RATING</td><td>10</td></tr>
<tr><td rowspan="2">6.</td><td rowspan="2">ADJUSTMENT FOR DISCONTINUITY ORIENTATIONS</td><td></td><td>Drive against dip (45^o – 90^o), Fair</td></tr>
<tr><td>RATING</td><td>-5</td></tr>
<tr><td colspan="2" rowspan="2">RMR</td><td></td><td>7+8+15+15+10-5</td></tr>
<tr><td>TOTAL</td><td>50</td></tr>
</table>

Table F-2: RMR for Arkose

PARAMETER			VALUES
1.	STRENGTH OF INTACT ROCK MATERIAL	POINT-LOAD STRENGTH INDEX	9.101 *MPa*
		RATING	**12**
2.	DRILL CORE QUALITY (RQD)		65 – 80%
		RATING	**13**
3.	JOINT SPACING		0.6*m* – 2.0*m*
		RATING	**15**
4.	JOINT CONDITIONS		Slightly rough surfaces, separation <1*mm*
		RATING	**15**
5.	GROUNDWATER CONDITIONS		<10*l* per minute inflow, damp conditions
		RATING	**10**
6.	ADJUSTMENT FOR DISCONTINUITY ORIENTATIONS		Drive against dip (45^o – 90^o), Fair
		RATING	**-5**
RMR			**12+13+15+15+10-5**
		TOTAL	**60**

Table F-3: RMR for Nchanga Basement Granite

PARAMETER			VALUES
1.	STRENGTH OF INTACT ROCK MATERIAL	POINT-LOAD STRENGTH INDEX	10.930 *MPa*
		RATING	**15**
2.	DRILL CORE QUALITY (RQD)		80 – 100%
		RATING	**17**
3.	JOINT SPACING		0.6*m* – 2.0*m*
		RATING	**15**
4.	JOINT CONDITIONS		Slightly rough surfaces, separation <1*mm*
		RATING	**15**
5.	GROUNDWATER CONDITIONS		<10*l* per minute inflow, damp conditions
		RATING	**10**
6.	ADJUSTMENT FOR DISCONTINUITY ORIENTATIONS		Drive against dip (45^o – 90^o), Fair
		RATING	**-5**
RMR			**15+17+15+15+10-5**
		TOTAL	**67**

Appendix G: NUG Development Dimensions

Table G-1: Standard Metric Development Dimensions

	DEVELOPMENT END	DIMENSIONS (W x H)
LOB - PRIMARY	HAULAGE - DOUBLE	6.7 X 3.9
	" - TRACKLESS	4.8 X 3.9
	" - SUB & AUX.	4.3 X 3.9
	DEWATERING - PROSPECT DRIVES	3.0 X 3.7
	" - DRAIN DRIVES	1.2 X 2.1
	MAT. X/CUT - TO D/D AREA.	4.3 X 3.0
	" - TO SERV/D ACC. X/C	2.4 X 2.4
	" - ACC. X/C TO T/D	1.8 X 2.1
	" - ACC. X/C TO SERV/D	1.8 X 2.1
	T/C RAISE	2.4 X 2.4
	ACC. RSE (TO T/D & FWVD)	2.4 X 2.4
	ACC. RSE D/D SITE (5.5m HT)	3.0 X 3.0
	ACC. X/CUT TO T/D EX. ACC. RSE	1.8 X 2.1
	FOOTWALL VENT DRIFT	3.0 X 3.0
	FWVD - TC RAISE	1.5 X 1.5
	FWVD - ACC. X/CUT EX. ACC. RAISE	1.8 X 2.1
	FWVD - VCR X/CUT & RAISE	1.5 X 1.5
	EMERGENCY X/CUT & RAISE	1.5 X 1.5
	INSPECTION X/CUT & RAISE	1.5 X 1.5
LOB - SECONDARY	TRANSFER DRIFT	1.8 X 3.0
	TRANSFER DRIFT (Thin Rich)	1.8 X 2.1
	" - SUB T/C X/CUT	1.5 X 1.5
	" - SUB T/C RAISE	1.5 X 1.5
	" - MUCKING POINTS	1.2 X 1.2
	" - ACC. RSE TO SERV/D	1.5 X 1.5
	SERVICE DRIFT	1.8 X 2.1
	SCRAPER DRIFT	1.4 X 1.5
	FINGER RSE X/CUT	1.4 X 1.4
	FINGER RSE (TO 2.4m ABOVE GRADE)	1.8 X 1.8

	FINGER RSE (EX 3.4m ABOVE GRADE)	**2.4 X 2.4**
	SLOT RAISE	1.8 X 1.8
	UPPER VENT	1.5 X 1.5
	TROUGH DRIVE	1.8 X 2.1
	" - SLOT X/CUT (N / SOUTH)	1.8 X 2.1
	" - MICKEY MOUSE X/CUT	1.2 X 1.2
	ARKOSE OR SHALE U/CUT	1.8 X 2.1
	" - SLOT X/CUT	1.8 X 2.1
	GRIZZLEY DRIVE	1.8 X 2.1
	DIP SCRAPE	1.4 X 1.5
UOB – DEVELOPMENT ENDS	BSS ACCESS HAULAGE	4.9 X 4.0
	UOB TRAM DRIVE	3.7 X 3.7
	" DOLOMITE DRIVE	3.0 X 3.7
	" LOADER X/CUT	3.0 X 3.0
	" SLC X/CUT	2.4 X 2.1
	" VENT CONNECTIONS	2.4 X 2.1
	" CONTOUR DRIVE (CAVO LASH)	2.4 X 2.1
	" CHAMBER DRIVE	1.8 X 2.1
	" CONTOUR DRIVE (HAND LASH)	1.4 X 1.5

NB: The transfer drifts and the service drifts are laid out at ½ position and 25 degrees inclination. The scraper drifts are laid out between ½ degree and 18 degrees inclination

Appendix H: MRMR Data Calculation Sheet

Table H -1: MRMR for Ore Zone in the HSI Complex

<table>
<tr><th colspan="2">PARAMETER</th><th colspan="33">RANGE OF VALUES</th></tr>
<tr><td rowspan="3">1.</td><td>Intact rock strength (MPa)</td><td>A</td><td>185</td><td>B</td><td>A</td><td>184 to 165</td><td>B</td><td>A</td><td>164 to 145</td><td>B</td><td>A</td><td>144 to 125</td><td>B</td><td>A</td><td>124 to 105</td><td>B</td><td>A</td><td>104 to 85</td><td>B</td><td>A</td><td>84 to 65</td><td>B</td><td>A</td><td>64 to 45</td><td>B</td><td>A</td><td>44 to 25</td><td>B</td><td>A</td><td>24 to 5</td><td>B</td><td>A</td><td>5 to 0</td><td>B</td></tr>
<tr><td>Rating</td><td colspan="3">20</td><td colspan="3">18</td><td colspan="3">16</td><td colspan="3">14</td><td colspan="3">12</td><td colspan="3">10</td><td colspan="3">8</td><td colspan="3">6</td><td colspan="3">4</td><td colspan="3">2</td><td colspan="3">0</td></tr>
<tr><td>Input Data</td><td colspan="3"></td><td colspan="3"></td><td colspan="3"></td><td colspan="3"></td><td colspan="3"></td><td colspan="3">10</td><td colspan="3"></td><td colspan="3"></td><td colspan="3"></td><td colspan="3"></td><td colspan="3"></td></tr>
<tr><td rowspan="3">2.</td><td>RQD (%)</td><td colspan="6">100 to 97</td><td colspan="3">96 to 84</td><td colspan="3">83 to 71</td><td colspan="3">70 to 56</td><td colspan="3">55 to 44</td><td colspan="3">43 to 31</td><td colspan="3">30 to 17</td><td colspan="3">16 to 4</td><td colspan="6">3 to 0</td></tr>
<tr><td>Rating</td><td colspan="6">15</td><td colspan="3">14</td><td colspan="3">12</td><td colspan="3">10</td><td colspan="3">8</td><td colspan="3">6</td><td colspan="3">4</td><td colspan="3">2</td><td colspan="6">0</td></tr>
<tr><td>Input Data</td><td colspan="6"></td><td colspan="3"></td><td colspan="3"></td><td colspan="3">11</td><td colspan="3"></td><td colspan="3"></td><td colspan="3"></td><td colspan="3"></td><td colspan="3"></td><td colspan="3"></td></tr>
<tr><td rowspan="2">3.</td><td>Joint spacing (m)</td><td colspan="33">See Note A below</td></tr>
<tr><td>Rating</td><td colspan="33">25 to 0</td></tr>
<tr><td>4.</td><td>Joint condition including groundwater (m)</td><td colspan="33">See Table H-2 overleaf</td></tr>
<tr><td></td><td>Rating</td><td colspan="33">40 to 0</td></tr>
</table>

Note A: For 1 Joint sets spacing at 1.5m (X = Spacing in m)

$$Rating = 25 \times \left[\frac{(26.4 \times log_{10}X) + 45}{100}\right] = 12$$

Table H-2: Assessment of Joint and Groundwater Conditions

PARAMETER	DESCRIPTION		DRY CONDITIONS (% OF POSSIBLE RATING OF 40)	WET CONDITIONS (% OF POSSIBLE RATING OF 40)		
				MOIST	MODERATE PRESSURE (25 to 125l/min)	SEVERE PRESSURE (>125l/min)
A Large-scale joint expression	Wavy	Multi-directional	100	100	95	90
		Uni-directional	95	90	85	80
	Curved		85	80	75	70
	Slight Undulation		80	75	70	65
	Straight		75	**70**	65	60
B Small-scale joint expression	Rough stepped/irregular		95	90	85	80
	Smooth stepped		90	85	80	75
	Slickensided stepped		85	80	75	70
	Rough undulating		80	75	70	65
	Smooth undulating		75	70	65	60
	Slickensided undulating		70	65	60	55
	Rough planar		65	60	55	50
	Smooth planar		60	55	50	45
	Polished		55	50	45	40
C Joint wall alteration zone	Stronger than wall rock		100	100	100	100
	No alteration		100	**100**	100	100
	Weaker than wall rock		75	70	65	60
D Joint filling	No fill – surface staining only		100	100	100	100
	Non-softening and sheared material (clay or free)	Coarse	90	**85**	80	75
		Medium	85	80	75	70
		Fine	80	75	70	65
	Soft sheared material (e.g. talc)	Coarse	70	65	60	55
		Medium	60	55	50	45
		FIne	50	45	40	35
	Gouge thickness <amplitude of irregularity		45	**40**	35	30
	Gouge thickness > amplitude of irregularity		30	20	15	10

$$Rating = \left[\left(\frac{A}{100\%} \times \frac{B}{100\%} \times \frac{C}{100\%} \times \frac{D}{100\%}\right) \times 40\right] = 10$$

$$\therefore \boldsymbol{MRMR = 10 + 11 + 12 + 10 = 43}$$

Appendix I: Reliability Estimates for HSI Dump Trucks

Table I-1: Reliability Estimates for Engine Sub System of MT09 Dump Truck

Time (Hours)	R(t) Lower 95.0% Confidence Limit	R(t) Point Estimate	R(t) Upper 95.0% Confidence Limit
112.8	0.9157	0.9797	0.9985
247.9	0.8679	0.9506	0.9894
376.1	0.8262	0.9215	0.9755
501.9	0.7875	0.8924	0.9588
627.2	0.7507	0.8634	0.9402
753.0	0.7154	0.8343	0.9202
880.1	0.6811	0.8052	0.8992
1,009.0	0.6479	0.7762	0.8772
1,140.4	0.6153	0.7471	0.8544
1,274.7	0.5836	0.7180	0.8309
1,412.3	0.5524	0.6890	0.8068
1,553.8	0.5218	0.6599	0.7821
1,699.7	0.4918	0.6308	0.7569
1,850.6	0.4623	0.6017	0.7312
2,007.0	0.4332	0.5727	0.7049
2,169.6	0.4047	0.5436	0.6782
2,339.3	0.3766	0.5145	0.6511
2,516.9	0.3489	0.4855	0.6234
2,703.5	0.3218	0.4564	0.5953
2,900.3	0.2951	0.4273	0.5668
3,108.9	0.2688	0.3983	0.5377
3,331.0	0.2431	0.3692	0.5082
3,568.9	0.2179	0.3401	0.4782
3,825.4	0.1932	0.3110	0.4476
4,104.3	0.1691	0.2820	0.4164
4,410.3	0.1456	0.2529	0.3847
4,750.1	0.1228	0.2238	0.3521
5,132.9	0.1008	0.1948	0.3189
5,572.6	0.0798	0.1657	0.2846
6,090.7	0.0598	0.1366	0.2493
6,724.5	0.0412	0.1076	0.2125
7,546.2	0.0245	0.0785	0.1738
8,729.7	0.0106	0.0494	0.1321
10,937.9	0.0015	0.0203	0.0843

Table I-2: Reliability Estimates for Transmission Sub System of MT11 Dump Truck

Time (Hours)	R(t) Lower 95.0% Confidence Limit	R(t) Point Estimate	R(t) Upper 95.0% Confidence Limit
1,368.6	0.9079	0.9777	0.9983
1,775.9	0.8559	0.9459	0.9884
2,039.2	0.8106	0.9140	0.9731
2,244.3	0.7685	0.8822	0.9547
2,417.0	0.7286	0.8503	0.9342
2,568.9	0.6904	0.8185	0.9122
2,706.3	0.6533	0.7866	0.8889
2,833.2	0.6174	0.7548	0.8646
2,952.0	0.5823	0.7229	0.8394
3,064.8	0.5481	0.6911	0.8134
3,172.8	0.5146	0.6592	0.7866
3,277.2	0.4817	0.6274	0.7592
3,378.8	0.4496	0.5955	0.7312
3,478.4	0.4180	0.5637	0.7025
3,576.7	0.3870	0.5318	0.6733
3,674.2	0.3566	0.5000	0.6434
3,771.5	0.3267	0.4682	0.6130
3,869.3	0.2975	0.4363	0.5820
3,968.0	0.2688	0.4045	0.5504
4,068.5	0.2408	0.3726	0.5183
4,171.4	0.2134	0.3408	0.4854
4,277.6	0.1866	0.3089	0.4519
4,388.2	0.1606	0.2771	0.4177
4,504.7	0.1354	0.2452	0.3826
4,628.9	0.1111	0.2134	0.3467
4,763.7	0.0878	0.1815	0.3096
4,913.0	0.0658	0.1497	0.2714
5,084.0	0.0453	0.1178	0.2315
5,289.4	0.0269	0.0860	0.1894
5,559.5	0.0116	0.0541	0.1441
6,001.9	0.0017	0.0223	0.0921

Table I-3: **Reliability Estimates for Hydraulic Sub System of MTK02 Dump Truck**

Time (Hours)	R(t) Lower 95.0% Confidence Limit	R(t) Point Estimate	R(t) Upper 95.0% Confidence Limit
462.7	0.7942	0.9478	0.9961
723.8	0.6837	0.8731	0.9719
924.0	0.5899	0.7985	0.9340
1,100.2	0.5054	0.7239	0.8873
1,265.6	0.4274	0.6493	0.8343
1,427.1	0.3548	0.5746	0.7760
1,590.0	0.2870	0.5000	0.7130
1,759.2	0.2240	0.4254	0.6452
1,940.7	0.1657	0.3507	0.5726
2,143.1	0.1127	0.2761	0.4946
2,381.9	0.0660	0.2015	0.4101
2,692.1	0.0281	0.1269	0.3163
3,198.8	0.0039	0.0522	0.2058

Appendix J: EBITDA Calculations

	UNIT	AMOUNT	
RESERVE TONNAGE @ DILUTION ENTRY	Tonnes	747,214	
TOTAL WEIGHTED AVERAGE GRADE	%	5.27%	
AICu GRADE	%	3.91%	
ASCu GRADE	%	1.36%	
AICu RECOVERY AT NEW WEST MILL	%	42.9%	
ASCu RECOVERY IN CONCENTRATE	%	3.78%	
TLP RECOVERY	%	79%	
PRIMARY Cu	Tonnes	7,725	
Cu IN CONCENTRATES	Tonnes	24,651	
TOTAL COPPER PRODUCED	Tonnes	32,375	
OPEX FACTORS			
MINING	$/t	33.95	
CONCENTRATING	$/t	307.06	
TAILINGS LEACH PLANT	$/t	1,785.75	
SMELTER	$/t	524.04	
ADMINSTRATION AND ENGINEERING	$/t	724.45	
TOTAL	$/t	3,375.25	
DIRECT OPEX INCURRED			
MINING	$	25,367,907.30	
CONCENTRATING	$	8,971,082.83	
TAILINGS LEACH PLANT	$	17,461,026.97	
SMELTER	$	6,769,452.62	
ADMINSTRATION AND ENGINEERING	$	23,454,257.58	
TOTAL DIRECT OPEX	$		82,023,727.31
UNIT PRODUCTION RETURNS			
NSR Cu IN CONCENTRATES	$/t	4,928.00	
NSR PRIMARY Cu	$/t	6,275.00	
TOTAL	$/t	11,203.00	
OVERALL PRODUCTION EARNINGS			
NSR Cu IN CONCENTRATES	$	121,478,436.77	
NSR PRIMARY Cu	$	48,471,889.10	
GROSS PRODUCTION RETURNS	$		169,950,325.87
EBITDA	$		87,926,598.56
SUSTAINING CAPEX			
MT09 SPARES AND OVERHAUL	$	69,420.00	
DEWATERING	$	268,800.00	
OTHERS	$	4,680,000.00	
TOTAL DIRECT CAPEX	$		5,018,220.00
NET EBITDA	$		82,908,378.56
DISCOUNT RATE		12%	
ANNUAL PRODUCTION RATE	tpy	308,500	
LIFE-OF-MINE BY DEP TONNAGES	Years	2.42	
NET DISCOUNTED EBITDA	**$**		**63,006,898.32**